

---

**Pacific Northwest  
National Laboratory**

Operated by Battelle for the  
U.S. Department of Energy

**STOMP  
Subsurface Transport Over  
Multiple Phases**

**Version 3.0**

**An Introductory Short Course**

M. Oostrom  
D.H. Meck  
M. D. White

October, 2003

Prepared for the U.S. Department of Energy  
under Contract DE-AC06-76RL01830



## DISCLAIMER

This report was prepared as an account of work sponsored by an agency of the United States Government. Neither the United States Government nor any agency thereof, nor Battelle Memorial Institute, nor any of their employees, makes **any warranty, express or implied, or assumes any legal liability or responsibility for the accuracy, completeness, or usefulness of any information, apparatus, product, or process disclosed, or represents that its use would not infringe privately owned rights.** Reference herein to any specific commercial product, process, or service by trade name, trademark, manufacturer, or otherwise does not necessarily constitute or imply its endorsement, recommendation, or favoring by the United States Government or any agency thereof, or Battelle Memorial Institute. The views and opinions of authors expressed herein do not necessarily state or reflect those of the United States Government or any agency thereof.

PACIFIC NORTHWEST NATIONAL LABORATORY

*operated by*

BATTELLE

*for the*

UNITED STATES DEPARTMENT OF ENERGY

*under Contract DE-AC06-76RL01830*

# **STOMP**

## **Subsurface Transport Over Multiple Phases**

**Version 3.0**

**An Introductory Short Course**

M. Oostrom  
D.H. Meck  
M.D. White

October, 2003

Prepared for the U.S. Department of Energy  
under Contract DE-AC06-76RLO 1830

**Pacific Northwest National Laboratory**  
Richland, Washington 99352

## Preface

This guide describes an introductory short course on the STOMP (Subsurface Transport Over Multiple Phases) simulator, a scientific tool for analyzing single and multiple phase subsurface flow and transport. This 10-problem manual was initially developed for a short course given at Delft University of Technology, The Netherlands in June 2003 by M. Oostrom and M.D. White. After the short course, the problems and associated exercises were improved and refined. Each problem consists of the following sections: Problem Description, Exercises, Input File, and Solutions to Selected Exercises. The solutions to the exercises were obtained and described by co-author D.H. Meck during the completion of a Science Undergraduate Laboratory Internship (SUNI) at PNNL. The 10 problems are of increased complexity, ranging from simple one-dimensional saturated flow of a single phase, to problems describing flow and transport of several phases. Electronic versions of the problems are presented on the STOMP website <http://www.pnl.org/etd/stomp>.

A description of the general use, *input* file formatting, compilation and execution of the simulator is provided in a companion user's guide (White and Oostrom, 2003). In writing these guides for the STOMP simulator, the authors have assumed that the reader comprehends concepts and theories associated with multiple-phase hydrology, heat transfer, thermodynamics, radioactive chain decay, and relative permeability-saturation-capillary pressure constitutive relations. The authors further assume that the reader is familiar with the computing environment on which they plan to compile and execute the STOMP simulator.

The STOMP simulator is written in the FORTRAN 77 and 90 languages, following American National Standards Institute (ANSI) standards. The simulator utilizes a variable source code configuration, which allows the execution memory and speed be tailored to the problem specifics, and essentially requires that the source code be assembled and compiled through a software maintenance utility. The memory requirements for executing the simulator are dependent on the complexity of physical

system to be modeled and the size and dimensionality of the computational domain. Likewise execution speed depends on the problem complexity, size and dimensionality of the computational domain, and computer performance.

## Compilation and Execution

The reader is referred to Chapter 5 of the User's Guide (White and Oostrom, 2003) for detailed information on execution of STOMP runs. In its native form, the STOMP simulator is a collection of files, which contain either global routines or those associated with a particular operational mode. For users outside of the Pacific Northwest National Laboratory, the STOMP simulator is distributed as assembled source coding for a particular operational mode, with associated include files, modules, example *input* files and required external packages (e.g., SPLIB). Assembly of the source coding occurs through the make utility (Talbot, 1988) before the code is distributed. For users within the Laboratory, the "make" utility additionally can be used to directly create an executable. Except for external packages, the STOMP simulator is coded in Fortran. Distributing an open source allows users to read and modify the simulator; hopefully, promoting an open exchange of scientific ideas. The penalty of an open source; however, is that the user is responsible for compiling and linking the source code to generate an executable. This inherently assumes that the user has a Fortran compiler and is familiar with its use for generating code. Advanced users, interested in modifying the code, should additionally be familiar, if not skilled with using a symbolic debugger (often provided with the Fortran compiler). The unassembled STOMP source is coded in a combination of Fortran 77 and Fortran 90. With respect to memory allocation, the assembled source code can be configured in two forms: static and dynamic memory.

For those users with only access to a Fortran 77 compiler, (e.g., g77, f77, pgf77) the code must be configured in static memory form. In this form the source code will include a parameters and a commons file. As Fortran 77 is unable to dynamically allocate memory, the user is responsible for editing the parameters file to define array dimensions to statically allocate memory during compilation. For users with access to a Fortran 90 compiler (e.g., f90, pgf90, ifc), the source code can be configured for dynamic memory allocation. In the dynamic memory form, both the parameters and commons

files are replaced with a series of Fortran 90 modules, in the file `allo.f`. As described below this module file must be compiled prior to compiling the source code. When configured under the dynamic memory option a utility named `step` is included in the source code. When incorporated, the `step` utility becomes the first subroutine called and reads a STOMP *input* file to determine dimensioned array requirements. These values (i.e., parameters) are then used to allocate memory for the dimensioned arrays, via a call to the subroutine `alloc`. Subroutine `alloc` makes a series of memory allocations and memory checks. If STOMP attempts to allocate more memory than available on the computer, the simulation stops and an error message is printed. Memory allocation under the dynamic memory option only occurs during the execution startup, (i.e., memory is never deallocated until the execution stops). The dynamic memory option is generally preferred as it allows the user to execute problems without having to create a parameters file and recompile the code with changes in the *input* file. Table 1 summarizes the memory allocation options.

**Table 1.** Memory Options

Memory Option	Fortran Compiler	Include Files	Module File	Notes
static	f77	commons parameters		<ul style="list-style-type: none"> <li>• user generated parameters</li> <li>• recompilation w/ input change</li> </ul>
dynamic	f90		allo.f	<ul style="list-style-type: none"> <li>• no recompilation w/ input change</li> <li>• greater 1GB memory on Linux</li> </ul>

Compiling the source code into an executable differs between operating systems, compilers, and memory options. This section will describe the differences between memory options, using the UNIX<sup>1</sup> as an example operating system. For the static memory option, the following files will be provided with the assembled source coding: `stomp#_[sp,bd].f`, `commons`, and `parameters`; where the # in the filename

---

<sup>1</sup> UNIX is a registered trademark of AT&T Information Systems

stomp#\_[sp,bd].f refers to the operational mode number and the solver options sp and bd refer to the conjugate gradient or banded solvers, respectively, (e.g., stomp4\_bd.f is the source code for the Water-Oil operation mode with the banded solver. To create an executable on a UNIX system, assuming the commons and parameters files were in the same directory as the source code, the user would issue the following command:

```
f77 -I . -o stomp4_bd.e stomp4_bd.f
```

For the conjugate gradient solver, the compiler must link to the splib library, and the compilation command would be:

```
f77 -I . -o stomp4_sp.e stomp4_sp.f $SPLIB_PATH/splib.a
```

where, \$SPLIB\_PATH is the path to the splib library. For the dynamic memory option, the following files will be provided with the assembled source coding:

stomp#\_[sp,bd].f, and allo.f. To create an executable on a UNIX system, assuming the commons and parameters files were in the same directory as the source code, the user would issue the following command:

```
f90 -c allo.f
f90 -c stomp4_bd.f
f90 -o stomp4_bd.e allo.o stomp4_bd.o
```

For the conjugate gradient solver, the compiler must link to the splib library, and the compilation command would be:

```
f90 -c allo.f
f90 -c stomp4_bd.f
f90 -o stomp4_bd.e allo.o stomp4_bd.o $SPLIB_PATH/splib.a
```

where, \$SPLIB\_PATH is the path to the splib library.

For the static memory option, the user is responsible for creating a parameters file. Parameters are used by the FORTRAN programming language and compilers to statically allocate memory for storage of variables. The FORTRAN 77 language is unable to allocate memory dynamically, therefore all memory storage requirements must be defined at compilation time. No execution errors will occur if the memory allocated is greater than required by the simulation, unless the memory requirements exceed the computer's capabilities. Unless necessary, the user should avoid executing simulations which require the use of virtual memory. The time required to swap data between the virtual memory storage device and the active memory typically yields poor execution speeds. The STOMP simulator requires two types of parameters (declared and computed) to be defined, prior to compilation. The user is responsible for properly assigning all of the declared parameters. Declared parameters are assigned by modifying the parameters file supplied with the STOMP simulator using a text editor (word processor) or by creating a new parameters file. The equations for the computed parameters must be included in each parameters file after the declared parameters. The parameter definitions given in this manual represent minimum acceptable values. All declared parameters, except for switch type parameters, must have minimum values of 1. Undersized parameters will generally yield execution errors, which may or may not be detected by the system. Oversized parameters are permissible, but can result in excessive memory allocation.

Executing the simulator is straight forward and only requires that the executable version of the code and an *input* file named input reside in the current directory. For restart simulations a *restart* file named restart must also reside in the current directory. Because *restart* files are created with an extension that corresponds with the generating time step, the user must rename the appropriate *restart* file to restart. For a UNIX operating system, execution is started by typing in the name of the executable file.

Execution will be indicated by the printing of a STOMP title banner and program disclaimer to the standard input/output device (e.g., screen). Two types of error messages may be generated, during an STOMP execution. The first type is a system generated message that typically indicates a memory, FORTRAN, or other system error identified by the system. The second type of error messages refer to those generated by the STOMP code, which typically refer to input, parameter, or convergence failure type messages. STOMP generated messages are divided into three categories according to severity. The most severe are ERROR messages, which abort the program execution. Undersized parameters are typical of errors which yield ERROR messages, because execution of the simulator with undersized parameters may yield gross errors, or even worse subtle errors which may pass undetected in the results. Next on the severity level are the WARNING messages, which generally warrant notice by the user that a problem with the *input* file probably exists. The least severe are NOTE messages, which are used to record events like the absence of an optional input card.

## Acknowledgements

Development of the STOMP simulator is partly supported by the Groundwater/Vadose Zone Integration Project funded through the U.S. Department of Energy's Richland Operations Office. In addition to programmatic support, the continued development of the STOMP simulator in its sequential and parallel implementations has been funded by the Laboratory Directed Research and Development (LDRD) program at the Pacific Northwest National Laboratory. In particular development of a scalable implementation has been funded through the Computational Science and Engineering Initiative and development of new operational modes for modeling carbon dioxide sequestration has been supported through the Carbon Management Initiative. Laboratory Directed Research and Development (LDRD) at Pacific Northwest National Laboratory is a productive and efficient program that develops technical capabilities for solving complex technical problems that are important to the Department of Energy and to the nation. DOE Order 413.2A sets forth the Department's LDRD policy and guidelines for DOE multiprogram laboratories and authorizes the national laboratories to allocate up to six percent of their operating budgets to fund the program.

The ten problems described in this manual were originally developed for a short course organized by Prof. S.M. Hassanizadeh at the Faculty of Civil Engineering and Geosciences, Delft University of Technology, The Netherlands on June 19 and 20, 2003.

# Table of Contents

Preface.....	v
Compilation and Execution .....	vii
Acknowledgements .....	xiii
Table of Contents .....	xv
1. Aqueous flow in saturated and unsaturated porous media .....	1
2. Aqueous flow to a well in a confined multi-layer system .....	19
3. Solute transport in a saturated porous medium .....	33
4. Salt-water intrusion and density-driven flow: Henry's Problem .....	47
5. Formation of residual NAPL saturation in unsaturated porous media .....	59
6. NAPL infiltration and redistribution in a 2D aquifer system .....	71
7. DNAPL vapor behavior in unsaturated porous media .....	87
8. Simulation of partitioning tracer transport to detect and quantify NAPLs ..	99
9. Simulation of supercritical CO <sub>2</sub> into a deep saline aquifer (CO <sub>2</sub> sequestration) .....	115
10. Simulation of countercurrent flow and heat transport with local evaporation and condensation (natural heat pipe) .....	127

# 1. Aqueous flow in saturated and unsaturated porous media

**Abstract:** *The user is introduced to the development of input files for successful simulation of flow problems. The first problem is a simple 1D vertical, single phase aqueous flow system. Through manipulation of input file parameter values and boundary conditions, various saturated and unsaturated systems are obtained.*

## 1.1 Problem Description

One dimensional, single-phase aqueous flow is simulated with the Water mode (STOMP1) of the STOMP simulator. As for all modes of the simulator, solute transport can be included. An example of solute transport for STOMP1 will be discussed in Problem 3. The input file for this basic one-dimensional problem is presented in its entirety in Section 1.3. In this section, the input for the individual cards is discussed. The simulation described flow in a 1-m long column. At the top of the column, a pressure head of 10-cm of water is imposed. The bottom outlet is set to be level with the top of the column. The boundary conditions at the top and bottom result in a pressure difference of 10 cm of water and causes vertical flow in a downward direction.

The standard information regarding the simulation is stated in the Simulation Title Card. Among other information, it contains the name of the authors and a short description of the problem.

```
#-----  
~Simulation Title Card  
#-----  
1,
```

STOMP Tutorial Problem 1,  
Mart Oostrom/Mark White,  
PNNL,  
June 03,  
15:00,  
1,  
Vertical flow in 1D column,

The Solution Control Card specifies that the execution mode option is Normal and that the Water mode (STOMP1) is used. There is one execution time period that starts at  $t = 0$  s and lasts for one day. The initial time step is 1 sec. and the maximum time step 1 day. The time step acceleration factor is 1.25, the maximum number of Newton-Raphson iterations is 8, and the convergence criterion is  $1.e-6$ . A total of 10000 time steps are allowed and all interfacial averaging occurs according to the defaults listed in Table 4.3 (page 4.28) in the User's Guide.

```
#-----  
~Solution Control Card  
#-----  
Normal,  
Water,  
1,  
0,s,1,d,1,s,1,d,1.25,8,1.e-6,  
10000,  
0,
```

The domain is divided into 10 uniform cells in the z-direction. The dimensions of each cell are  $0.1 \times 0.1 \times 0.1$  m.

```
#-----  
~Grid Card  
#-----  
Uniform Cartesian,  
1,1,10,  
0.1,m,
```

0.1,m,  
0.1,m,

A porous medium named 'sand' is assigned to all cells.

```
#-----  
~Rock/Soil Zonation Card  
#-----  
1,  
Sand,1,1,1,1,1,10,
```

The sand is assigned a particle density of 2650 kg/m<sup>3</sup> and a specific storage of 9.816e-4 1/m. Since these values and units are default inputs, input of the actual values is not necessary.

```
#-----  
~Mechanical Properties Card  
#-----  
Sand,2650,kg/m^3,0.4,0.4,9.816e-4,1/m,
```

The hydraulic conductivity in the z-direction is 10.0 m/day. Conductivities in the other two directions are not needed.

```
#-----  
~Hydraulic Properties Card  
#-----  
Sand,,,,,10.0,hc m/day,
```

The air-water retention relations have to be provided in the Saturation Function Card. If the domain remains saturated during a run, the specified values are not used. The sand has a Van Genuchten  $\alpha$  of 2.5 1/m, an n of 2.0, and a irreducible water saturation of 0.10. The Van Genuchten m value is computed according  $m = 1-1/n$ .

```
#-----
~Saturation Function Card
#-----
Sand, Van Genuchten, 2.5, 1/m, 2.0, 0.10,,
```

The Aqueous Relative Permeability Card is required for all modes. For this simulation, the Mualem pore-size distribution model is used.

```
#-----
~Aqueous Relative Permeability Card
#-----
Sand, Mualem,,
```

It is assumed that the column is initially completely saturated with a hydrostatic pressure gradient of  $-9793.52 \text{ Pa/m}$ . This gradient is the product of the liquid density and gravitational acceleration. It is further assumed that the aqueous pressure at the top of the column is atmospheric at  $101325 \text{ Pa}$ . Given the distance from the top to the lowest node is  $0.95 \text{ m}$ , the aqueous pressure at the lowest node is computed as  $101325 + 0.95 * 9793.52 = 110629 \text{ Pa}$ .

```
#-----
~Initial Conditions Card
#-----
Gas Pressure, Aqueous Pressure,
1,
Aqueous Pressure, 110629, Pa,,,,, -9793.52, 1/m, 1, 1, 1, 1, 10,
```

The pressure is described at both boundaries using a Dirichlet boundary conditions. The aqueous pressure at the top is equivalent to a head of  $10 \text{ cm}$  of water. The prescribed value at the bottom boundary indicates an outlet water level located at the top boundary. This value is computed as  $101325 + 1.0 * 9793.52 = 111119 \text{ Pa}$ .

```

#-----
~Boundary Conditions Card
#-----
2,
top,dirichlet,
1,1,1,1,10,10,1,
0,d,102304,Pa,
bottom,dirichlet,
1,1,1,1,1,1,1,
0,d,111119,Pa,

```

The Output Card indicates that Reference Node Variables will be written to the screen and the output file for all nodes in the problem after completion of every time step. The default output time units are in hr and the output length units in cm. The screen, output file, and plot file significant digits are all 6. The reference node variables are aqueous saturation, aqueous pressure, aqueous hydraulic head and the node-centered volumetric aqueous flux in the vertical direction. The reference node variables are written to the *output* file. Besides the final *plot* file, there is one additional *plot* file being generated at  $t = 12$  hr. A total of 5 plot file variables are specified. The first one is included to avoid the writing of restart files at the prescribed plot file times. The rest of the plot file variables are identical to the reference node variables.

```

#-----
~Output Options Card
#-----
10,
1,1,10,
1,1,9,
1,1,8,
1,1,7,
1,1,6,
1,1,5,
1,1,4,
1,1,3,

```

```

1,1,2,
1,1,1,
1,1,hr,cm,6,6,6,
4,
aqueous saturation,,
aqueous pressure,Pa,
aqueous hydraulic head,cm,
znc aqueous volumetric flux,cm/day,
1,
12,hr,
5,
no restart,,
aqueous saturation,,
aqueous pressure,Pa,
aqueous hydraulic head,cm,
znc aqueous volumetric flux,cm/day,

```

A total of 2 fluxes and associated integral amounts will be written to a file called *surface*.

```

#-----
~Surface Flux Card
#-----
2,
Aqueous Volumetric Flux,l/day,l,top,1,1,1,1,10,10,
Aqueous Volumetric Flux,l/day,l,bottom,1,1,1,1,1,1,

```

## 1.2 Exercises

1. Run the base STOMP1 problem by executing an appropriate executable. Look at the output on the screen for all individual nodes. Verify that one output file, two plot files and one surface file are created. View the contents of each file.
2. Decrease the porosity in the Mechanical Properties Card to 0.2. Execute the run and view the results. Change variable back to old value.

3. Reduce the hydraulic conductivity by a factor 10. Run the simulation and view the results. Change variable back to old value.
4. Increase the pressure at the top of domain to represent a 20-cm water head. Execute run and view results. Change variable back to old value.
5. Add a second porous medium named 'silt' to the input file. The silt should occupy the lower 50 cm of the flow cell. The upper half of the column should still be sand. Give the silt the same properties as the sand, except for a 1 m/day hydraulic conductivity. Additions are needed to the Rock/Soil Zonation, Mechanical Properties, Hydraulic Properties, Saturation Function, and Aqueous Relative Permeability Cards. Execute simulation and view results.
6. Reduce the hydraulic conductivity of the silt to 0.1 m/day. Run simulation and view results. Change variable back to 1 m/day.
7. Change the final time in the Solution Control Card to 10 days. Change the number of Rock/Soil Types to 1 and allow the sand to occupy the complete column. Leave all the silt-related lines in the input file because they are needed later. However, they will not be read when the number of Rock/Soil Types is set to 1. Change the boundary conditions card to the following:

```

1,
bottom,dirichlet,
1,1,1,1,1,1,3,
0,d,111119,Pa,
1,d,102304,Pa,
10,d,102304,Pa,

```

Comment on the changes in this card. Predict the effect of the imposed change. Run simulation and view results.

8. Change Van Genuchten  $\alpha$ -parameter to 1.25 1/m. Run simulation and view results. Change variable back to original value.

9. Change Van Genuchten n-parameter to 4.0. Run simulation and view results. Change variable back to original value.
10. Change the Van Genuchten saturation function of the sand to Brooks and Corey as follows:

Sand,Brooks and Corey,0.4,m,1.0,0.10,,

Run simulation and view results. Change line back to original line containing the Van Genuchten saturation function.

11. Increase Rock/Soil Types back to 2 to include the silt. Change the Van Genuchten  $\alpha$ -parameter of the silt to 1.25 1/m. Run simulation and view results. Change variable back to original value.

### 1.3 Input File

```
#-----
~Simulation Title Card
#-----
1,
STOMP Tutorial Problem 1,
Mart Oostrom/Mark White,
PNNL,
June 03,
15:00,
1,
Vertical flow in 1D column,

#-----
~Solution Control Card
#-----
Normal,
Water,
1,
0,s,1,d,1,s,1,d,1.25,8,1.e-6,
10000,
0,

#-----
~Grid Card
#-----
```

Uniform Cartesian,  
1,1,10,  
0.1,m,  
0.1,m,  
0.1,m,

#-----  
~Rock/Soil Zonation Card  
#-----  
1,  
Sand,1,1,1,1,1,10,

#-----  
~Mechanical Properties Card  
#-----  
Sand,2650,kg/m<sup>3</sup>,0.4,0.4,9.816e-4,1/m,

#-----  
~Hydraulic Properties Card  
#-----  
Sand,,,,,10.0,hc m/day,

#-----  
~Saturation Function Card  
#-----  
Sand, Van Genuchten,2.5,1/m,2.0,0.10,,

#-----  
~Aqueous Relative Permeability Card  
#-----  
Sand, Mualem,,

#-----  
~Initial Conditions Card  
#-----  
Gas Pressure, Aqueous Pressure,  
1,  
Aqueous Pressure,110629,Pa,,,,,-9793.52,1/m,1,1,1,1,1,10,

#-----  
~Boundary Conditions Card  
#-----  
2,  
top,dirichlet,  
1,1,1,1,10,10,1,  
0,d,102304,Pa,  
bottom,dirichlet,  
1,1,1,1,1,1,1,  
0,d,111119,Pa,

#-----  
~Output Options Card

#-----

10,  
1,1,10,  
1,1,9,  
1,1,8,  
1,1,7,  
1,1,6,  
1,1,5,  
1,1,4,  
1,1,3,  
1,1,2,  
1,1,1,  
1,1,hr,cm,6,6,6,  
4,  
aqueous saturation,,  
aqueous pressure,Pa,  
aqueous hydraulic head,cm,  
znc aqueous volumetric flux,cm/ day,  
1,  
12,hr,  
5,  
no restart,,  
aqueous saturation,,  
aqueous pressure,Pa,  
aqueous hydraulic head,cm,  
znc aqueous volumetric flux,cm/ day,

#-----

~Surface Flux Card

#-----

2,  
Aqueous Volumetric Flux,l/ day,l,top,1,1,1,1,10,10,  
Aqueous Volumetric Flux,l/ day,l,bottom,1,1,1,1,1,1,

## 1.4 Solutions to Selected Exercises

### Exercise 1

Initially the pressure distribution in the column is hydrostatic, resulting in no flow conditions. Suddenly 10 cm of water is imposed above the cylinder, creating a hydraulic gradient and in resulting downward flow. The system reacts quickly to the boundary condition and the steady state flow of  $q = -100$  cm/day is reached rapidly.

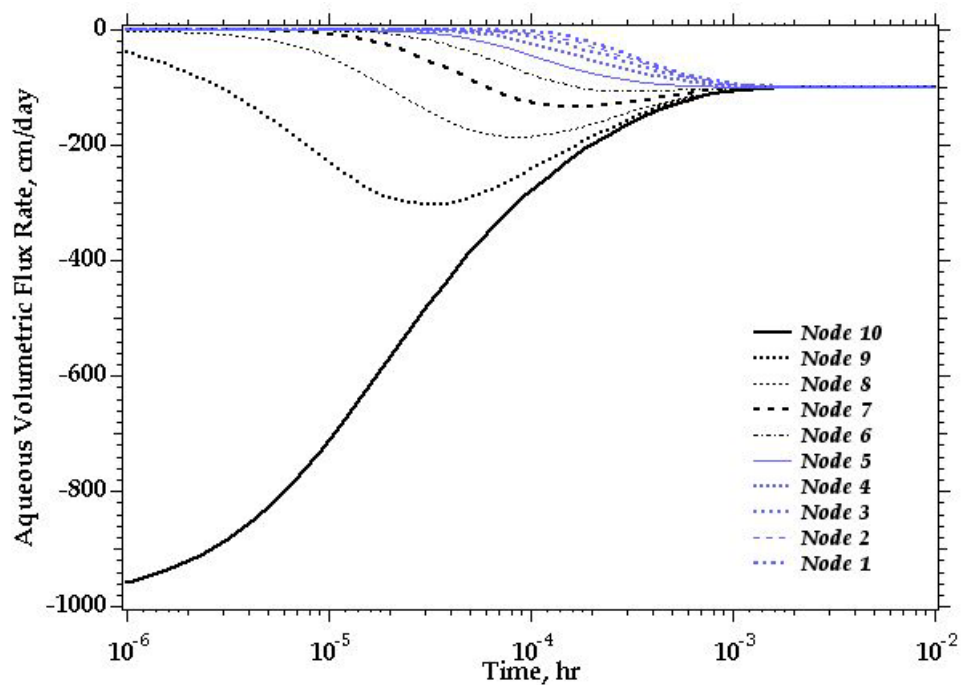


**Figure 1.1.** Flow in a saturated porous media column in response to a suddenly imposed 10-cm head (Darcy Velocity transients).

### Exercise 2

The simulator allows changes in porous media porosity independent of other hydrologic properties. For an aqueous saturated system at moderate

pressures, the Darcy velocity is independent of porosity; therefore, the transient and steady-state flow field is identical to that shown in Figure 1.1.

### Exercise 3

Darcy's Law implies that the flow rate is proportional to the hydraulic conductivity. Reducing the hydraulic conductivity by a factor of 10 reduces the flow rate and the time required to reach steady-flow conditions by a factor of 10, as seen by comparing Figures 1.2 and 1.1. The steady state flow rate is  $q = -10$  cm/day.

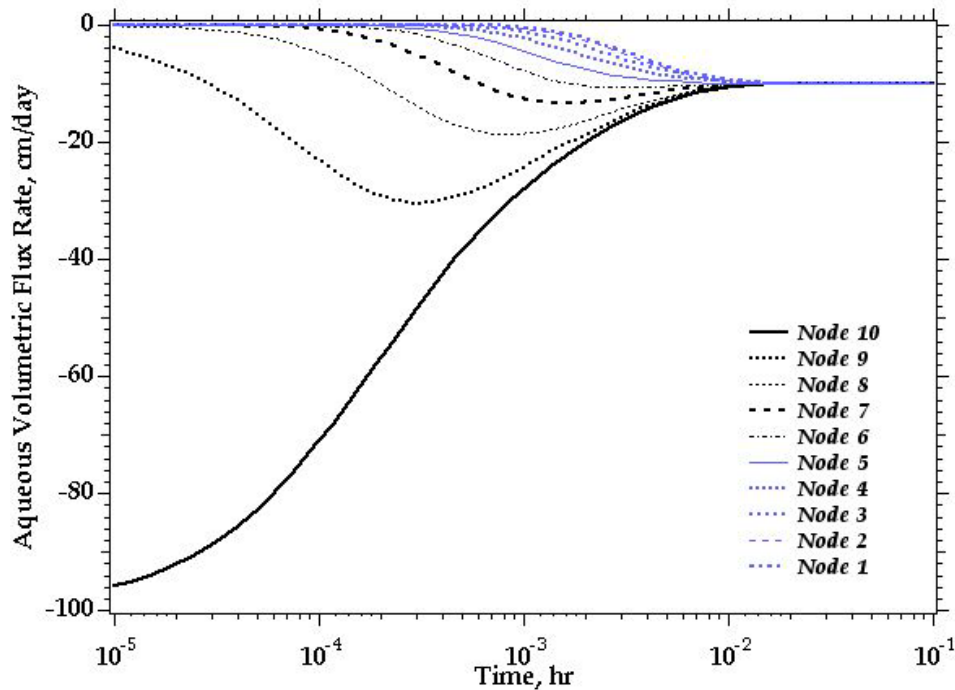


**Figure 1.2.** Flow in a saturated porous media column in response to a suddenly imposed 10-cm head (Hydraulic conductivity = 10 cm/day, Darcy velocity transients).

### Exercise 4

A 20-cm water head is imposed by increasing the boundary pressure on the column top from 102304 to 103283 Pa. Darcy's Law states that flow rate is proportional to the hydraulic gradient. Doubling the hydraulic gradient doubles

the flow rate to  $q = -200$  cm/day, but does not alter the time required to reach steady-flow conditions, as shown in Figure 1.3.

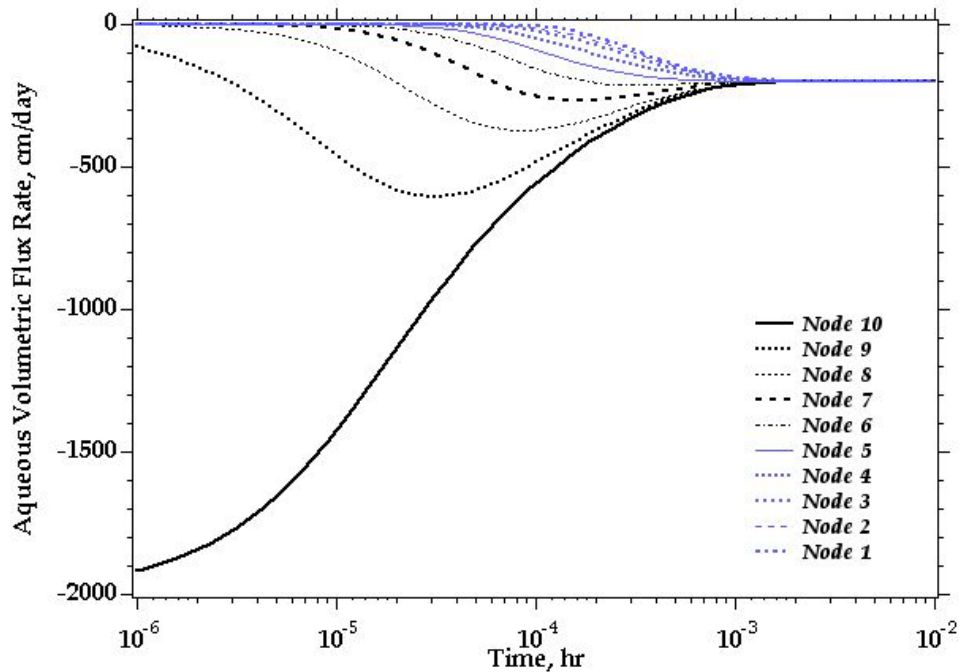


**Figure 1.3.** Flow in a saturated porous media column in response to a suddenly imposed 20-cm head (Ponded head = 20 cm, Darcy velocity transients).

### Exercise 5

The addition of the silt decreases the overall hydraulic conductivity of the system and reduces the steady state flow rate to  $-36.78$  cm/day. Continuity requires that the flow rate is the same throughout the sand and the silt. The hydraulic head in each soil is linearly distributed, but there is a slope discontinuity at the soils interface. The pressure gradient in the silt is greater than the sand, as seen in Figure 1.4

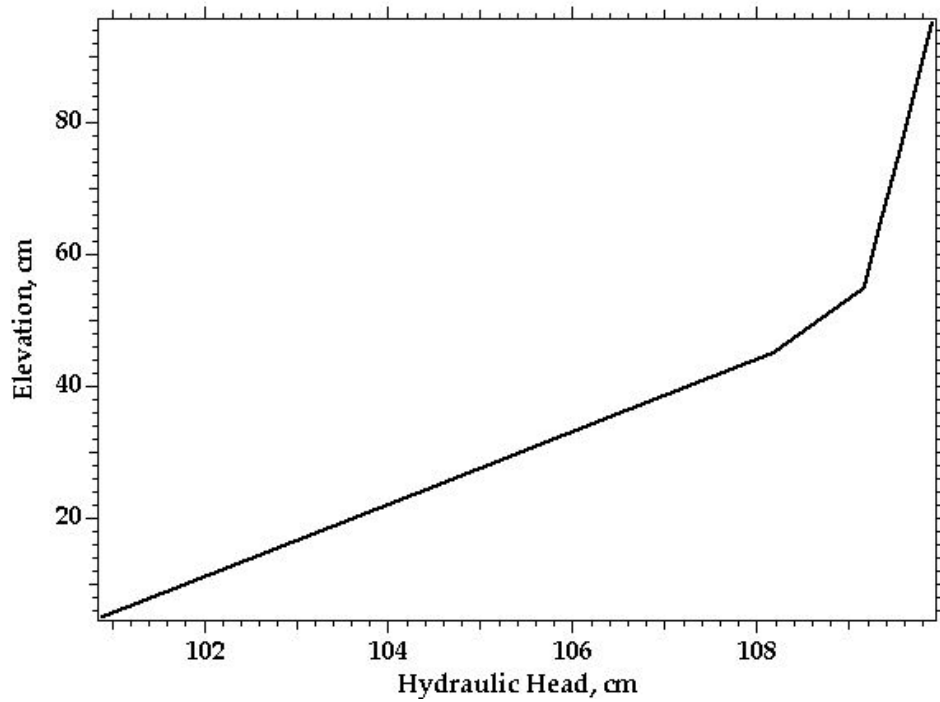


**Figure 1.4.** Flow in a saturated porous media column in response to a suddenly imposed 10-cm head (Silt hydraulic conductivity = 1.0 cm/day, Hydraulic head at 10 days).

### Exercise 6

Reducing the hydraulic conductivity of the silt to 0.1 m/day reduces the flow rate to -1.98 cm/day. The 10.0 cm of head is mostly being used to force the fluid through the silt.

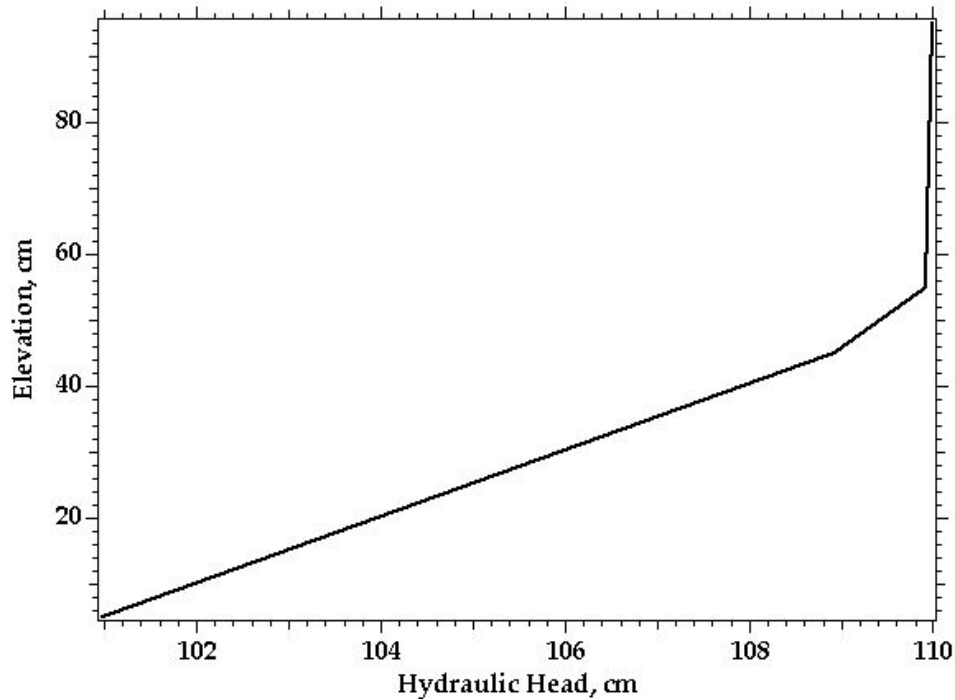


**Figure 1.5.** Flow in a saturated porous media column in response to a suddenly imposed 10-cm head (Silt hydraulic conductivity = 0.1 cm/day, Hydraulic head at 10 days).

### Exercise 7

For this exercise the upper pressure boundary condition is removed, eliminating the ponded water. The lower boundary condition is converted to transient form, representing a falling pressure over the first day, followed by a constant pressure boundary for 9 days. These boundary conditions model controlled drainage of a saturated soil column; where, the pressure head on the column bottom drops 90 cm over 1 day, followed by a constant head condition for 9 days. Initially water drains quickly from the soil column, until desaturation slows the drainage rate. The drainage rate as indicated by the Darcy velocity at each grid cell is shown in Figure 1.6. Column drainage becomes minimal after 60 hours. The final drained-column saturation profile is shown in Figure 1.7.

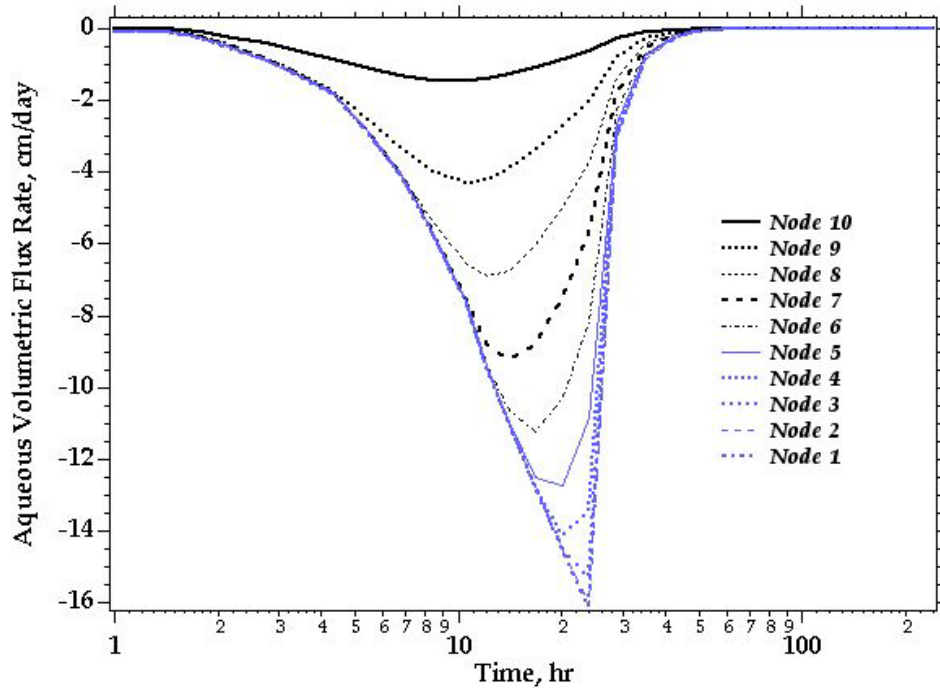


**Figure 1.6.** Flow in a saturated porous media column in response to a suddenly imposed 10-cm head (Column drainage, Darcy velocity transients).

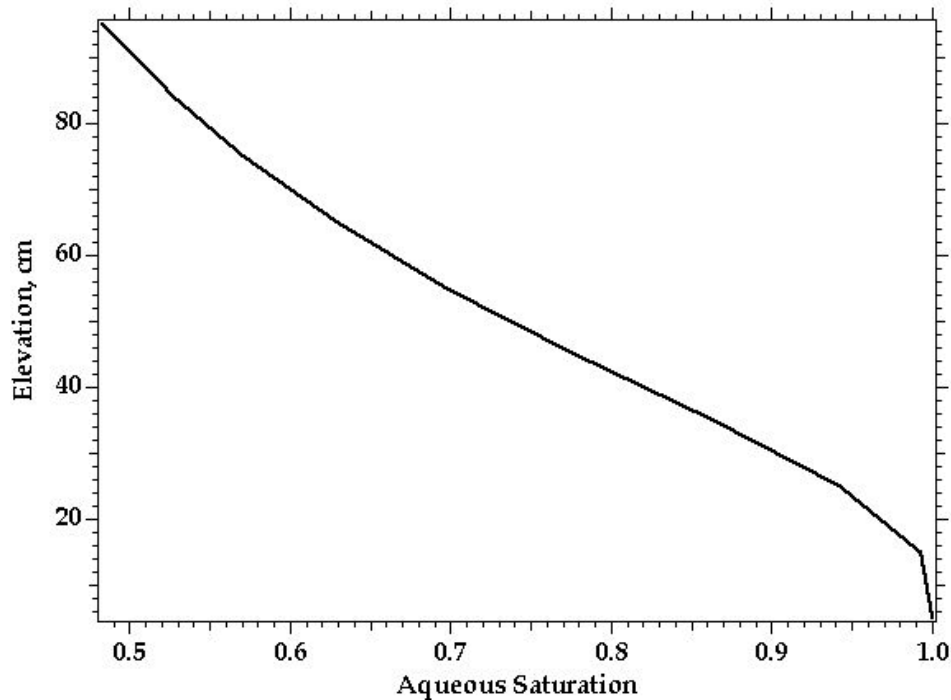


**Figure 1.7.** Flow in a saturated porous media column in response to a suddenly imposed 10-cm head (Column drainage, aqueous saturation at 10 days).

## Exercises 8, 9 & 10

This series of drainage simulations demonstrate differences in saturation profiles for variations in the soil-moisture retention characteristics. Because the simulations are carried to steady-state or near steady-state conditions the resulting saturation profiles are insensitive to the relative permeability function, as shown in Figure 1.8.

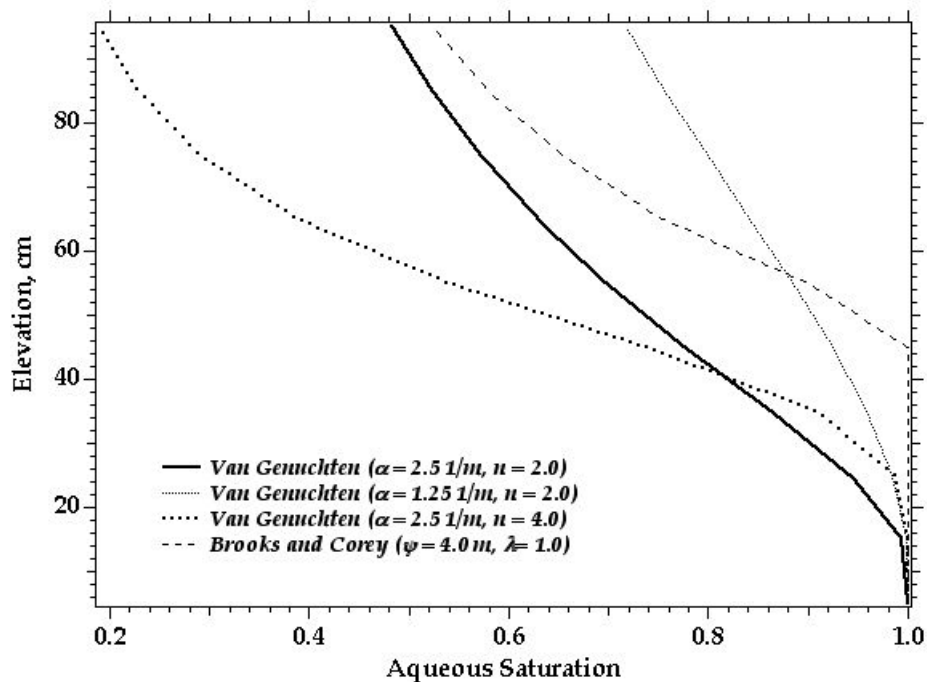


**Figure 1.8.** Flow in a saturated porous media column in response to a suddenly imposed 10-cm head (Saturation function variants, aqueous saturation at 10 days).

## Exercise 11

The lower hydraulic conductivity of the silt prevents the drainage from completing in the 10-day period, as shown in Figure 1.9. Although drainage was incomplete, the splitsoil system yields a composite drainage curve, as shown in Figure 1.10.

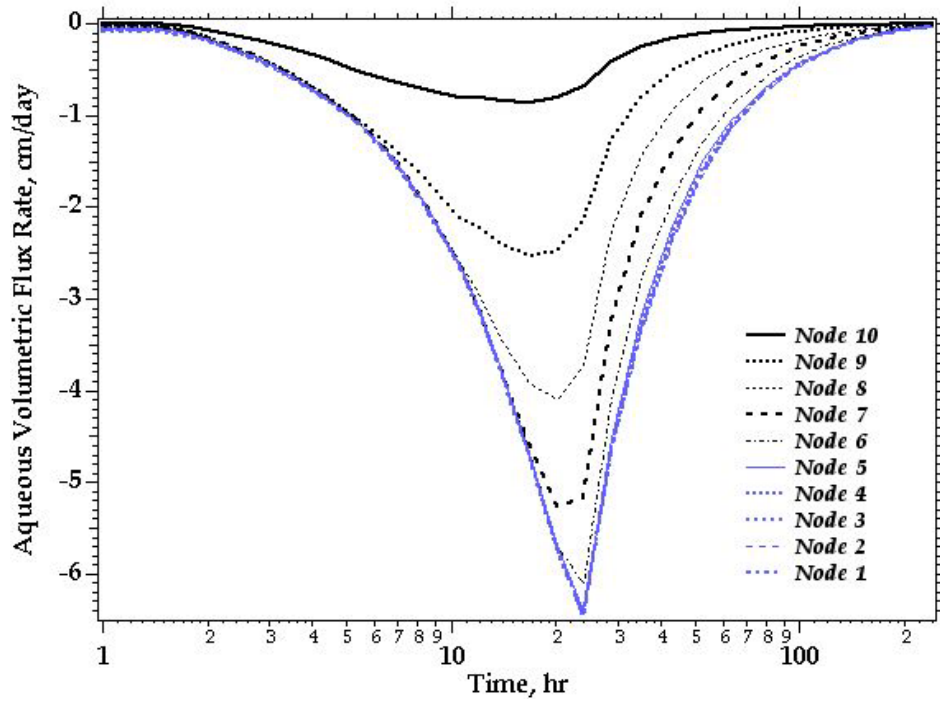


**Figure 1.9.** Flow in a saturated porous media column in response to a suddenly imposed 10-cm head (Silt layer, Darcy velocity transients).

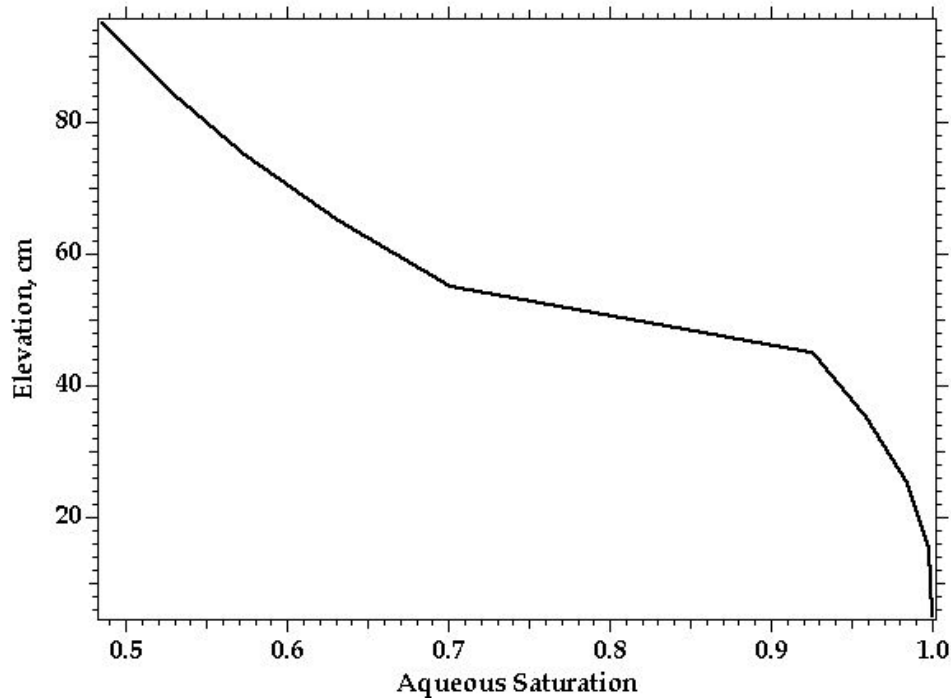


**Figure 1.10.** Flow in a saturated porous media column in response to a suddenly imposed 10-cm Head (Silt layer, aqueous saturation at 10 days).

## 2. Aqueous flow to a well in a confined multi-layer system

**Abstract:** *This test case illustrates flow to a well in a confined multi-layer system, where two identical aquifers (upper and lower) are separated by an aquitard. The well produces only from the lower aquifer, where it is fully penetrating. This problem is known in the literature as the leaky aquifer problem. The user is introduced to a two-dimensional domain, a cylindrical coordinate system, and Neumann boundary conditions.*

### 2.1 Problem Description

The input file for this problem is presented in section 2.3. Two identical aquifers, confined, horizontal, homogeneous, isotropic, 5 m thick, with hydraulic conductivity of  $2 \times 10^{-5}$  m/s and a storage coefficient of  $10^{-4}$  m<sup>-1</sup>, are separated by an aquitard. The aquitard has a thickness of 10 m, hydraulic conductivity of  $10^{-8}$  m/s, and storage coefficient of  $8 \times 10^{-4}$  m<sup>-1</sup>. Figure 2.1 shows a sketch of the conceptual model. A pumping well penetrates through to the lower aquifer. The well is only open to the full thickness of the lower aquifer, and it is sealed to the aquitard and upper aquifer. In addition, it is assumed the well is of small diameter, and there are no head losses due to well construction. The well is pumped at a constant rate  $Q$ , for  $t > 0$ . Uniform head prevails over the entire domain at  $t = 0$ , i.e. zero drawdown, and no drawdown is allowed at a radial distance of 10,000 m for  $t > 0$ .

The governing equation for transient flow in radial coordinates is

$$\frac{S_s}{K} \frac{\partial h}{\partial t} - \frac{\partial^2 h}{\partial r^2} - \frac{1}{r} \frac{\partial h}{\partial r} = 0 \quad 2.1$$

where  $S_s$ ,  $K$ ,  $h$ ,  $t$ , and  $r$ , are the specific storage coefficient, hydraulic conductivity, hydraulic head, time, and radial distance from the well, respectively.

A STOMP simulation with a duration of 100 years, an initial time-step of 36 s, and a time-step growth factor of 1.414 is shown in section 2.3. The simulation was started with uniform head initial conditions (hydrostatic pressure). Pumping at the well was implemented via a Neumann boundary condition, while a Dirichlet boundary condition was prescribed at  $r = 10,000$  m. The Boundary Conditions Card reads:

```
#-----
~Boundary Conditions Card
#-----
2,
west,neumann,
1,1,1,1,5,1,
0,d,-5.02929620e-05,m/s,
east,hydraulic gradient,
13,13,1,1,1,20,1,
0,d,684115,Pa,
```

The initial conditions of the problem were such that a uniform aqueous phase head of 60.0 m of water was imposed on the system. To obtain this initial distribution, the following Initial Conditions Card was imposed:

```
#-----
~Initial Conditions Card
#-----
Gas Pressure,Aqueous Pressure,
1,
Aqueous Pressure,684115,Pa,,,,,-9793.5,1/m,1,13,1,1,1,20,
```

Simulation of this problem requires a closely spaced grid near the well, in order to accurately represent the steep head gradient caused by pumping. Thus, a grid with progressively finer spacing close to the well is used in the radial

direction. Uniform grid spacing is used to discretize the vertical direction. The resulting grid has 13 nodes in the radial direction and 20 nodes in the vertical direction. The radial symmetry of the problem allows the use of the cylindrical grid feature of STOMP. An 18° arc is used for the third dimension. Since the third dimension is not active, this angle is arbitrary. The Grid Card for this problem is:

```
#-----
~Grid Card
#-----
Cylindrical,
13,1,20,
1.0,m,1.195,m,2.365,m,3.955,m,7.285,m,12.715,m,22.885,m,40.315,m,72.085,m,127.915,m,
504.485,m,1495.515,m,4828.485,m,10000,m,
0.,deg,18.,deg,
0,m,20@1.0,m,
```

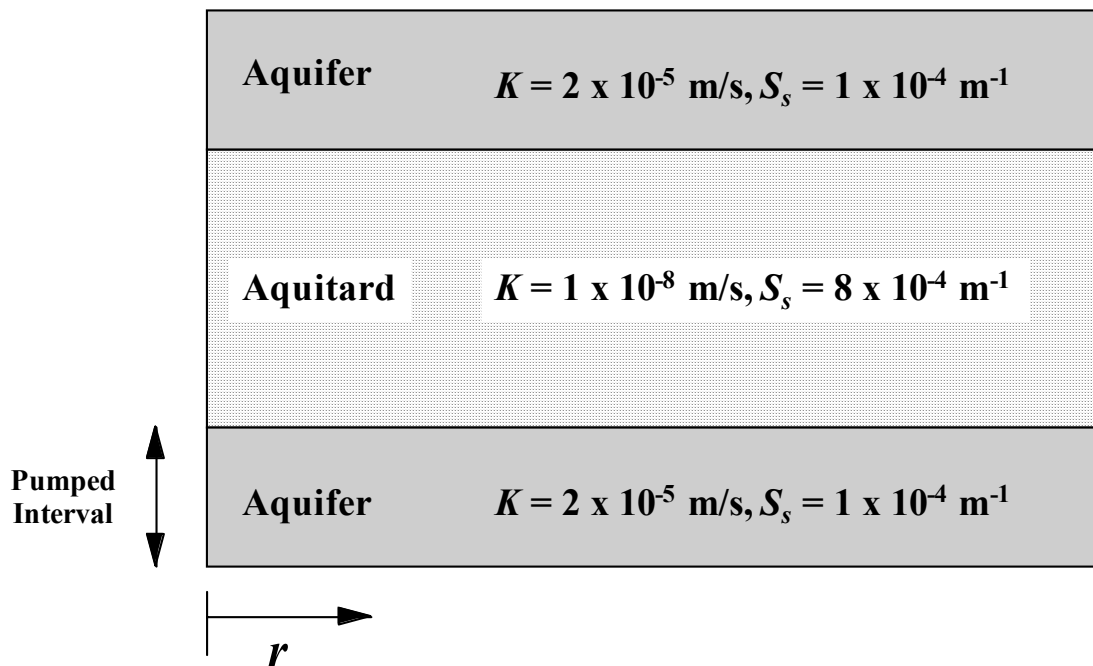
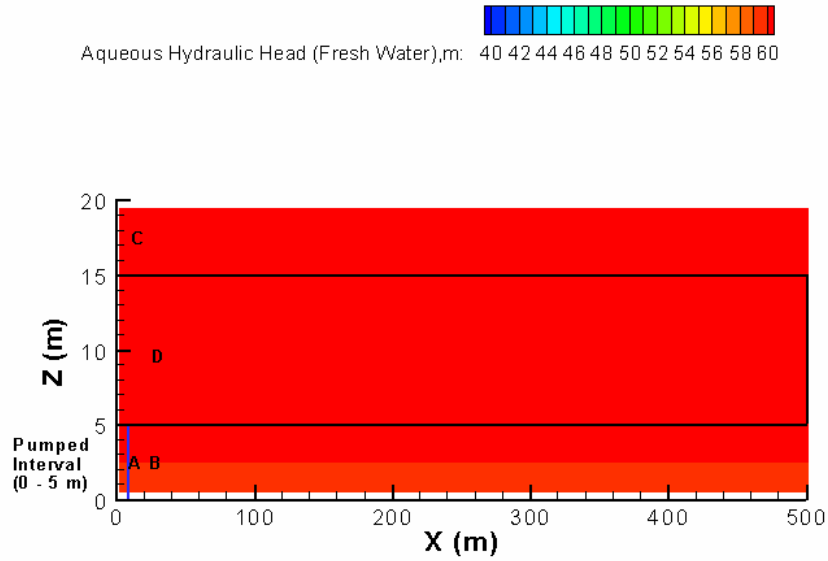


Figure 2.1 Schematic sketch of two-aquifer problem.

## 2.2 Exercises

1. Explain why the imposed initial conditions for the aqueous phase result in a uniform aqueous head of 60 m throughout the domain.
2. Compute the water production rate for the well in  $\text{m}^3/\text{day}$ .
3. Run the simulation using an appropriate executable and input file.
4. Compare the data in the *surface* file with the number computed in Exercise 2.
5. View the *output* file and plot the aqueous phase heads at the 4 reference nodes as a function of time. The location of the reference nodes are shown in Figure 2.2. Compare the produced plot with the results shown in Figure 2.3 and explain the differences.
6. Manipulate the final *plot* file to produce a plot that shows the head distribution for the whole or part of the domain. The plot has to look similar to Figure 2.4.
7. Increase the hydraulic conductivity of the aquitard to equal that of the two aquifers. Run the simulation and make a plot of the final aqueous phase head distribution. Compare the results with the plot made in Exercise 6. Reset the hydraulic conductivity value in the *input* file.
8. Impose an anisotropy ratio of 10:1 in the aquitard only. Run the simulation and make a plot of the final aqueous phase head distribution. Compare the results with the plots made in Exercises 6 and 7. Reset the hydraulic conductivity value in the *input* file.
9. Instead of using the Neumann boundary condition, create a Source Card to obtain similar results. Use the User's Guide and the first example on Page B. 185 for guidance. Run the simulation and compare the results.



**Figure 2.2** Location of specified reference nodes and initial aqueous head distribution.

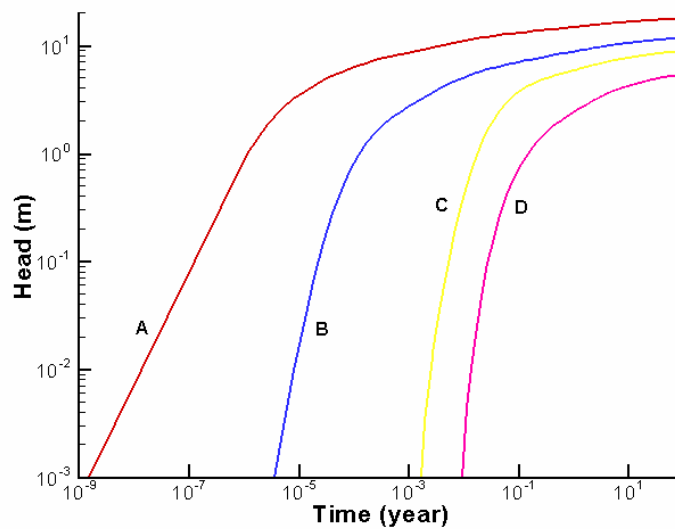


**Figure. 2.3.** Drawdown at location A, B, C, D.

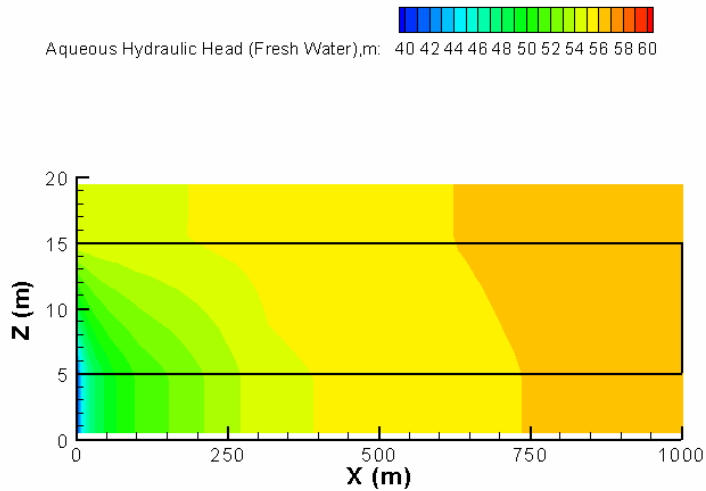


**Figure 2.4.** Final aqueous head distribution.

### 2.3 Input File

```

#-----
~Simulation Title Card
#-----
1,
STOMP Tutorial Problem 2,
Mart Ostrom/Mark White,
PNNL,
June 03,
15:00,
4,
Two aquifer problem (Segol 1994, p. 423-432),
Two aquifers (5 m thick) separated by an aquitard (10 m thick),
Pumping well is screened in the lower aquifer only,
No drawdown allowed on other end,

#-----
~Solution Control Card
#-----
Normal,
Water,
1,
0,s,100,yr,36,s,50,d,1.414,24,1.e-6,
10000,
,

```

```

#-----
~Grid Card
#-----
Cylindrical,
13,1,20,
1.0,m,1.195,m,2.365,m,3.955,m,7.285,m,12.715,m,22.885,m,40.315,m,72.085,m,127.915,m,
504.485,m,1495.515,m,4828.485,m,10000,m,
0.,deg,18.,deg,
0,m,20@1.0,m,

#-----
~Rock/Soil Zonation Card
#-----
3,
Aquifer1,1,13,1,1,16,20,
Aquitard,1,13,1,1,6,15,
Aquifer2,1,13,1,1,1,5,

#-----
~Mechanical Properties Card
#-----
Aquifer1,2650,kg/m^3,0.30,0.30,1.e-04,1/m,
Aquitard,2650,kg/m^3,0.43,0.43,8.e-04,1/m,
Aquifer2,2650,kg/m^3,0.30,0.30,1.e-04,1/m,

#-----
~Hydraulic Properties Card
#-----
Aquifer1,2.e-05,hc m/s,,,2.e-05,hc m/s,
Aquitard,1.e-08,hc m/s,,,1.e-08,hc m/s,
Aquifer2,2.e-05,hc m/s,,,2.e-05,hc m/s,

#-----
~Saturation Function Card
#-----
Aquifer1,van Genuchten,0.133,1/cm,1.88,0.268,,
Aquitard,van Genuchten,0.133,1/cm,1.88,0.268,,
Aquifer2,van Genuchten,0.133,1/cm,1.88,0.268,,

#-----
~Aqueous Relative Permeability Card
#-----
Aquifer1,Mualem,,
Aquitard,Mualem,,
Aquifer2,Mualem,,

#-----
~Initial Conditions Card
#-----
Gas Pressure,Aqueous Pressure,
1,
Aqueous Pressure,684115,Pa,,,,,-9793.5,1/m,1,13,1,1,1,20,

```

#-----  
~Boundary Conditions Card

#-----  
2,  
west,neumann,  
1,1,1,1,1,5,1,  
0,d,-5.02929620e-05,m/s,  
east,hydraulic gradient,  
13,13,1,1,1,20,1,  
0,d,684115,Pa,

#-----  
~Output Options Card

#-----  
4,  
3,1,3,  
7,1,3,  
3,1,18,  
7,1,10,  
1,1,yr,m,deg,6,6,6,  
3,  
aqueous saturation,,  
aqueous pressure,Pa,  
aqueous hydraulic head,m,  
5,  
0.5,d,  
1,d,  
1,yr,  
10,yr,  
50,yr,  
8,  
no restart,,  
aqueous hydraulic head,m,  
aqueous pressure,Pa,  
aqueous saturation,,  
XNC aqueous volumetric flux,m/hr,  
ZNC aqueous volumetric flux,m/hr,  
X aqueous volumetric flux,m/hr,  
Z aqueous volumetric flux,m/hr,

#-----  
~Surface Flux Card

#-----  
2,  
aqueous volumetric flux,m<sup>3</sup>/day,m<sup>3</sup>,west,1,1,1,1,1,5,  
aqueous volumetric flux,m<sup>3</sup>/day,m<sup>3</sup>,east,13,13,1,1,1,20,

## 2.4 Solutions to Selected Exercises

### Exercise 1

Initial conditions for aqueous pressure for this problem are specified by specifying a base pressure and pressure gradient on the *Initial Conditions Card*. The vertical pressure gradient of -9793.52 is equivalent to uniform total head conditions (i.e., hydrostatic conditions) for an aqueous density of 998.32 kg/m<sup>3</sup> (i.e., pure water at 20 C). Using the domain bottom as the reference point for computing total head, the base pressure of 684115 Pa is computed as

$$[(60-0.5) m * 9793.52 Pa/m] + 101325.0 Pa = 684115 Pa$$

where, 0.5 m is the distance from the domain bottom to the base node elevation, and 101325 Pa is the default gas pressure.

### Exercise 2

The water production rate is 136.5 m<sup>3</sup>/day (1502.6 gal/hr), calculated using the specified boundary flux of 5.0292962e-05 m/s and the well geometry, as

$$5.0292962 \times 10^{-5} m/s * 2\pi * 1 m * 5 m = 1.58 \times 10^{-3} m^3/s = 136.5 m^3/day$$

where, the screened interval area equals 31.416 m<sup>2</sup>.

### Exercises 3 and 4

The surface flux file reports a steady-flow flow rate into the well of 6.8256 m<sup>3</sup>/day, which can be converted to a well production rate, as

$$6.8256 \text{ m}^3/\text{day} * 18.0^\circ/360.0^\circ = 136.5 \text{ m}^3/\text{day}$$

which agrees with the prescribed water production rate for the well.

### Exercise 5

The plot of hydraulic head at each location as a function of time, as shown in Figure 2.4, shows decreasing head with time. This plot differs from the results shown in Figure 2.3, as it shows hydraulic head drawdown, calculated as the initial hydraulic head (i.e., 60 m) less hydraulic head.

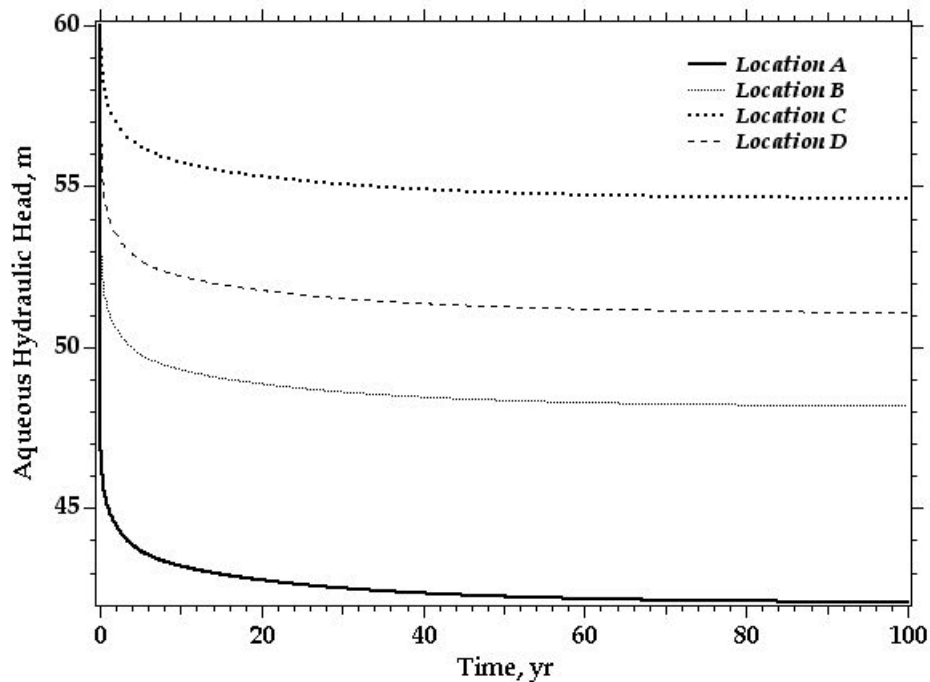


**Figure 2.4.** Hydraulic head in response to pumping

### Exercise 6

As requested in the *input* file, the *plot* file contains data for the aqueous hydraulic head (m) for all nodes in the domain. This file can be converted to a format for the plotting packages Tecplot and Surfer using the *plotTo.pl* Perl script. For Tecplot the command would appear as:

```
plotTo.pl Tecplot plot.dat plot.766
```

where, the file *plot.dat* is the Tecplot formatted file. The resulting Tecplot contour plot of hydraulic head appears as shown in Figure 2.5.

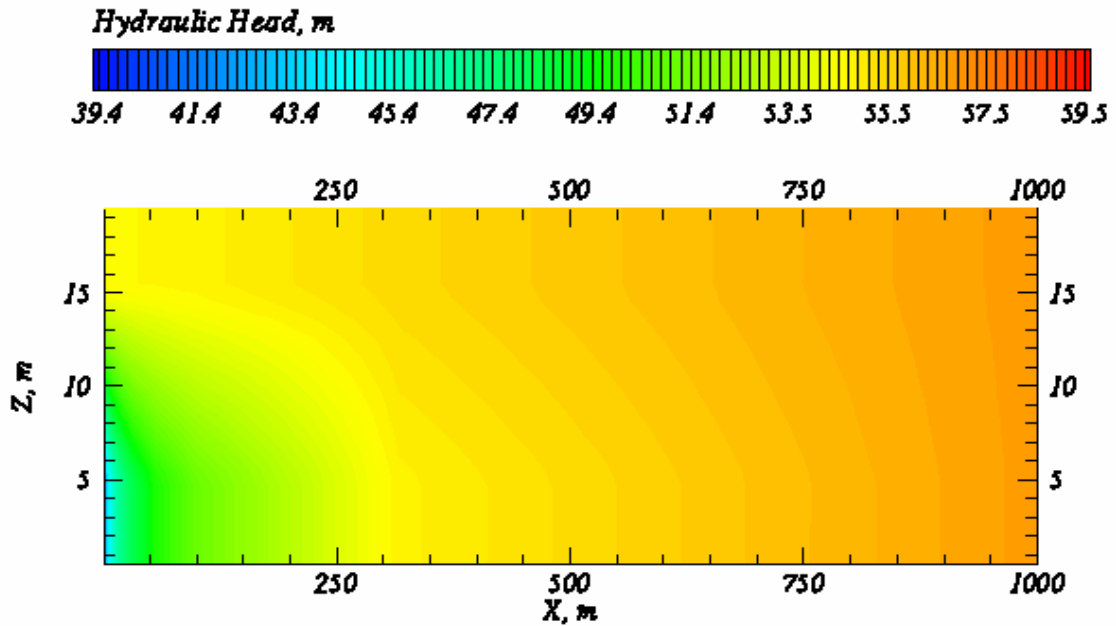
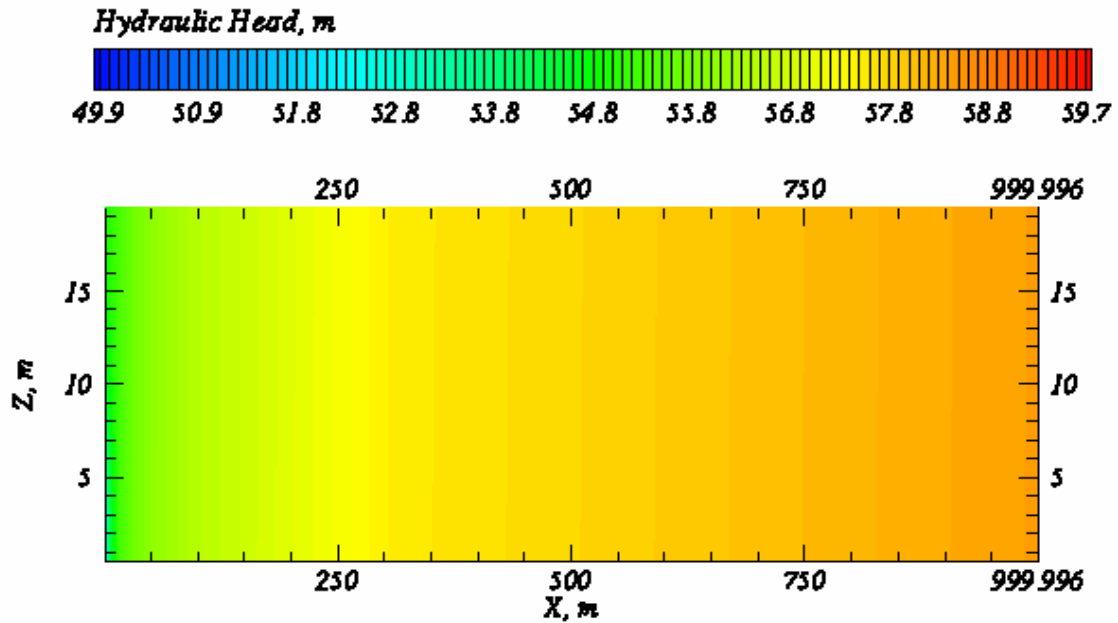


Figure 2.5. Contours of hydraulic head in response to pumping

### Exercise 7

Increasing the hydraulic conductivity of the aquitard to the value of the aquifers reduces the overall flow resistance and homogenizes the aquifer. The lower resistance reduces the gradient in hydraulic head and the homogenization flattens the head contours, as shown in Figure 2.6.



**Figure 2.6.** Contours of hydraulic head in response to pumping (homogeneous aquifer).

### Exercise 8

Increasing the horizontal hydraulic conductivity of the aquitard by a factor of 10, reduces the horizontal flow resistance of the aquitard, but not enough to significantly change the response in hydraulic head, as shown in Figure 2.7.

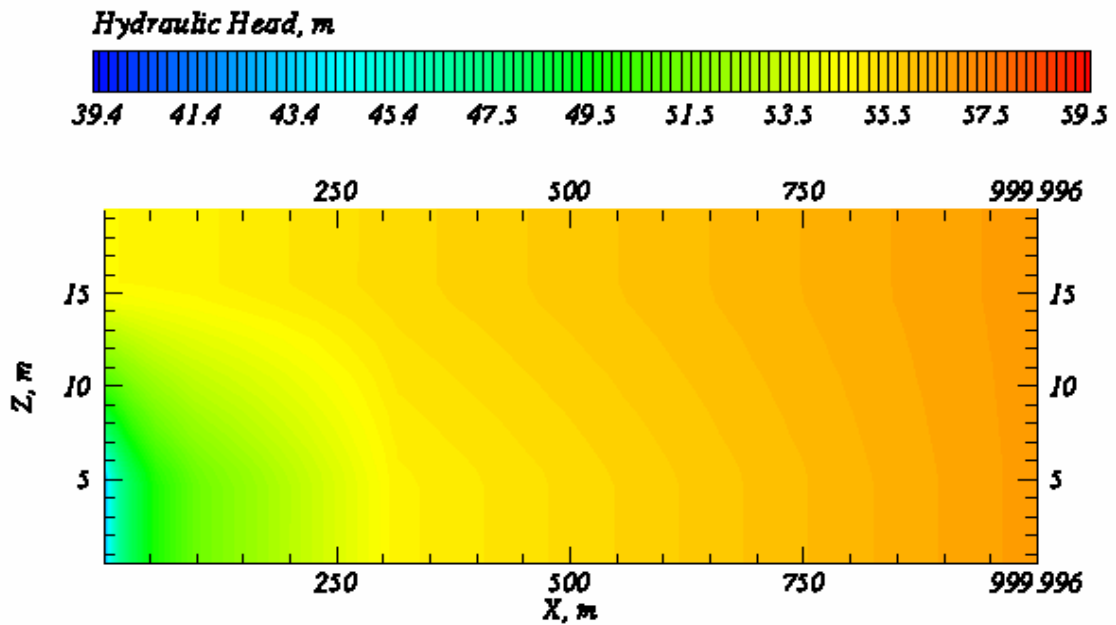


**Figure 2.7.** Contours of hydraulic head in response to pumping (10:1 anisotropy ratio).

### Exercise 9

Many boundary conditions can be imposed as sources, giving the user considerable flexibility in developing *input* files. The following changes to the *Boundary Condition Card* and *Source Card* will yield nearly identical results reported in Exercise 6.

*~Boundary Conditions Card*

1,  
*east,hydraulic gradient,*  
 13,13,1,1,1,20,1,  
 0,d,684115,Pa,

*~Source Card*

1,  
*Aqueous Volumetric,1,1,1,1,1,5,1,*  
 0,d,-1.58e-05,m<sup>3</sup>/s,

### 3. Solute transport in a saturated porous medium

**Abstract:** *This test case illustrates transport of a solute within a steady state, uniform flow field. An initial square pulse of solute mass is instantaneously introduced into the flow field and transported downstream. The pulse undergoes advection, dispersion and molecular diffusion. The user is introduced to solute transport input file cards, standard and higher order transport options, and the importance of controlling Peclet and Courant numbers.*

#### 3.1 Problem Description

The input file for this problem is presented in section 3.3. The governing equation for advection-dispersion in a saturated porous media is

$$\frac{\partial}{\partial t}(RC) + \frac{\partial}{\partial x_j}(q_j C) - \frac{\partial}{\partial x_i} \left( D_{ij} \frac{\partial C}{\partial x_j} \right) = Q \quad \text{for } i,j = 1,2,3 \quad 3.1$$

where  $C$  is the time ( $t$ ) and space dependent ( $x$ ) solute concentration,  $R$  is the retardation factor,  $q$  is the Darcy velocity,  $D$  is the dispersion tensor, and  $Q$  is a sink/source term. In the STOMP simulator, the solute transport equation is solved after the flow field has been computed.

The accuracy of the results obtained from numerical simulation of transport is usually affected by the values of the grid Courant,  $Cr$ , and Peclet,  $Pe$ , numbers. The Courant number controls the oscillations in the solution arising from the discretization of time derivative, and is defined as

$$Cr = \frac{v\Delta t}{\Delta x} \quad 3.2$$

where  $\Delta t$  is the size of the time-step and  $\Delta x$  is the grid spacing.

The Peclet number is a measure of the ratio between the advective and the dispersive components of transport, and controls the oscillations in the solution due to the spatial discretization of the domain. The Peclet number is defined as

$$Pe = \frac{v\Delta x}{D} \quad 3.3$$

The initial value problem discussed here was recommended by the Convection-Diffusion Forum during the VII International Conference on Computational Methods in Water Resources (Baptista et al., 1988), with the purpose of having a common comparison. The following numerical values for the problem dimensions and parameters are those suggested by the Forum. The one-dimensional domain extends from  $0 < x < 20000$  m, the pore water velocity is 0.5 m/day, and the initial pulse is located at  $1400 \text{ m} < x < 2600$  m. Grid spacing is specified as 200 m, time-steps are 96 days, and total simulation time is 9600 days. An effective dispersion coefficient of 50 m<sup>2</sup>/day is used by specifying a dispersivity of 100 m. When solute transport is considered the Solute/Fluid Interaction Card and the Solute/Porous Medium Interaction Card have to be included. For this problem, the cards are

```
#-----
~Solute/Fluid Interaction Card
#-----
1,
Tracer, conventional, 0.0, m^2/d, continuous, 1.0e+12, d,
0,
```

```

#-----
~Solute/Porous Media Interaction Card
#-----
Porous Medium,100,m,,m,
Tracer,0.,,

```

Initial and boundary conditions for the solute have to be provided in the Initial Conditions and Boundary Conditions Card, respectively.

An analytical solution given by van Genuchten and Alves (1982) is available for comparison with the simulated results. The analytical solution is modified to account for a translation of the initial pulse in the positive  $x$ -axis direction. Assuming the solute to be conservative, and given the initial and boundary conditions

$$\begin{aligned}
C(x,0) &= 0 & \text{for } 0 \leq x \leq 1400 \text{ and } 2600 \leq x & & 3.4 \\
C(x,0) &= 1 & \text{for } 1400 \leq x \leq 2600 & & \\
C(0,t) &= 0 & \text{for } t > 0 & & \\
\frac{\partial C}{\partial x}(\infty,t) &= 0 & \text{for } t > 0 & &
\end{aligned}$$

the solution to the advection-dispersion equation is

$$\begin{aligned}
C(x,t) &= \frac{1}{2} \left\{ \operatorname{erfc} \left[ \frac{x-x_2-vt}{(4Dt)^{1/2}} \right] - \operatorname{erfc} \left[ \frac{x-x_1-vt}{(4Dt)^{1/2}} \right] \right\} \\
&+ \frac{1}{2} \exp\left(\frac{vx}{D}\right) \left\{ \operatorname{erfc} \left[ \frac{x-x_2-vt}{(4Dt)^{1/2}} \right] - \operatorname{erfc} \left[ \frac{x-x_1-vt}{(4Dt)^{1/2}} \right] \right\} & 3.5
\end{aligned}$$

*References*

Baptista A, P Gresho, and E Adams. 1988. Reference Problems for the Convection-Diffusion Forum. VII International Conference on Computational Methods in Water Resources, Cambridge, Massachusetts.

van Genuchten MT, and WJ Alves. 1982. Analytical Solutions of the One-Dimensional Convective-Dispersive Solute Transport Equation. ARS Technical Bulletin 1661, USDA.

### 3.2 Exercises

1. Based on the initial location of the solute, the flow rate and the duration of the simulation, determine the location of the peak concentration at the end of the simulation.
2. Compute the Peclet and Courant numbers of the simulation described in the *input* file shown in section 3.3.
3. Show through a calculation why the imposed pressure of 121225 Pa at node 1,1,1,1,1,1, in the Initial Conditions Card is consistent with the -1.0 Pa/m gradient and the Dirichlet boundary condition of 101325 Pa at the east side of the domain.
4. Run the simulation and post process the *plot* file. Make a graph of the solute concentration vs. distance.
5. Repeat the simulation for Peclet numbers of 20 and 50 by manipulating the horizontal dispersivity. Make graphs of the spatial solute concentration distribution.
6. Repeat the simulation for Courant numbers of 0.12 and 0.015 by manipulating the time stepping. Make graphs of the spatial solute concentration distribution.
7. Repeat the simulation for  $Pe = 20$  and  $Cr = 0.24$  using standard Patankar transport. Compare the results with the results obtained with

TVD transport. Reset the time step and dispersivity values after completion of the simulation.

8. The retardation coefficient,  $R$ , for linear retardation is given as

$$R = 1 + \frac{K_d(1 - n_D)\rho_s}{s_l n_D}$$
 where  $K_d$  is the partitioning coefficient ( $L^3/M$ ),  $n_d$  the

diffusive porosity,  $s_l$  the aqueous saturation and  $\rho_s$  the particle density. In the Solute/Porous Media Interaction Card, enter a value for  $K_d$  such that  $R$  equals 2. Run the simulation and compare the results with the base simulation.

9. Edit the Initial Conditions and Boundary Conditions Cards to reflect the following: The Peclet number is 20. Initially, there is no solute present in the entire domain. From  $t = 0$  to  $t = 2400$  days, solute is injected with the aqueous phase from the west boundary using a Aqueous Concentration boundary condition for the solute with a concentration of  $1.0 \text{ l/m}^3$ . From  $t = 2400$  to  $t = 9600$  days, the Aqueous Concentration is  $0.0 \text{ l/m}^3$ . Add a plot time at  $t = 2400$  days. Make graphs of the solute distribution at 2400 and 9600 days.

### 3.3 Input File

```
#-----  
~Simulation Title Card  
#-----  
1,  
STOMP Tutorial Problem 3,  
Mart Ostrom/Mark White,  
PNNL,  
June 03,  
15:00,  
2,  
Classic test problem for 1D Transport problem,  
Water mode (STOMP1) with transport,  
  
#-----  
~Solution Control Card
```

#-----

Normal,  
Water w/TVD transport,  
1,  
0,s,9600,d,96,d,96,d,1.0,8,1.e-6,  
10000,  
,

#-----

~Grid Card

#-----

Uniform Cartesian,  
100,1,1,  
200,m,  
1,m,  
1,m,

#-----

~Rock/Soil Zonation Card

#-----

1,  
Porous Medium,1,100,1,1,1,1,

#-----

~Mechanical Properties Card

#-----

Porous Medium,,,0.5,0.5,,,Millington and Quirk,

#-----

~Hydraulic Properties Card

#-----

Porous Medium,2448.3743,hc m/day,,,,,

#-----

~Saturation Function Card

#-----

Porous Medium,van Genuchten,0.015,1/cm,2.0,0.05,,

#-----

~Aqueous Relative Permeability Card

#-----

Porous Medium,Mualem,,

#-----

~Solute/Fluid Interaction Card

#-----

1,  
Tracer,conventional,0.0,m<sup>2</sup>/d,continuous,1.0e+12,d,  
0,

#-----  
~Solute/Porous Media Interaction Card

#-----  
Porous Medium,100,m,,m,  
Tracer,0,,

#-----  
~Initial Conditions Card

#-----  
Gas Pressure,Aqueous Pressure,  
2,  
Aqueous Pressure,121225,Pa,-1.0,1/m,,,,,1,100,1,1,1,1,  
Solute Aqueous Volumetric,Tracer,1.0,1/m^3,,,,,8,13,1,1,1,1,

#-----  
~Boundary Conditions Card

#-----  
2,  
west,neumann,aqueous conc,  
1,1,1,1,1,1,1,  
0,s,0.25,m/d,0.0,1/m^3,  
east,dirichlet,outflow,  
100,100,1,1,1,1,1,  
0,s,101325,Pa,,

#-----  
~Output Options Card

#-----  
7,  
8,1,1,  
13,1,1,  
33,1,1,  
34,1,1,  
35,1,1,  
36,1,1,  
37,1,1,  
1,1,d,m,6,6,6,  
3,  
solute aqueous concentration,tracer,1/m^3,  
x aqueous volumetric flux,m/day,  
aqueous courant number,,  
0,  
3,  
no restart,,  
solute aqueous concentration,tracer,1/m^3,  
x aqueous volumetric flux,m/day,

### 3.4 Solutions to Selected Exercises

#### Exercise 1

This problem considers an unretarded (unsorbed) solute, therefore, the migration of the center of mass is governed by the pore-water velocity. Initially, the center of mass of the solute is located at an x-direction distance of 2,000 m. A horizontal Darcy velocity of 0.25 m/d with a porosity of 0.5 converts to a pore-water velocity of 0.50 m/d; therefore, after a period of 9,600 d the solute center of mass will have moved 4,800 m and be located at an x-direction distance of 6,800 m.

#### Exercise 2

The Peclet number is a function of the pore-water velocity, grid dimension, and effective diffusion-dispersion coefficient, according to the following expression

$$Pe = v \delta x / D_e = (0.5 \text{ m/day})(200 \text{ m}) / (50 \text{ m}^2/\text{day}) = 2.0$$

where,  $v$  is the pore-water velocity (m/d),  $\delta x$  is the grid spacing (m), and  $D_e$  is the effective diffusion-dispersion coefficient ( $\text{m}^2/\text{day}$ ). The Courant number is a function of the pore-water velocity, time step, and grid dimension, according to the following expression

$$Cr = v \delta t / \delta x = (0.5 \text{ m/d})(96 \text{ d}) / (200 \text{ m}) = 0.24$$

where,  $v$  is the pore-water velocity (m/d),  $\delta t$  is the time step (d), and  $\delta x$  is the grid spacing (m).

#### Exercise 3

The pressure at the east boundary surface is specified as atmospheric (101325 Pa). The centroid of node (1,1,1) is located 99.5 node dimensions away from the east boundary surface. Therefore, with a uniform x-direction grid spacing of 200 m, the initial pressure at node (1,1,1) is calculated as

$$(99.5 \text{ nodes})(200 \text{ m/nodes})(1 \text{ Pa/m}) + 101325 \text{ Pa} = 121225 \text{ Pa}$$

#### Exercise 4

As requested in the *input* file, the *plot* file contains data for the solute aqueous concentration for all nodes in the domain. This file can be converted to a format for plotting packages Tecplot and Surfer using the *plotTo.pl* Perl script. For Tecplot the command would appear as

```
plotTo.pl Tecplot plot.dat plot.100
```

where, the file *plot.dat* is the Tecplot formatted file. The resulting Tecplot contour plot of hydraulic head appears as shown in Figure 3.1.

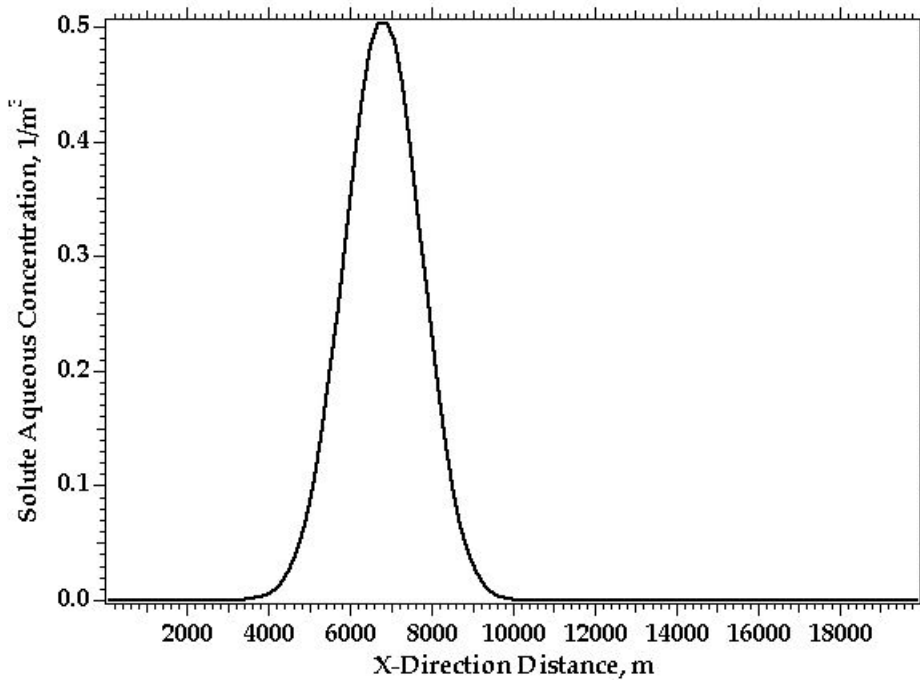


**Figure 3.1.** Solute aqueous concentration profile at 9600 days

## Exercise 5

Peclet numbers of 20 and 50 are created by using a solute longitudinal dispersivity of 10 and 4 m, respectively on the *Solute/Porous Media Interaction Card*. The results for all Peclet numbers are shown in Figure 3.2. The higher Peclet numbers yield lower solute dispersion.

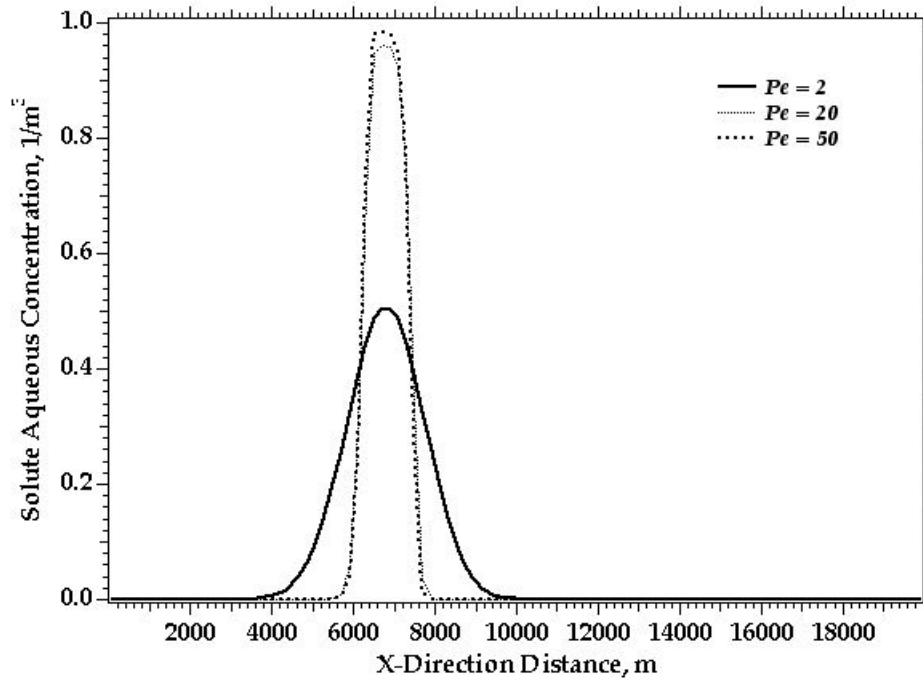


**Figure 3.2.** Solute aqueous concentration profile at 9600 days ( $Pe = 2, 20, 50$ )

## Exercise 6

Courant numbers of 0.12 and 0.015 are created by using a time steps of 48 and 6 d, respectively on the *Solution Control Card*. The results for all Courant numbers are shown in Figure 3.3; where, the lower Courant numbers yield slightly higher solute dispersion.

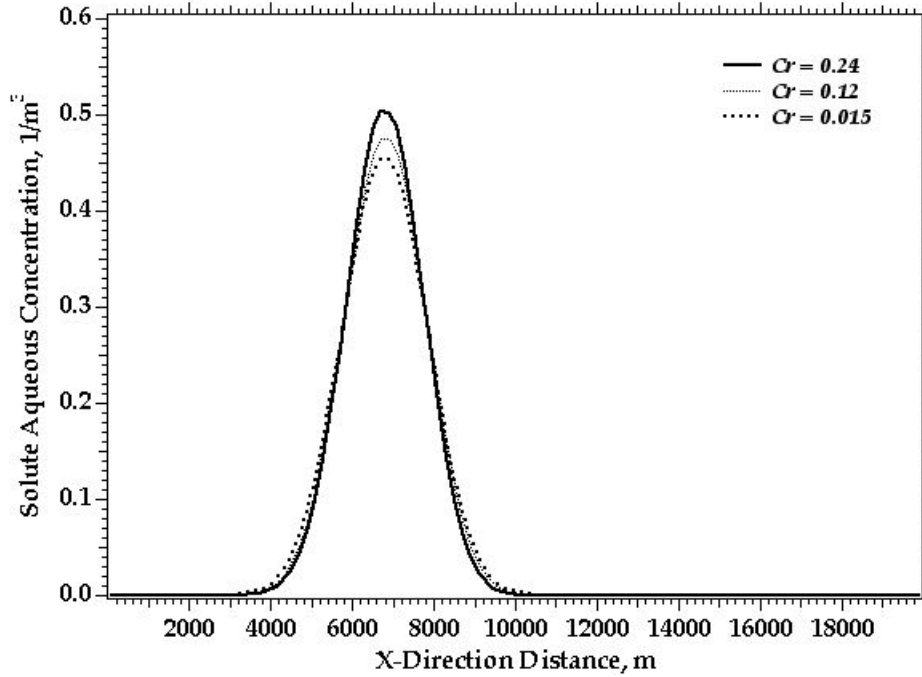


**Figure 3.3.** Solute aqueous concentration profile at 9600 days ( $Cr = 0.24, 0.12, 0.015$ ).

## Exercise 7

Whereas the Patankar transport scheme is generally more computationally efficient, it can often generate unacceptable amounts of numerical dispersion. The TVD (Total Variational Diminishing) transport method was designed to reduce the amount of numerical dispersion, but it is more computationally demanding and also requires a smaller time step. For problems with large Peclet numbers the TVD scheme must be used, as shown in Figure 3.4. A rule of thumb is to use  $Cr < .8$  for Patankar and  $Cr < .2$  for TVD.

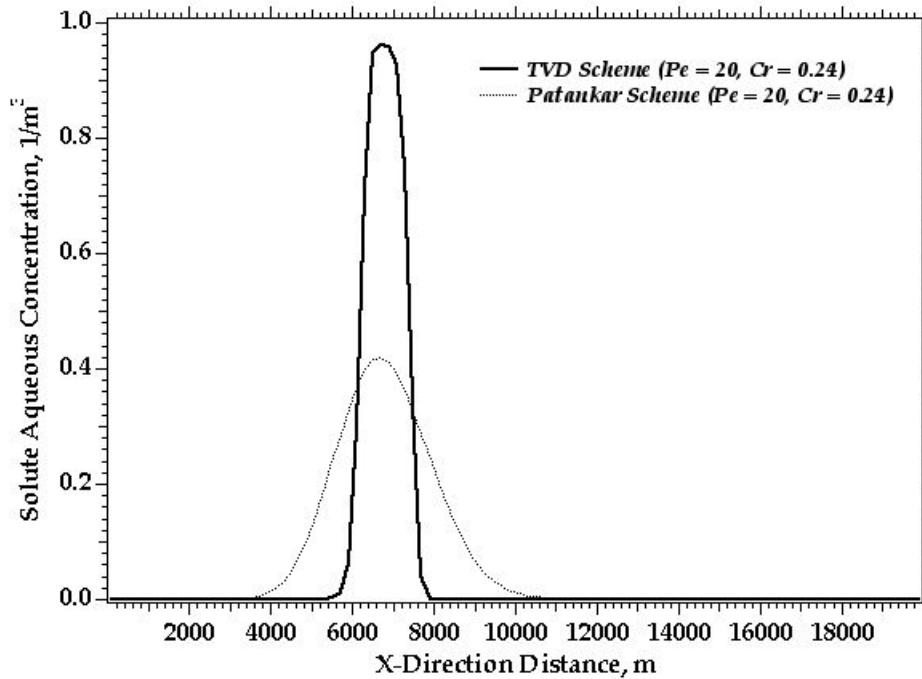


**Figure 3.4.** Solute aqueous concentration profile at 9600 days (TVD and Patankar Schemes).

### Exercise 8

A partition coefficient of  $3.7736 \times 10^{-4} \text{ m}^3/\text{kg}$  produces a retardation coefficient of 2.0. The base simulation used a partition coefficient of  $0 \text{ m}^3/\text{kg}$ , or a retardation coefficient of 1.0. As shown in Figure 3.5, doubling the retardation coefficient acts to retard the migration of the solute center of mass by a factor of 2.

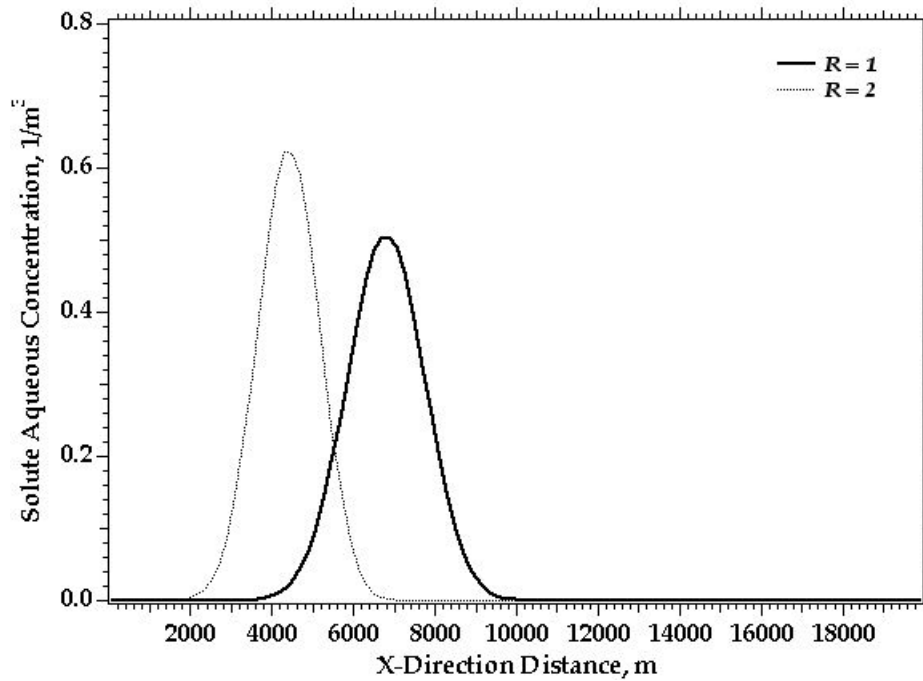


**Figure 3.5.** Solute aqueous concentration profile at 9600 days (Retardation Coefficients = 1.0, 2.0).

## Exercise 9

The base simulation specified a slug of solute within the domain to investigate solute transport. This exercise uses a boundary condition to specify solute influent. The effect of dispersion on the influent solute slug is shown in Figure 3.6.

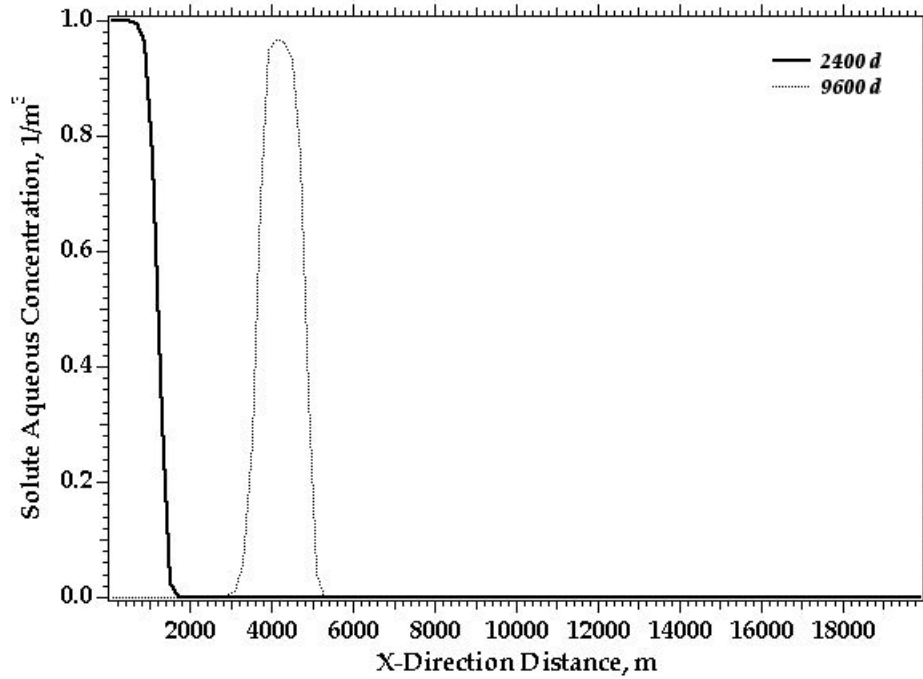


**Figure 3.6.** Solute aqueous concentration profile (2400 and 9600 days).

## 4. Salt-water intrusion and density-driven flow: Henry's Problem

**Abstract:** *Henry's problem addresses the steady-state solution of a diffused salt-water wedge within a confined aquifer balanced against a flowing fresh-water field. Fresh water enters the confined aquifer at a constant rate from a hypothetical inland boundary and discharges into a hypothetical coastal boundary. Salt water from the coastal boundary advances and mixes with the discharging fresh water. The user is introduced to modifications to the input file that allow appropriate transport of density and viscosity altering dissolved components. The Water-Salt mode (STOMP11) is used for this application.*

### 4.1 Problem Description

This application was chosen to demonstrate the coupled flow and salt transport capabilities of the STOMP simulator. Although these capabilities have been specifically written for salt-water brines, other solutes could be considered by changing the algorithms for computing the brine properties (e.g., density and viscosity).

Henry's problem addresses the steady-state solution of a diffused salt-water wedge within a confined aquifer balanced against a flowing fresh-water field. Fresh water enters the confined aquifer at a constant rate from a hypothetical inland boundary and discharges into a hypothetical coastal boundary. Salt water from the costal boundary advances and mixes with the discharging fresh water. Because both the inland and costal boundary conditions are invariant a steady-state condition is reached, which balances the intruding sea-water wedge against the fresh-water flow field. Henry (1964a; 1964b) published an analytical solution to this problem in a U.S. Geological Survey

publication, and the problem has henceforth become a classical test for numerical simulators with solute dependent density capabilities. Unfortunately, no other numerical method has been able to successfully duplicate Henry's solution, which accordingly resulted in some doubt about its validity. Ségol (1994) revisited Henry's solution and noted several discrepancies in the published solution. Ségol's revisited solution to this classical problem shows close agreement with the numerical solution of Voss and Souza (1987).

Henry's problem involves a two-dimensional rectangular domain with no flow conditions along the top and bottom boundaries to simulate a confined aquifer of infinitesimal width, as shown in Figure 4.1. This problem description follows that developed by Voss and Souza (1987) from Henry's original formulation. The rectangular domain has dimensions of 2 m in the horizontal direction and 1 m in the vertical direction, which is aligned with the gravitational vector. The computational grid comprises 200 square nodes of uniform size. A constant fresh-water flux (Neumann condition) is imposed on the inland (west) boundary; whereas, a hydrostatic pressure boundary (hydraulic gradient condition) of salt water is imposed on the coastal (east) boundary. Parameters used in this simulation are consistent with the non-dimensional parameters chosen by Henry (1964a; 1964b). Initially the aquifer was filled with freshwater under hydrostatic conditions. The pressure boundary conditions on the coastal boundary were hydrostatic conditions for sea water. Henry's problem was solved with the STOMP simulator by executing from fresh-water hydrostatic conditions in the aquifer until steady state conditions were reached. The time step acceleration factor of 1.25 allows the user to over specify the time required to reach steady-state conditions without excessive execution time costs. As the simulation approaches steady-state conditions the number of Newton-Raphson iterations will diminish to one, and all of the output variables will become invariant with time. Steady-state conditions for this problem were achieved

roughly after 1 day of simulation time. The relatively small initial time step of 1.0 s was chosen to prevent convergence failures during the first time step.

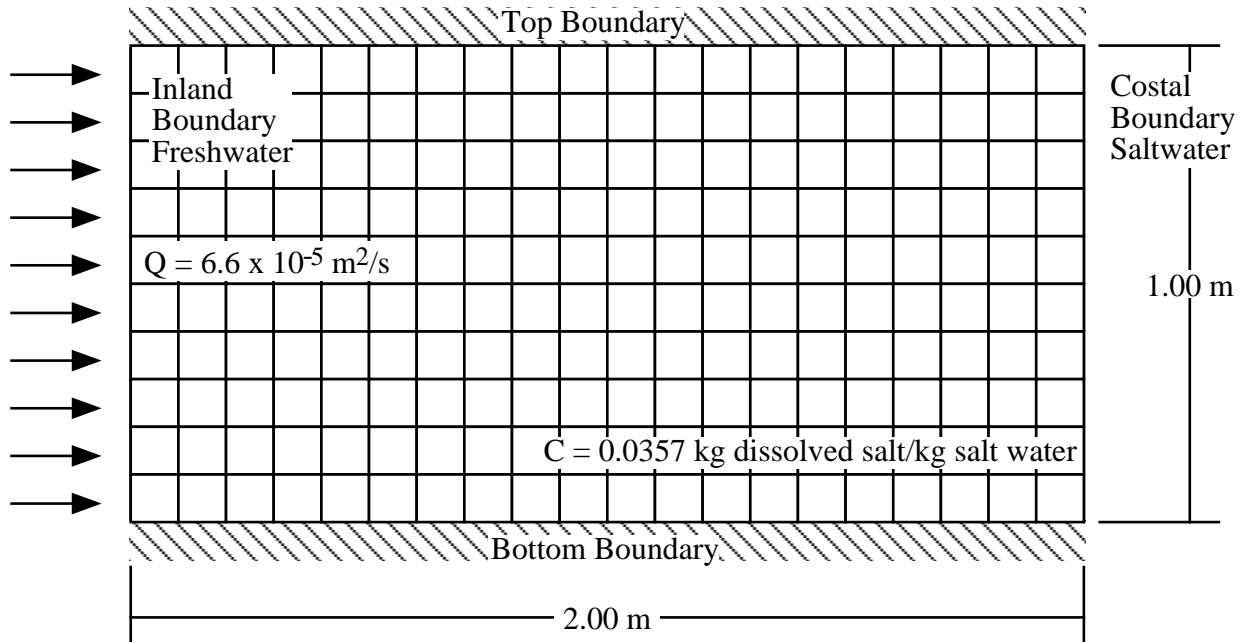


Figure 4.1 Henry's problem and computational grid

The salt interactions with the aqueous phase and the porous medium are specified in the Salt Transport Card.

```
#-----
~Salt Transport Card
#-----
Henry Sodium Chloride,
Constant,18.86e-6,m^2/s,
Porous Medium,0.0,m,0.0,m,
```

Two modifications, involving the computation of salt-water properties, were made to the source coding of the STOMP simulator to execute this application. Salt-water density in the STOMP simulator is normally computed using the function of Leijnse (1992), according to Eq. 4.1. For our application this function was replaced with the one specified by Henry, as shown in Eq. 4.2. The

variation in salt-water viscosity was ignored in Henry's problem; therefore, the expression for salt-water viscosity was modified from the function of Leijnse (1992), according to Eq. 4.3 to that shown in Eq. 4.4. The simulator is prompted to use the special density and viscosity equations for this problem by including the word 'Henry' in the first line of the Salt Transport Card. The second line shows the salt diffusion coefficient in the aqueous phase, and the third line the dispersivity values. The boundary conditions for the salt equation are given in the Boundary Conditions Card. In this case, constant aqueous salt concentrations are prescribed at both the west and east boundaries.

$$\rho_{\ell}^s = \rho_{\ell}^w \exp(0.7\omega_{\ell}^s) \quad 4.1$$

$$\rho_{\ell}^s = \rho_{\ell}^w + 0.6829C_{\ell}^s \quad 4.2$$

$$\mu_{\ell}^s = \mu_{\ell}^w \left[ 1.0 + 1.85\omega_{\ell}^s + 4.1(\omega_{\ell}^s)^2 + 44.5(\omega_{\ell}^s)^3 \right] \quad 4.3$$

$$\mu_{\ell}^s = \mu_{\ell}^w \quad 4.4$$

### References

- Henry H.R. 1964a. Effects of Dispersion on Salt Encroachment in Coastal Aquifers. Water-Supply Paper 1613-C, Sea Water in Coastal Aquifers: C71-84, U.S. Geological Survey.
- Henry H.R. 1964b. Interfaces between salt water and fresh water in coastal aquifers. Water-Supply Paper 1613-C, Sea Water in Coastal Aquifers: C35-70, U.S. Geological Survey.
- Leijnse A. 1992. Three-Dimensional Modeling of Coupled Flow and Transport in Porous Media, Ph.D., University of Notre Dame, Notre Dame, Indiana.
- Ségol G. 1994. Classic Groundwater Simulations: Proving and Improving Numerical Models, trans., Prentice-Hall, Englewood Cliffs, New Jersey.
- Voss C.I. and W.R. Souza. 1987. Variable density flow and solute transport simulation of regional aquifers containing a narrow freshwater-saltwater transition zone. Water Resources Research, 23:1851-1866.

## 4.2 Exercises

1. Run the simulation and produce a plot of the salt distributions after 10 days.
2. Remove the word 'Henry' from the Salt Transport Card and rerun the simulation. Make a plot of the salt distribution at  $t = 10$  days and compare graph with the results obtained in Exercise 1. Restore input file.
3. Reduce the west Neumann aqueous phase inflow rate by a factor 10. Run the simulation and make a plot of the salt distribution at  $t = 10$  days. Compare graph with the results obtained in Exercises 1 and 2. Restore input file.
4. Reduce salt diffusion coefficient by a factor 10. Run the simulation and make a plot of the salt distribution at  $t = 10$  days and compare graph with the results obtained in Exercises 1 - 3 Restore input file.
5. Add an aqueous volumetric source at node 15,1,1. Allow the source to extract water with a rate of 10 l/min. Run the simulation and make a plot of the salt distribution at  $t = 10$  days and compare the graph with the results obtained in Exercises 1 - 4. If the differences are small compared to the base case, increase the pumping rate until a change is observed.

## 4.3 Input File

```
#-----  
~Simulation Title Card  
#-----  
1,  
STOMP Tutorial Problem 4,  
Mart Oostrom/Mark White,  
PNNL,  
June 03,  
15:00,  
2,  
Henry's Problem for Salt Water Intrusion,  
Classic test problem for simulators with water and salt equations,
```

#-----  
~Solution Control Card

#-----  
Normal,  
Water-Salt,  
1,  
0,yr,10,d,1,s,1,d,1.25,8,1.e-6,  
1000,  
,

#-----  
~Grid Card

#-----  
Uniform Cartesian,  
20,1,10,  
10,cm,  
10,cm,  
10,cm,

#-----  
~Rock/Soil Zonation Card

#-----  
1,  
Porous Medium,1,20,1,1,1,10,

#-----  
~Mechanical Properties Card

#-----  
Porous Medium,,,0.35,0.35,,,Constant Diffusion,1.0,

#-----  
~Hydraulic Properties Card

#-----  
Porous Medium,1.020408e-9,m^2,,,1.020408e-9,m^2,

#-----  
~Saturation Function Card

#-----  
Porous Medium,van Genuchten,0.2,1/cm,1.8,0.0,,

#-----  
~Aqueous Relative Permeability Card

#-----  
Porous Medium,Mualem,,

#-----  
~Salt Transport Card

#-----  
Henry Sodium Chloride,  
Constant,18.86e-6,m^2/s,  
Porous Medium,0.0,m,0.0,m,

#-----  
~Initial Conditions Card  
#-----  
Gas Pressure,Aqueous Pressure,  
1,  
Aqueous Pressure,121325,Pa,,,,,-9793.5331,1/m,1,20,1,1,1,10,

#-----  
~Boundary Conditions Card  
#-----  
2,  
west,neumann,aqueous conc,  
1,1,1,1,1,10,1,  
0,s,6.6e-05,m/s,0.0,kg/m^3,  
east,hydraulic gradient,aqueous conc,  
20,20,1,1,1,10,1,  
0,s,121557.98,Pa,36.5921,kg/m^3,

#-----  
~Output Options Card  
#-----  
10,  
20,1,1,  
20,1,3,  
20,1,5,  
20,1,7,  
20,1,10,  
15,1,1,  
15,1,3,  
15,1,5,  
15,1,7,  
15,1,10,  
1,1,d,m,6,6,6,  
5,  
salt aqueous concentration,kg/m^3,  
aqueous viscosity,cp,  
aqueous density,kg/m^3,  
xnc aqueous volumetric flux,m/s,  
znc aqueous volumetric flux,m/s,  
2,  
0.5,d,  
1,d,  
6,  
no restart,,  
salt aqueous concentration,kg/m^3,  
aqueous viscosity,cp,  
aqueous density,kg/m^3,  
xnc aqueous volumetric flux,m/s,  
znc aqueous volumetric flux,m/s,

#-----

~Surface Flux Card

#-----

4,

aqueous volumetric flux,m<sup>3</sup>/day,m<sup>3</sup>,east,20,20,1,1,1,5,

aqueous volumetric flux,m<sup>3</sup>/day,m<sup>3</sup>,east,20,20,1,1,6,10,

salt mass flux,kg/day,kg,east,20,20,1,1,1,5,

salt mass flux,kg/day,kg,east,20,20,1,1,6,10,

## 4.4 Solutions to Selected Exercises

### Exercise 1

The steady-state solution to Henry's problem is shown in Figure 4.2. The salt water is moving in through diffusion from the east boundary. The density effects are clearly visible as the salt water tends to sink in the domain. The fresh water, moving from west to east, is diverted to flow over the salt water.

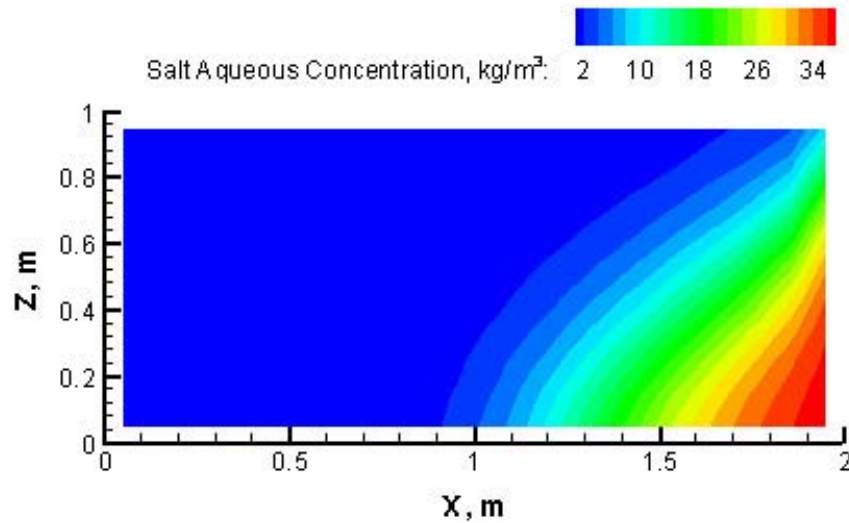


**Figure 4.2** Salt concentrations for the standard Henry simulation at  $t = 10$  days.

### Exercise 2

By removing the 'Henry' provision in the input file, the simulator defaults to the Leijnse (1992) viscosity and density functions. As is shown in Figure 4.3, differences with standard solution to Henry's problem are relatively small. Figures 4.2 and 4.3 do not exhibit major differences.

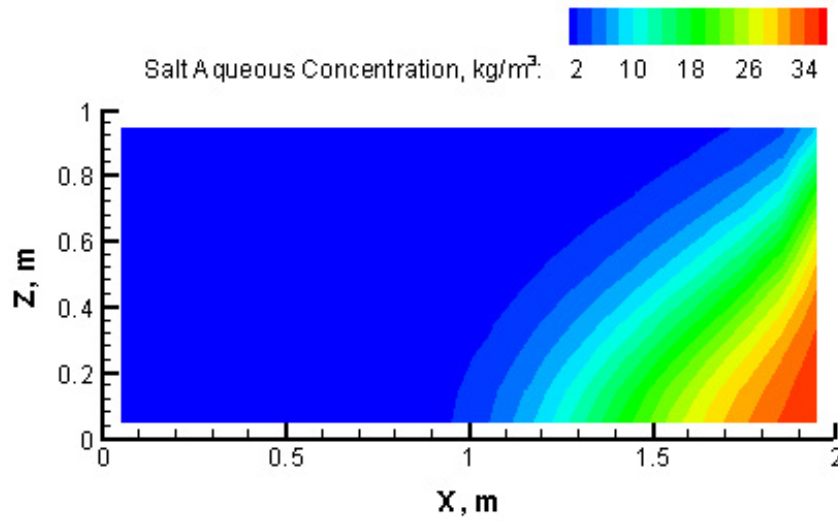


**Figure 4.3** Salt concentrations for simulation with the Leijnse (1992) viscosity and density functions.

### Exercise 3

A reduction of the aqueous flux at the west boundary results in an increased diffusion of salt into the domain from the east boundary (Figure 4.4). The amount of salt that is transported into the domain is considerably more than the amount for the standard problem (Figure 4.2).

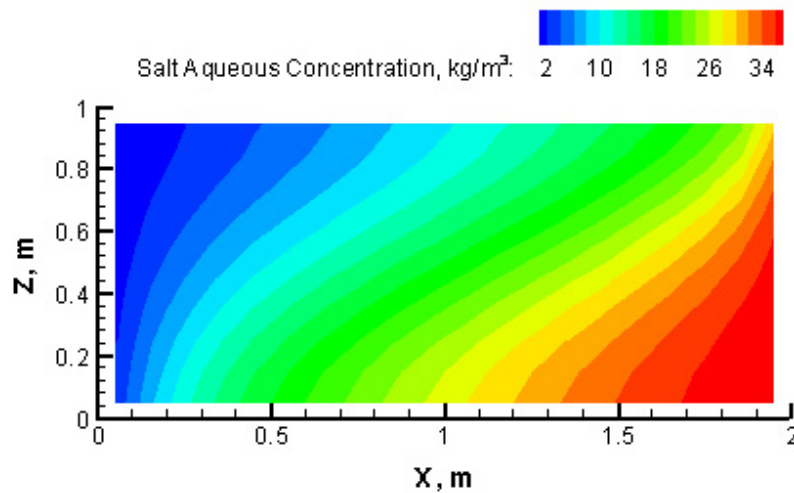


**Figure 4.4** Salt concentrations following the reduced fresh-water inflow rate.

#### Exercise 4

A reduction in the diffusion coefficient causes decreased mixing of the salt with the fresh water (Figure 4.5). The sinking of the wedge is more pronounced as greater density gradients occur in the domain.

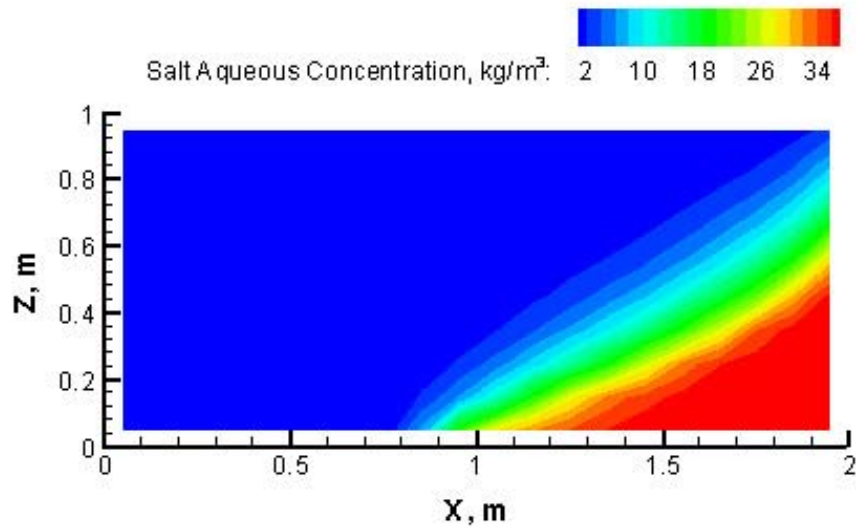


**Figure 4.5** Salt concentrations as a result of a reduced salt diffusion coefficient.

#### Exercise 5

As a result of pumping, the salt wedge is reduced compared to the base case. The steady-state situation, depicted in Figure 4.6, occurs after less than one hour.

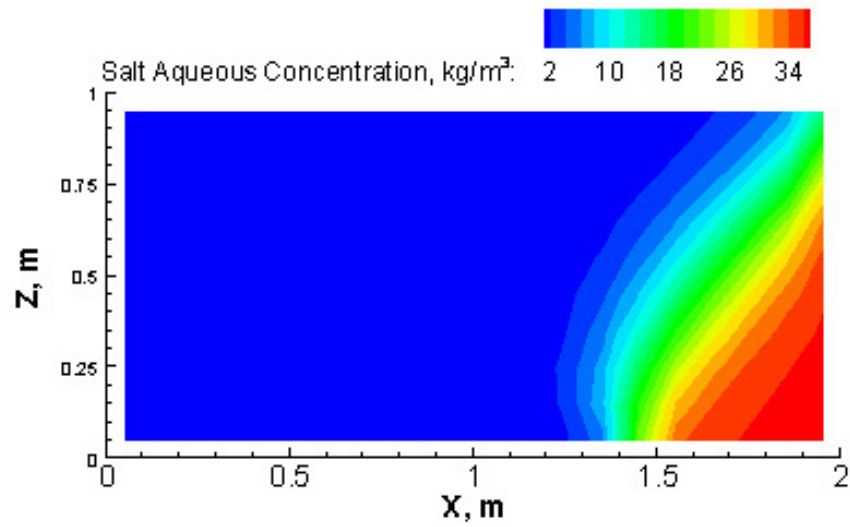


**Figure 4.6** Salt concentrations resulting from well pumping at node 15, 1, 1, extracting 10 L/hour. The steady state situation is reached in about one hour.

## 5. Formation of residual NAPL saturation in unsaturated porous media

**Abstract:** *The user is introduced to NAPL flow in porous media. The example problem demonstrates how residual NAPL saturation formation in the unsaturated zone affects NAPL flow. Residual saturation formation in the vadose zone is a process that is often ignored in multi-fluid flow simulators. The user will simulate an actual column experiment and evaluate the impact of residual NAPL saturation on fluid flow. The Water-Oil mode (STOMP4) is used for this application.*

### 5.1 Problem Description

Groundwater contamination as a result of subsurface leakage or surface spills of immiscible organic liquids, such as solvents and hydrocarbon products, is a widespread problem in the industrialized world. Many organic liquids existing as a separate phase are in fact often slightly miscible with water and their solubility often exceeds the drinking water standards by orders of magnitude. To accurately describe the movement of such liquids in the subsurface, separate Nonaqueous Phase Liquid (NAPL), aqueous, and, in the case of volatile organic liquids, gas phase flow has to be considered.

Descriptions of mobile and entrapped NAPL behavior are standard features of multifluid flow simulators. However, these models do not generally incorporate retention of nonaqueous phase liquid (NAPL) in the vadose zone following NAPL imbibition events (e.g., surface spills, tank leaks). Commonly used constitutive relations assume a nonzero NAPL relative permeability when the non-trapped NAPL saturation is greater than zero. As a result, the non-trapped NAPL is allowed to drain from the pore spaces. As NAPL retained in the

vadose zone can serve as a long-term source for groundwater contamination, via transport through the gas or aqueous phase, understanding and predicting the processes of residual NAPL formation and remobilization is critical when considering restoration or management of a contaminated subsurface site. A theory describing the formation of residual NAPL saturation (Lenhard et al., 2003) has recently been implemented into the simulator. Simulation results have been compared to experimental data (White et al, 2003).

The theory of Lenhard et al. (2003) recognizes residual NAPL formation within the pore-space region between the apparent aqueous saturation and the maximum apparent total-liquid saturation. This theory is based on fluid displacement physics in pore spaces. The Lenhard et al. model (2003) allows for residual NAPL collocated with mobile NAPL, which can reduce the mobile NAPL relative permeability. Ignoring air entrapment by NAPL, the effective residual NAPL saturation,  $\bar{S}_{nr}$ , is computed as

$$\bar{S}_{nr} = \bar{S}_{nr}^{max} \left( \bar{S}_t^{max} - \bar{S}_l \right)^{1/2} \left( 1 - \bar{S}_l \right)^{3/2} \quad 5.1$$

where  $\bar{S}_{nr}^{max}$  is the maximum residual NAPL saturation that can be obtained in a porous medium,  $\bar{S}_l$  is the apparent aqueous phase saturation, and  $\bar{S}_t^{max}$  is the historic maximum apparent total-liquid saturation. The first and second terms between brackets are factors related to the volume of pore space occupied by NAPL, and the size of the pore containing the NAPL, respectively. The reader is referred to Lenhard et al. (2003) for a detailed description and derivation of 5.1.

The Soltrol®220 experiment was conducted in a 1-m-long column with a 5.0 cm inside diameter. The column was packed under saturated conditions with 90 cm of a medium-grained Hanford sand. Denoting the bottom as  $z = 0$  cm, the

column was calibrated for dual-energy gamma radiation measured at nine locations:  $z = 5, 15, 25, 35, 45, 55, 65, 75,$  and  $85$  cm. The column was subsequently drained at a rate of  $10$  cm/hr from  $z = 90$  cm to  $z = 20$  cm after which the porous medium system was allowed to reach quasi-static equilibrium by waiting seven days. After this period,  $120$  ml Soltrol<sup>®</sup>220 was injected at a rate of  $1$  ml/min for  $120$  minutes. After the injection, the LNAPL was allowed to infiltrate and redistribute. The column was scanned daily for the duration of the experiment ( $50$  days) to determine LNAPL and water saturations. The fluid properties and hydraulic properties of the porous medium, including the maximum entrapped Soltrol<sup>®</sup>220 saturation,  $\bar{S}_{ne}^{\max}$ , were obtained in independent procedures.

The Soltrol<sup>®</sup> 220 imbibition experiment was modeled, starting with a drained column (i.e., hydrostatic aqueous phase), with the water table set at  $20.0$  cm above the column bottom and injecting  $120$  ml of NAPL over a  $2$ -hour period in the top grid cell. The experiment was simulated over a  $50$ -day period, with time steps limited to  $0.5$  hr for the first  $100$  hrs and  $4.0$  hr for the remaining period. During the first  $7$ -hr period time stepping is limited by the convergence capabilities of the Newton-Raphson linearization scheme. The time step is cut to  $20\%$  of its previous value if a converged solution to the coupled nonlinear equations is not found. Beyond the first  $7$ -hr period, time stepping is controlled by the specified limits. The input files for STOMP modes with NAPL include the Oil Properties Card and the NAPL Relative Permeability Card. Boundary conditions for this phase have to specified in the Boundary Conditions Card. Results of simulations with and without the formation of residual saturation are compared with experimental results in Figures 5.1, 5.2, and 5.3.

### *References*

Lenhard, R.J., M. Oostrom, and J.H. Dane. 2004. A constitutive model for air-NAPL-water flow in the vadose zone accounting for residual NAPL in strongly water-wet porous media. *J. of Contaminant Hydrology* (in Press).

White, M.D., M. Oostrom, and R.J. Lenhard. 2004. A practical model for nonvolatile NAPL-aqueous flow in variably saturated porous media, distinguishing mobile, residual, and entrapped NAPL. *Ground Water* (in Press)

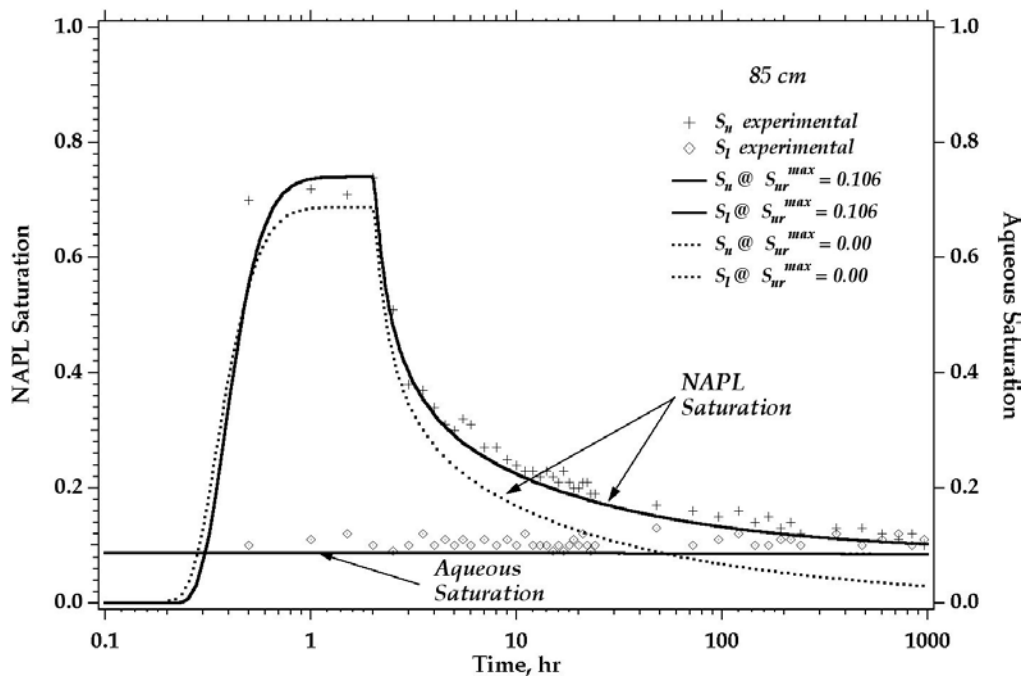


**Figure 5.1** Comparison of aqueous and NAPL saturation between laboratory observations and numerical simulations at  $z = 85$  cm for the Soltrol<sup>®</sup> 220 infiltration experiment.

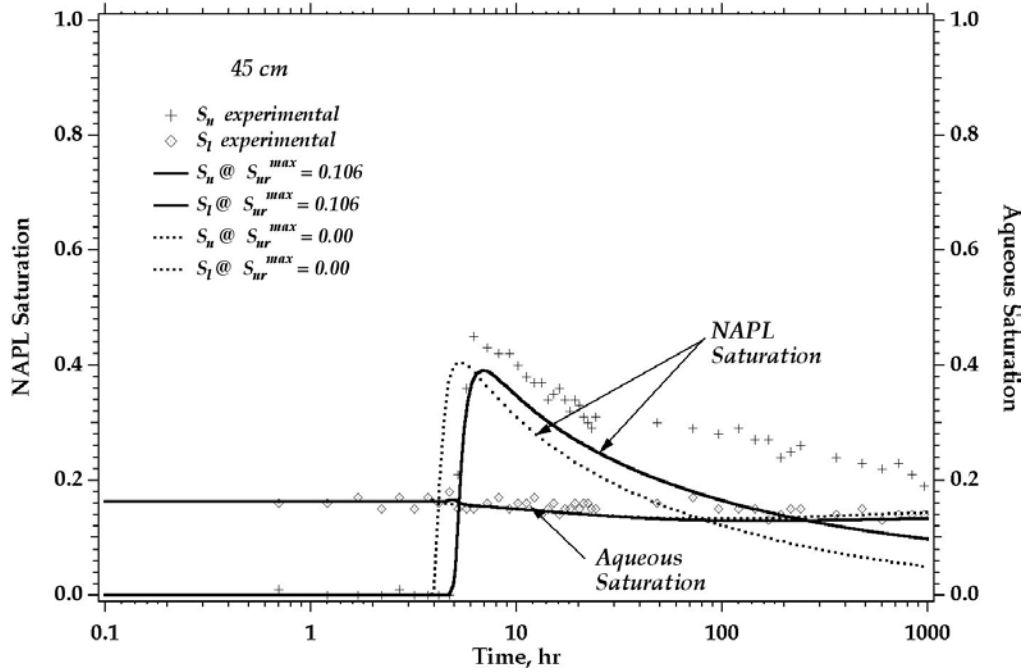


**Figure 5.2** Comparison of aqueous and NAPL saturation between laboratory observations and numerical simulations  $z = 45$  cm for the Soltrol<sup>®</sup> 220 infiltration experiment.

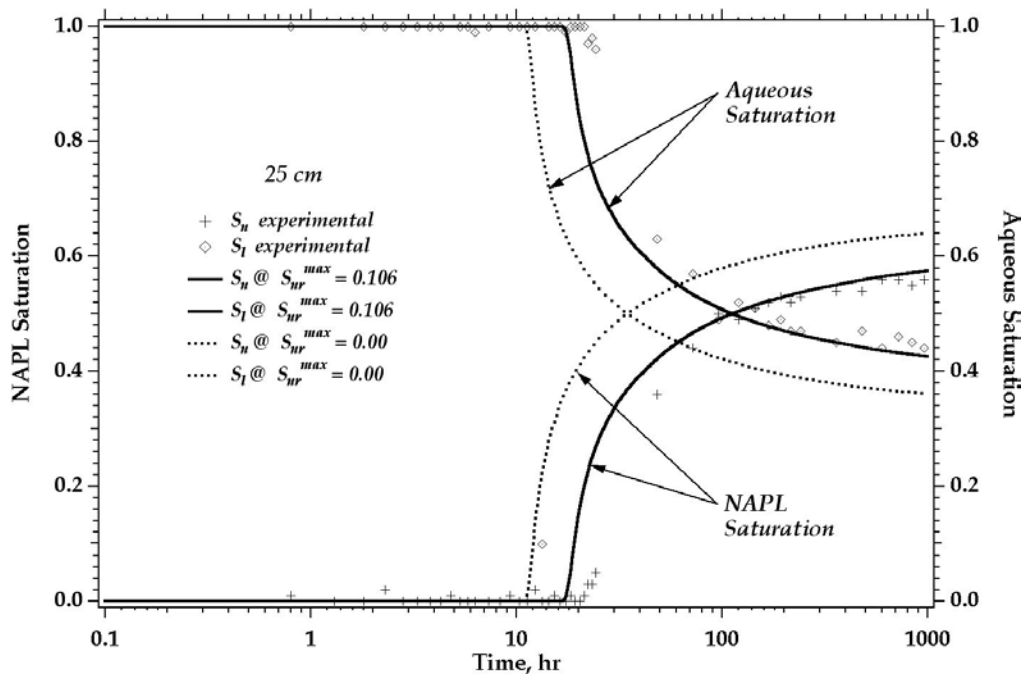


**Figure 5.3** Comparison of aqueous and NAPL saturation between laboratory observations and numerical simulations at  $z = 25$  cm for the Soltrol<sup>®</sup> 220 infiltration experiment.

## 5.2 Exercises

1. The experiment was conducted in a 1D column with a 5-cm diameter. Verify that the Grid Card has been set up properly.
2. Execute the simulation with the input file shown in section 5.3. Plot the NAPL saturation vs. elevation at  $z = 85, 45,$  and  $25$  cm and compare the simulated NAPL saturations with Figs. 5.1, 5.2, and 5.3.
3. The residual formation option is specified in the Saturation Function Card:

```
#-----
~Saturation Function Card
#-----
72.0,dynes/cm,38.0,dynes/cm,,,
Sand,Brooks and Corey w/ residual,10.12,cm,2.67,0.08,72.0,dynes/cm,0.106,
```

With the help of the User's Guide, complete the card for nonhysteretic conditions. Plot the NAPL saturation vs. elevation at  $z = 85, 45,$  and  $25$  cm and compare the simulated NAPL saturations with Figs. 5.1, 5.2, and 5.3.

4. Increase the maximum residual saturation to 0.212. Execute simulation, make plots at  $z = 85, 45,$  and  $25$  cm, and compare with previously obtained results.
5. Compute equivalent Van Genuchten values for this porous medium. Execute simulation, make plots at  $z = 85, 45,$  and  $25$  cm, and compare with previously obtained results.
6. Reduce the permeability by a factor 10. Execute simulation, make plots at  $z = 85, 45,$  and  $25$  cm, and compare with previously obtained results.

### 5.3 Input File

```
#-----  
~Simulation Title Card  
#-----  
1,  
STOMP Tutorial Problem 5,  
M.Ostrom/Mark White,  
Pacific Northwest National Laboratory,  
Jan 2003,  
3 PM PST,  
2,  
Soltrol 170 movement in coarse sand,  
Testing of new residual saturation formation theory,  
  
#-----  
~Solution Control Card  
#-----  
Normal,  
Water-Oil,  
2,  
0,s,100,hr,1,s,0.5,hr,1.25,8,1.e-6,  
100,hr,50,d,1,s,4.0,hr,1.25,8,1.e-6,  
10000,  
Variable Aqueous Diffusion,  
0,  
  
#-----  
~Grid Card  
#-----  
Cartesian,  
1,1,91,  
0.0,cm,4.431135,cm,  
0.0,cm,4.431135,cm,  
0.0,cm,0.5,cm,89@1,cm,90,cm,  
  
#-----  
~Rock/Soil Zonation Card  
#-----  
1,  
Sand,1,1,1,1,1,91,  
  
#-----  
~Mechanical Properties Card  
#-----  
Sand,,kg/ m^3,0.36,0.36,,,Millington and Quirk,  
  
#-----  
~Hydraulic Properties Card  
#-----  
Sand,,,,,1.41e-11,m^2,
```

```

#-----
~Saturation Function Card
#-----
72.0,dynes/cm,38.0,dynes/cm,,,
Sand,Brooks and Corey w/ residual,10.12,cm,2.67,0.08,72.0,dynes/cm,0.106,

#-----
~Aqueous Relative Permeability Card
#-----
Sand,Burdine,,

#-----
~NAPL Relative Permeability Card
#-----
Sand,Burdine,,

#-----
~Oil Properties Card
#-----
Soltrol 220,
153.82,g/mol,250.,K,349.9,K,556.4,K,
45.6,bar,275.9,cm^3/mol,0.272,0.193,0.0,debyes,
4.072e+1,2.0496e-1,-2.27e-4,8.843e-8,
Equation 1,-7.07139,1.71497,-2.89930,-2.49466,
Constant,810,kg/m^3,
Constant,4.5e-3,Pa s,
1.0e10,Pa,

#-----
~Initial Conditions Card
#-----
2,
Aqueous Pressure,103259,Pa,,,,,-9793.5192,1/m,1,1,1,1,1,91,
NAPL Pressure,-1.e9,Pa,,,,,1,1,1,1,1,91,

#-----
~Boundary Conditions Card
#-----
2,
Top,Zero Flux,Neumann,
1,1,1,1,91,91,2,
0,hr,-1.e9,Pa,0.0,-0.05093,cm/min,
2,hr,-1.e9,Pa,0.0,-0.05093,cm/min,
Bottom,Dirichlet,Zero Flux,
1,1,1,1,1,1,
0.0,hr,103284,Pa,0.0,101325,Pa,

#-----
~Output Control Card
#-----
9,

```

1,1,86,  
1,1,76,  
1,1,66,  
1,1,56,  
1,1,46,  
1,1,36,  
1,1,26,  
1,1,16,  
1,1,6,  
1,1,hr,cm,6,6,6,  
3,  
Aqueous Saturation,,  
NAPL Saturation,,  
Residual NAPL Saturation,,  
0,  
3,  
Aqueous Saturation,,  
NAPL Saturation,,  
Residual NAPL Saturation,,  
  
#-----  
~Surface Flux Card  
#-----  
3,  
NAPL volumetric flux,ml/min,ml,top,1,1,1,1,91,91,  
NAPL volumetric flux,ml/min,ml,bottom,1,1,1,1,1,1,  
aqueous volumetric flux,ml/min,ml,bottom,1,1,1,1,1,1,

## 5.4 Solutions to Selected Exercises

### Exercise 2

Simulated NAPL saturations at  $z = 25, 45,$  and  $85$  cm are shown in Figure 5.4. The results are identical to the solid NAPL lines in Figures 5.1, 5.2, and 5.3.

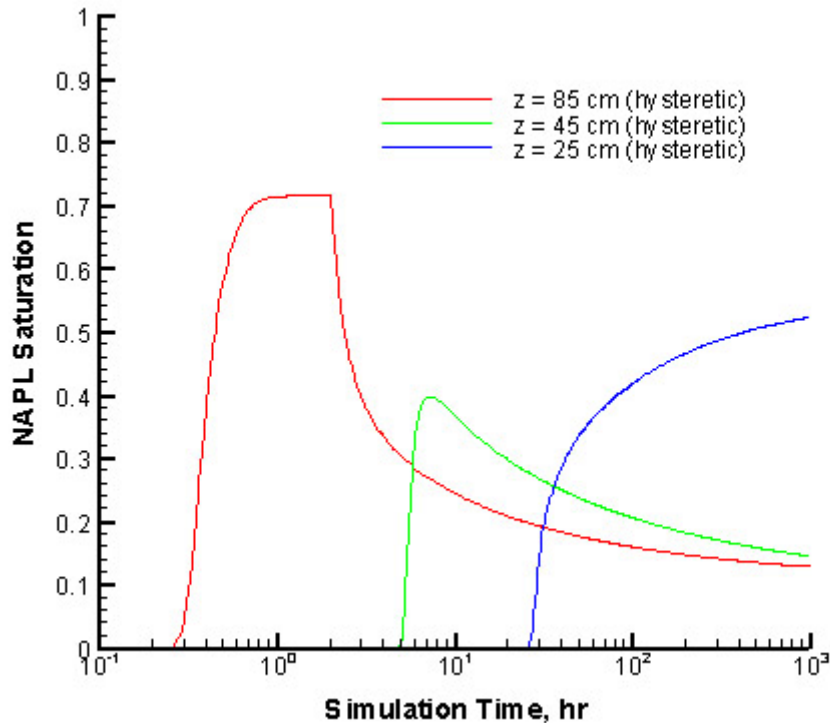


**Figure 5.4** Simulated NAPL saturation at  $z = 85, 45$  and  $25$  cm .

### Exercise 3

Simulated NAPL saturations at  $z = 25, 45,$  and  $85$  cm are shown in Figure 5.5. The results for the nonhysteretic simulation are identical to the dashed NAPL lines in Figures 5.1, 5.2, and 5.3. To simulate nonhysteretic conditions use the following Saturation Function Card:

```
#-----  
~Saturation Function Card  
#-----
```

72.0,dynes/cm,38.0,dynes/cm,,,  
 Sand, Brooks and Corey,10.12,cm,2.67,0.08,72.0,dynes/cm,

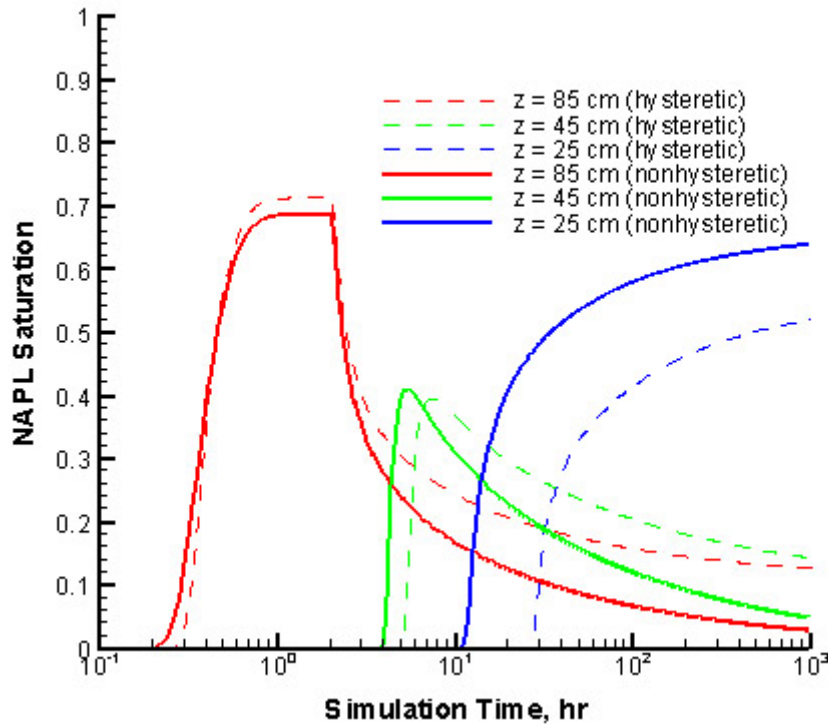
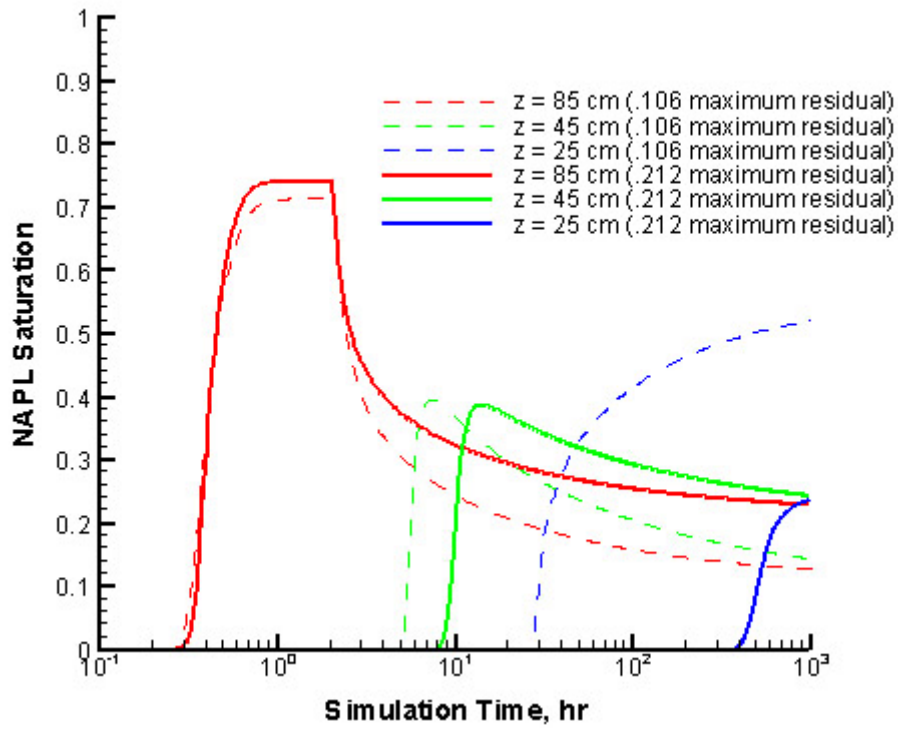


Figure 5.5 A comparison of hysteretic versus nonhysteretic NAPL 1-dimensional infiltration and redistribution.

**Exercise 4**

The effects of increasing the maximum residual saturation are illustrated in Figure 5.6. As the NAPL descends through the soil column it does not drain as easily and the NAPL saturation does not decline as rapidly as before. Since more NAPL is retained in the upper sections of the column, node 25 (blue line) does not see NAPL appearing until later in the simulation. Increasing the residual maximum saturation to 0.212 requires the following Saturation Function Card.

```
#-----
~Saturation Function Card
#-----
72.0,dynes/cm,38.0,dynes/cm,,,
Sand,Brooks and Corey w/Residual,10.12,cm,2.67,0.08,72.0,dynes/cm,.212,
```



**Figure 5.6** The effect of maximum residual saturation on NAPL 1-dimensional infiltration.

## 6. NAPL infiltration and redistribution in a 2D aquifer system

**Abstract:** *The first objective of this two-part example is to investigate the effects of fluid density and viscosity on the movement of NAPLs after a spill in a partly saturated, hypothetical, aquifer. The user will investigate the effects of NAPL fluid properties on infiltration and redistribution. The objective of the second part is to compute steady-state initial conditions through a separate simulation. The Restart file generated by this simulation is used to define the initial conditions for the actual infiltration event. The Water-Oil mode (STOMP4) is used for this application.*

### 6.1 Problem Description

#### Part 1.

A known amount of LNAPL, with a density of  $800 \text{ kg/m}^3$  and a viscosity of  $0.002 \text{ Pa s}$ , is injected into a hypothetical two-dimensional aquifer. The input file of this problem is shown in section 6.3.1. The simulation domain is 50-m long and 10-m high. A total of 25 and 20 uniform nodes are used in the  $x$ - and  $z$ -direction, respectively. The water table is at approximately 6 m from the surface. The NAPL is injected with a rate of  $0.25 \text{ m/day}$  at the top of node (13,1,20) for a period of 10 days. After the infiltration period, the NAPL is allowed to redistribute for 190 days. The total simulation time is 200 days.

#### Part 2

This problem differs from the problem in Part 1 in that the steady-state initial conditions prior to the NAPL infiltration can not be specified in the Initial Conditions Card because precipitation ( $100 \text{ ml/year}$ ) is included. When more complex initial conditions are required, a separate run has to be completed that

yields a *restart* file that contains the proper initial conditions. The input file for the simulation computing the steady-state initial conditions is shown in section 6.3.2. The input file shown in 6.3.3 uses the restart file created with the input file shown in section 6.3.2.

## 6.2 Exercises

### Part 1.

1. Run the problem outlined in section 6.3.1. Make a plot of the LNAPL saturation distribution at  $t = 10$  and  $t = 200$  days. Check the surface file and see if the proper amount of NAPL has entered the system.
2. Increase the density of the NAPL to  $1200 \text{ kg/m}^3$  and run the simulation. Make plots at  $t = 10$  and 200 days and compare results with plots made in Exercise 1
3. Increase the viscosity of the NAPL to  $0.02 \text{ Pa s}$ , while keeping the NAPL density at  $1200 \text{ kg/m}^3$ . Run the simulation and make plots at  $t = 10$  and 200 days. Compare results with plots made in Exercises 1 and 2. Change the viscosity and the density back to the original values.
4. Instead of using a Neumann boundary condition to allow NAPL into the domain, use an equivalent source at node (13,1,20). Run the simulation and compare results.

### Part 2.

5. Run the problem outlined in section 6.3.2. This simulation yields a *restart.x* file. Rename the *restart.x* file to *restart*. Check the output file or the screen and verify that the vertical aqueous flux is approximately  $100 \text{ mm/year}$  throughout the unsaturated domain. Compare the initial and steady-state aqueous saturations.

6. Run the problem in section 6.3.3. Comment on the differences between this input file and the file shown in section 6.3.1. Run the simulation and make plots at  $t = 10$  and 200 days. Compare results with plots made in Exercise 1.
7. Change the horizontal gradient on the water table from  $-40$  Pa/m to  $-70$  Pa/m. Make sure to change the necessary boundary conditions and initial conditions on both of the input files used in this simulation! Run the simulation and make plots at  $t = 10$  and 200 days. Compare results with the plots made in Exercise 6.

## 6.3 Input Files

### 6.3.1 Input File for Part 1

```
#-----
~Simulation Title Card
#-----
1,
STOMP Tutorial Problem 6a,
Mart Ostrom/Mark White,
PNNL,
June 03,
15:00,
1,
Simulation of NAPL spills in 2D domain,

#-----
~Solution Control Card
#-----
Normal,
Water-Oil,
2,
0,s,10,d,1,s,1,d,1.25,8,1.e-6,
10,d,200,d,1,s,10,d,1.25,8,1.e-6,
10000,
Variable Aqueous Diffusion,
,

#-----
~Grid Card
#-----
Uniform Cartesian,
25,1,20,
```

2,m,  
1,m,  
0.5,m,

#-----  
~Rock/Soil Zonation Card

#-----  
1,  
Sand,1,25,1,1,1,20,

#-----  
~Mechanical Properties Card

#-----  
Sand,2650,kg/m<sup>3</sup>,0.43,0.43,,,Millington and Quirk,

#-----  
~Hydraulic Properties Card

#-----  
Sand,10,hc m/day,,,10,hc m/day,

#-----  
~Saturation Function Card

#-----  
72.0,dynes/cm,,,32,dynes/cm,  
Sand, Van Genuchten,0.1,1/cm,2.0,0.10,72.0,dynes/cm,,

#-----  
~Aqueous Relative Permeability Card

#-----  
Sand,Mualem,,

#-----  
~NAPL Relative Permeability Card

#-----  
Sand,Mualem,,

#-----  
~Oil Properties Card

#-----  
NAPL,  
165.834,g/mol,251.,K,394.4,K,620.2,K,  
47.6,bar,289.6,cm<sup>3</sup>/mol,0.2758,0.2515,0.0,debyes,  
-1.431e+1,5.506e-1,-4.513e-4,1.429e-7,  
Equation 1,-7.36067,1.82732,-3.47735,-1.00033,  
Constant,800.0,kg/m<sup>3</sup>,  
Constant,0.002,Pa s,  
1.0e8,Pa,

#-----  
~Initial Conditions Card

#-----  
2,

Aqueous Pressure,140000,Pa,0.0,1/m,,,-9793.5192,1/m,1,25,1,1,1,20,  
NAPL Pressure,-1.e9,Pa,,,,,1,25,1,1,1,20,

#-----

~Boundary Conditions Card

#-----

3,  
top,zero flux,neumann,  
13,13,1,1,20,20,2,  
0,d,-1.e9,Pa,0.0,-0.25,m/day,  
10.0,d,-1.e9,Pa,0.0,-0.25,m/day,  
west,hydraulic gradient,dirichlet,  
1,1,1,1,1,20,1,  
0,d,140000,Pa,0.0,-1.e9,Pa,  
east,hydraulic gradient,dirichlet,  
25,25,1,1,1,20,1,  
0,d,140000,Pa,0.0,-1.e9,Pa,

#-----

~Output Options Card

#-----

9,  
13,1,20,  
13,1,15,  
13,1,10,  
13,1,8,  
13,1,6,  
13,1,4,  
1,1,7,  
1,1,6,  
1,1,4,  
1,1,day,m,6,6,6,  
2,  
napl saturation,,  
aqueous saturation,,  
2,  
10,d,  
100,d,  
3,  
no restart,,  
napl saturation,,  
aqueous saturation,,

#-----

~Surface Flux Card

#-----

3,  
NAPL volumetric flux,m^3/day,m^3,top,13,13,1,1,20,20,  
NAPL volumetric flux,m^3/day,m^3,west,1,1,1,1,1,20,  
NAPL volumetric flux,m^3/day,m^3,east,25,25,1,1,1,20,

### 6.3.2 Input File Part 2 (steady-state run).

```
#-----  
~Simulation Title Card  
#-----  
1,  
STOMP Tutorial Problem 6b (steady-state calculations),  
Mart Oostrom/Mark White,  
PNNL,  
June 03,  
15:00,  
2,  
Steady state calculations to set up flow field,  
Restart file will be used for subsequential NAPL infiltration simulation,  
  
#-----  
~Solution Control Card  
#-----  
Normal,  
Water-Oil,  
1,  
0,s,1000,yr,1,d,1000,yr,1.25,8,1.e-6,  
10000,  
Variable Aqueous Diffusion,  
,  
  
#-----  
~Grid Card  
#-----  
Uniform Cartesian,  
25,1,20,  
2,m,  
1,m,  
0.5,m,  
  
#-----  
~Rock/Soil Zonation Card  
#-----  
1,  
Sand,1,25,1,1,1,20,  
  
#-----  
~Mechanical Properties Card  
#-----  
Sand,2650,kg/m^3,0.43,0.43,,,Millington and Quirk,  
  
#-----  
~Hydraulic Properties Card  
#-----  
Sand,10,hc m/day,,,10,hc m/day,  
  
#-----
```

~Saturation Function Card

#-----  
72.0,dynes/cm,,,32,dynes/cm,  
Sand, Van Genuchten,0.1,1/cm,2.0,0.10,72.0,dynes/cm,,

#-----  
~Aqueous Relative Permeability Card

#-----  
Sand, Mualem,,

#-----  
~NAPL Relative Permeability Card

#-----  
Sand, Mualem,,

#-----  
~Oil Properties Card

#-----  
NAPL,  
165.834,g/mol,251.,K,394.4,K,620.2,K,  
47.6,bar,289.6,cm<sup>3</sup>/mol,0.2758,0.2515,0.0,debyes,  
-1.431e+1,5.506e-1,-4.513e-4,1.429e-7,  
Equation 1,-7.36067,1.82732,-3.47735,-1.00033,  
Constant,800.0,kg/m<sup>3</sup>,  
Constant,0.002,Pa s,  
1.0e8,Pa,

#-----  
~Initial Conditions Card

#-----  
2,  
Aqueous Pressure,140000,Pa,-40.0,1/m,,, -9793.5192,1/m,1,25,1,1,1,20,  
NAPL Pressure,-1.e9,Pa,,,,,1,25,1,1,1,20,

#-----  
~Boundary Conditions Card

#-----  
3,  
top,neumann,zero flux,  
1,25,1,1,20,20,1,  
0,d,-100.0,mm/year,0.0,-1.e9,Pa,  
west,hydraulic gradient,dirichlet,  
1,1,1,1,1,10,1,  
0,d,140040,Pa,0.0,-1.e9,Pa,  
east,hydraulic gradient,dirichlet,  
25,25,1,1,1,10,1,  
0,d,138040,Pa,0.0,-1.e9,Pa,

#-----  
~Output Options Card

#-----  
9,

1,1,20,  
 25,1,20,  
 13,1,20,  
 13,1,18,  
 13,1,16,  
 13,1,14,  
 13,1,12,  
 13,1,10,  
 13,1,8,  
 1,1,yr,m,6,6,6,  
 3,  
 napl saturation,,  
 aqueous saturation,,  
 z aqueous volumetric flux,mm/year,  
 0,  
 2,  
 aqueous saturation,,  
 z aqueous volumetric flux,mm/year,

### 6.3.3 Input File Part 2 (NAPL Infiltration).

```

#-----
~Simulation Title Card
#-----
1,
STOMP Tutorial Problem 6b (NAPL Infiltration),
Mart Oostrom/Mark White,
PNNL,
June 03,
15:00,
2,
Simulation of NAPL spill in 2D domain,
Simulation starts with Restart file,

#-----
~Solution Control Card
#-----
Restart,
Water-Oil,
2,
0,s,10,d,1,s,1,d,1.25,8,1.e-6,
10,d,200,d,1,s,10,d,1.25,8,1.e-6,
10000,
Variable Aqueous Diffusion,
,

#-----
~Grid Card
#-----
Uniform Cartesian,
25,1,20,
  
```

2,m,  
1,m,  
0.5,m,

#-----  
~Rock/Soil Zonation Card

#-----  
1,  
Sand,1,25,1,1,1,20,

#-----  
~Mechanical Properties Card

#-----  
Sand,2650,kg/m<sup>3</sup>,0.43,0.43,,Millington and Quirk,

#-----  
~Hydraulic Properties Card

#-----  
Sand,10,hc m/day,,,10,hc m/day,

#-----  
~Saturation Function Card

#-----  
72.0,dynes/cm,,,32,dynes/cm,  
Sand, Van Genuchten,0.1,1/cm,2.0,0.10,72.0,dynes/cm,,

#-----  
~Aqueous Relative Permeability Card

#-----  
Sand,Mualem,,

#-----  
~NAPL Relative Permeability Card

#-----  
Sand,Mualem,,

#-----  
~Oil Properties Card

#-----  
NAPL,  
165.834,g/mol,251.,K,394.4,K,620.2,K,  
47.6,bar,289.6,cm<sup>3</sup>/mol,0.2758,0.2515,0.0,debyes,  
-1.431e+1,5.506e-1,-4.513e-4,1.429e-7,  
Equation 1,-7.36067,1.82732,-3.47735,-1.00033,  
Constant,800.0,kg/m<sup>3</sup>,  
Constant,0.002,Pa s,  
1.0e8,Pa,

#-----  
~Initial Conditions Card

#-----  
0,

#-----  
~Boundary Conditions Card

#-----  
5,  
top,neumann,neumann,  
13,13,1,1,20,20,4,  
0,d,-100,mm/year,0.0,-0.25,m/day,  
10.0,d,-100,mm/year,0.0,-0.25,m/day,  
10.0,d,-100,mm/year,0.0,0.,m/day,  
100.0,d,-100,mm/year,0.0,0.,m/day,  
top,neumann,zero flux,  
1,12,1,1,20,20,1,  
0,d,-100.0,mm/year,0.0,-1.e9,Pa,  
top,neumann,zero flux,  
14,25,1,1,20,20,1,  
0,d,-100.0,mm/year,0.0,-1.e9,Pa,  
west,hydraulic gradient,dirichlet,  
1,1,1,1,1,10,1,  
0,d,140040,Pa,0.0,-1.e9,Pa,  
east,hydraulic gradient,dirichlet,  
25,25,1,1,1,10,1,  
0,d,138040,Pa,0.0,-1.e9,Pa,

#-----  
~Output Options Card

#-----  
9,  
13,1,20,  
13,1,15,  
13,1,10,  
13,1,8,  
13,1,6,  
13,1,4,  
1,1,20,  
1,1,15,  
1,1,10,  
1,1,day,m,6,6,6,  
3,  
napl saturation,,  
aqueous saturation,,  
z aqueous volumetric flux,mm/year,  
2,  
10,d,  
100,d,  
3,  
no restart,,  
napl saturation,,  
aqueous saturation,,

#-----  
~Surface Flux Card

#-----  
3,  
NAPL volumetric flux,m<sup>3</sup>/day,m<sup>3</sup>,top,13,13,1,1,20,20,  
NAPL volumetric flux,m<sup>3</sup>/day,m<sup>3</sup>,west,1,1,1,1,1,20,  
NAPL volumetric flux,m<sup>3</sup>/day,m<sup>3</sup>,east,25,25,1,1,1,20,

## 6.4 Solutions to Selected Exercises

### Part 1, Exercise 1

Figure 6.1 shows the NAPL distribution at the end of the 10-day infiltration period. Through capillary action, the NAPL spreads laterally in the unsaturated zone. The lower part of the NAPL bottom has reached the capillary fringe. The angular shape of the NAPL body is a direct result of the rather coarse discretization. The plots can be improved by using a smaller grid. Figure 6.2 shows the NAPL saturations at  $t = 200$  days. At this point in time, the NAPL had 190 days for redistribution after the source injection stopped. Most of the NAPL in the vadose zone has drained. Since the NAPL is lighter than water, the NAPL tends to spread above the capillary fringe.

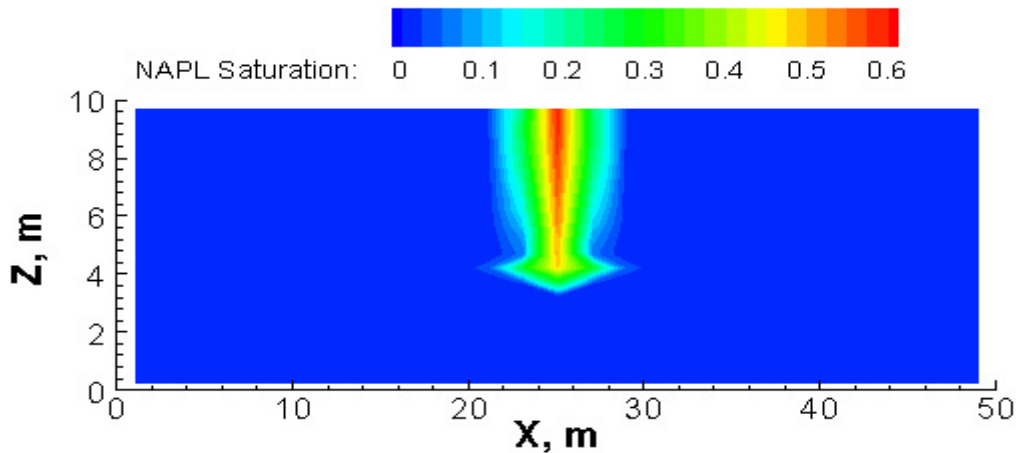


**Figure 6.1** LNAPL spill distribution in 2-dimensional aquifer after 10 days.

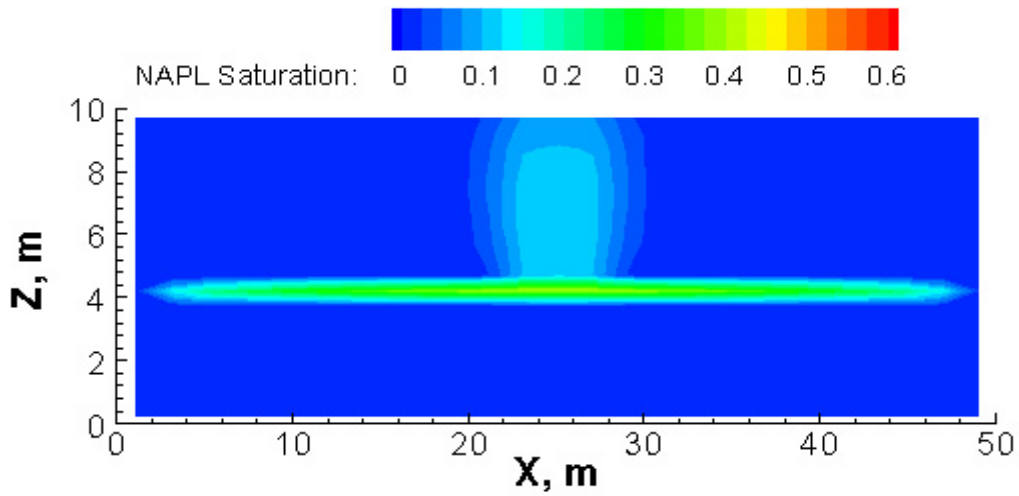


**Figure 6.2** LNAPL spill distribution in 2-dimensional aquifer after 200 days.

Part 2, Exercise 2

The NAPL in this problem is a dense NAPL (DNAPL). As a result, the fluid will move below the water table, as is shown in Figures 6.3 and 6.4. After 200 days, most of the DNAPL is located on top of the bottom boundary.

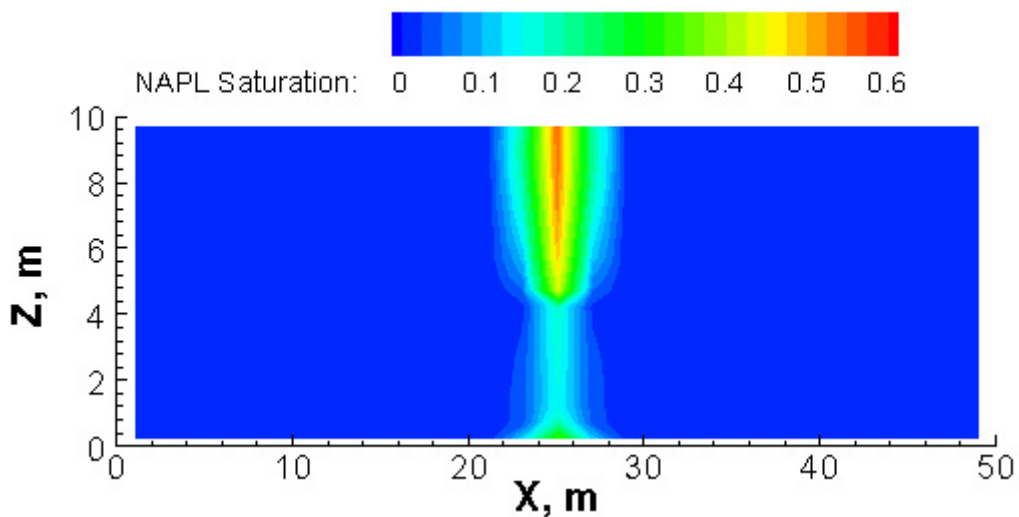


**Figure 6.3** DNAPL spill distribution in 2-dimensional aquifer after 10 days.

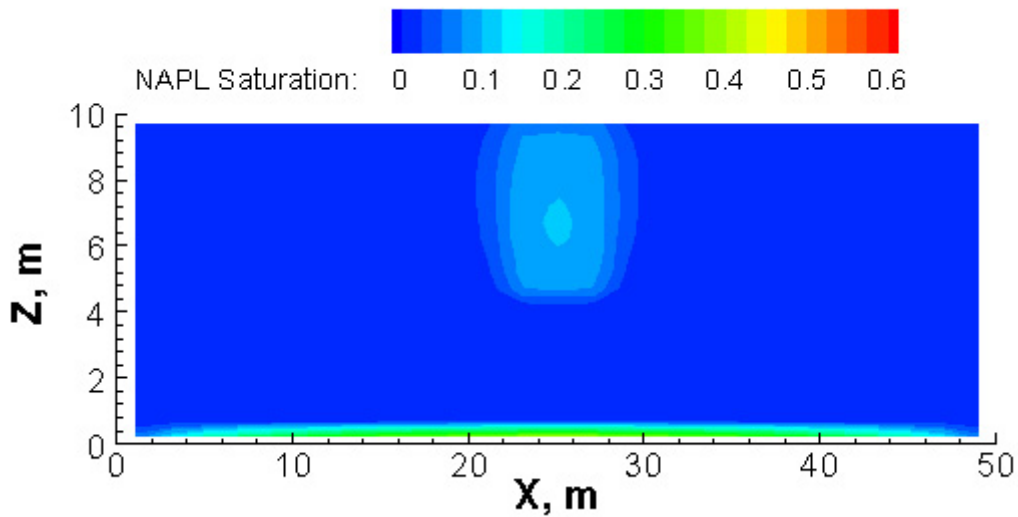


**Figure 6.4** LNAPL spill distribution in 2-dimensional aquifer after 200 days.

### Part 1, Exercise 3

An increase in the viscosity slows down the movement of the DNAPL. After 10 days, the DNAPL has not yet reached the water table (Figure 6.5). After 200 days, the DNAPL has migrated to the lower parts of the domain, below the water table (Figure 6.6). The lateral spreading is less than shown in Figure 6.4.

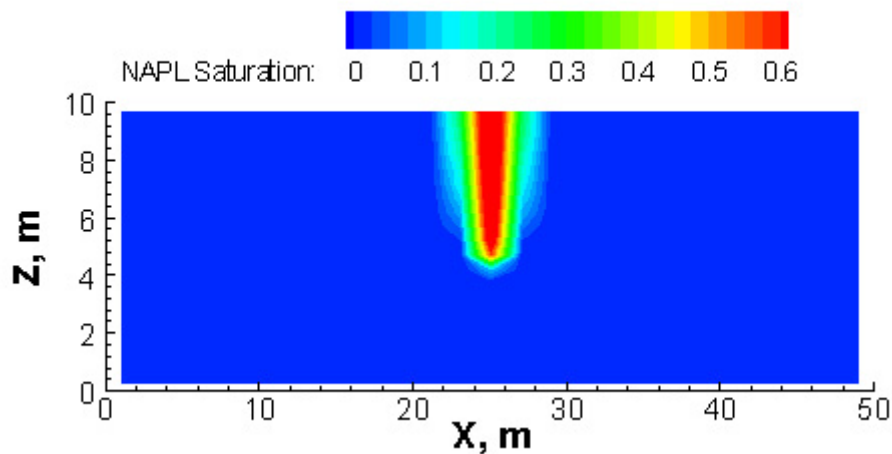


**Figure 6.5** LNAPL spill distribution in 2-dimensional aquifer after 10 days.

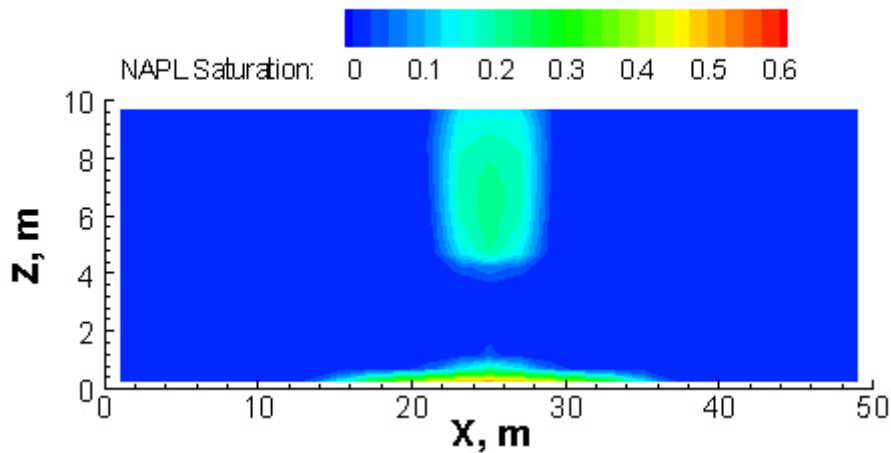


**Figure 6.6** LNAPL spill distribution in 2-dimensional aquifer after 200 days.

**Part1, Exercise 4**

To use a source instead of a boundary condition to introduce the NAPL into the domain use the following source card

```
#-----
~Source Card
#-----
1,
NAPL Volumetric,13,13,1,1,20,20,2,
0,d,.5,m^3/d,
10,d,.5,m^3/d,
```

(You will also have to change the LSTM parameter in the parameters file and the boundary conditions!)

**Part 2, Exercise 6**

The effects of the imposed gradients on LNAPL movement are not yet visible in Figure 6.7. However, as soon as the LNAPL moves below the water table, the LNAPL body is forced to move laterally. The lateral movement in the eastern direction is clearly visible in Figure 6.8.

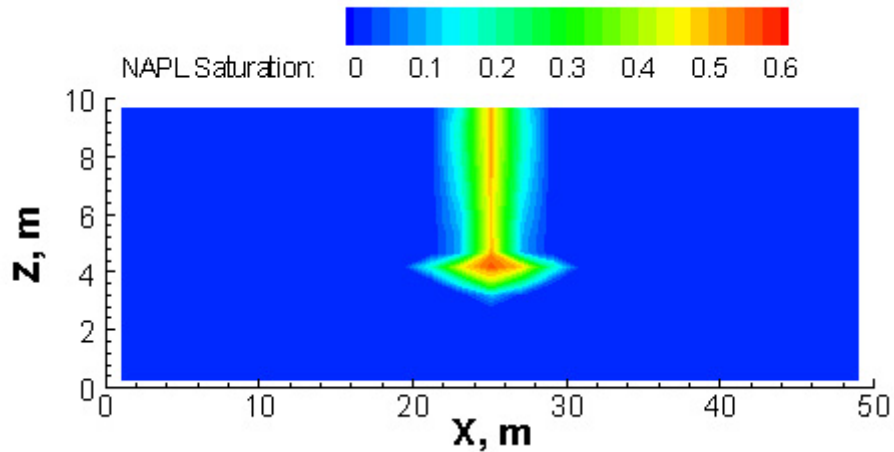


**Figure 6.7** LNAPL spill distribution in 2-dimensional aquifer after 10 days. The simulation included 100ml/year precipitation and a horizontal pressure gradient of 40 Pa/m.

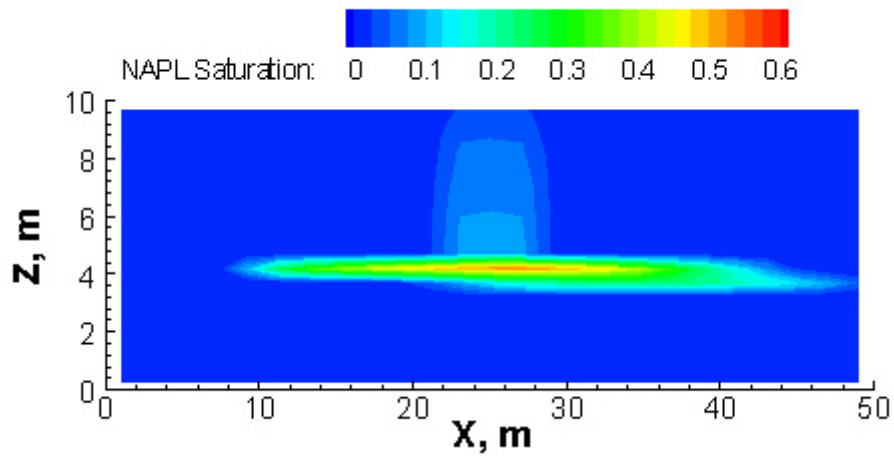


**Figure 6.8** LNAPL spill distribution in 2-dimensional aquifer after 200 days. The simulation included 100ml/year precipitation and a horizontal pressure gradient of 40 Pa/m.

### Part2, Exercise 7

The effects of the hydraulic gradient are clearly visible in Figures 6.9 and 6.10. The LNAPL is forced to move towards the East boundary of the domain.

The movement is considerably faster than for the previous case where the gradient was 40 Pa/m.

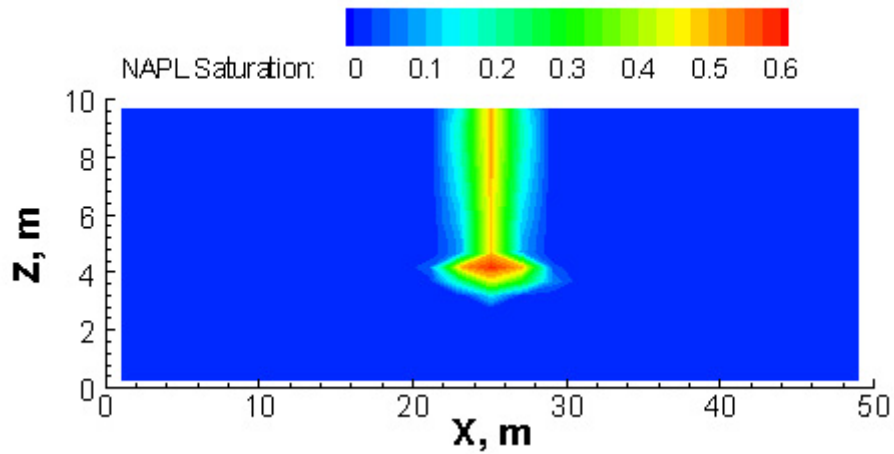


**Figure 6.9** LNAPL spill distribution in 2-dimensional aquifer after 10 days. The simulation included 100ml/year precipitation and a horizontal pressure gradient of 70 Pa/m.

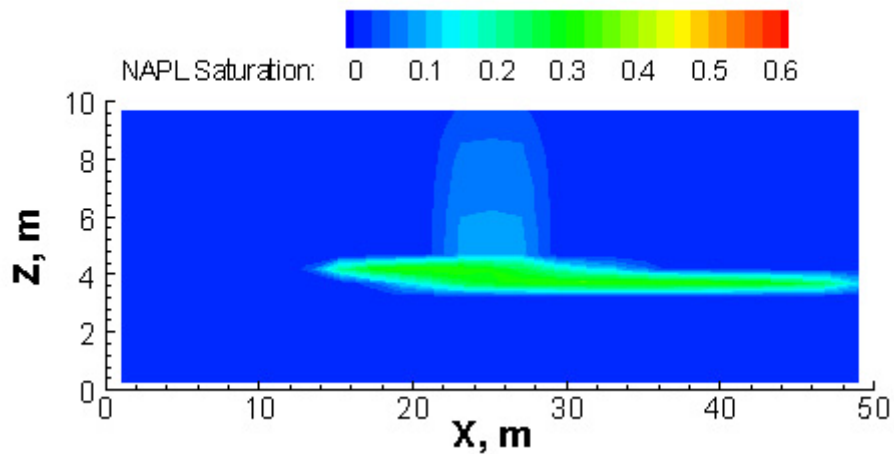


**Figure 6.10** LNAPL spill distribution in 2-dimensional aquifer after 200 days. The simulation included 100ml/year precipitation and a horizontal pressure gradient of 70 Pa/m.

## 7. DNAPL vapor behavior in unsaturated porous media

**Abstract:** *Density effects may be important when contaminant vapors are moved through the subsurface. Volatile organic compounds with a relatively high molecular weight such as trichloroethene (TCE) and carbon tetrachloride may cause density differences to occur in the gas phase. An example is presented that allows the user to investigate when density effects may be important. The user is also asked to develop a soil vapor extraction system that accelerates the removal of a residual NAPL source. The object of this problem is to introduce the user to transport of organic components in the gaseous phase. The Water-Air-Oil mode (STOMP5) is used for this application.*

### 7.1 Problem Description

Volatile organic compounds (VOCs) such as solvents and hydrocarbon fuels are commonly found in the subsurface at many sites. Typically, industrial VOCs have entered the subsurface as nonaqueous-phase liquids (NAPLs) via chemical spills, leaks in storage or transmission structures, and direct disposal to waste sites. VOCs have characteristically a high vapor pressure at normal temperatures and pressures near the earth's surface; therefore, a substantial mass of VOCs will likely be present in the gaseous phase of the subsurface.

Once in the subsurface, VOCs can exist as a separate phase (i.e., a NAPL), as a component of the gaseous phase, and as a component of the aqueous phase. VOCs may also be adsorbed on solid material, either organic or inorganic. The movement of VOCs in the subsurface can occur by advective, diffusive, and

dispersive fluxes of the separate fluid phases. Therefore, to model VOC transport in the gaseous phase, advection, diffusion, and dispersion processes need to be considered. In many fluid flow and transport models, however, gas-phase pressures are assumed to be atmospheric and diffusion the only mechanism with which chemicals in the gaseous phase migrate.

Gas-phase advection is controlled by the network of pores that contain gas, the viscosity of the gaseous phase, and a spatial difference in the gas-phase total potential, which is commonly defined as the sum of the gas-pressure potential and the gravitational potential. Very small gradients in the gas-phase total potential can yield significant advective fluxes because the resistance to gas flow is small (i.e., negligible gas-phase viscosities), and the gaseous phase is contained in the largest pores of liquid-unsaturated porous media. Several investigators have examined density-driven flow of gas caused by VOC contamination and concluded that VOC molecular mass and porous medium permeability are important factors in determining whether density-driven advection is an important transport mechanism.

The problem *input* file is given in section 7.3. The domain is 30 m long in the x-direction and 10 m high in the z-direction. The porous medium is uniform and the water table is located at the bottom of the domain. There is no gradient in the aqueous phase. A zone with residual NAPL saturation of 0.2 is located in a 1 m<sup>3</sup> zone near the west boundary. The DNAPL has a vapor pressure of 12,000 Pa and a molecular weight of 153.82 g/mol. Compared to STOMP4 simulations (Water-Oil), the only additional Card to be specified is the Gas Relative Permeability Card. The total simulation time is 100 days. Plot files are created at 4 additional times. Vapors develop from the NAPL and are transported through the domain via advection and diffusion.

## 7.2 Exercises

1. Given the vapor pressure and Henry's constant, compute the aqueous phase mole fraction of the NAPL.
2. Explain the choice of the values for the gas initial pressure at node (1,1,1) (101319.15 Pa) and the vertical gradient (-11.71 Pa/m).
3. Based on the *input* file, explain why the NAPL is forced to be residual.
4. Run the simulation. Plot the gas concentration at  $t = 100$  days.
5. Make changes in the *input* file to remove density-driven advection in the gaseous phase. Plot the gas concentration at  $t = 100$  days and compare with results of previous exercises.
6. Density effects are assumed to be strong functions of the porous medium permeability. Lower the permeability by a factor 10 and by a factor 100 and plot the results at  $t = 100$  days.
7. Install a vapor extraction system in node (10,1,1). Allow the pumping to start at  $t = 25$  days. Extract with a constant rate from  $t = 25$  to  $t = 100$  days. Choose various rates and observe the effect on the remaining NAPL in the source zone and the final gas concentrations at  $t = 100$  days.
8. Do the same at node (5,1,1). Comment on the differences with what was observed in Exercise 8.

## 7.3 Input File

```
#-----  
~Simulation Title Card  
#-----  
1,  
STOMP Tutorial Problem 7,  
Mart Oostrom/Mark White,  
PNNL,  
June 03,  
15:00,  
2,  
Simulation of 2D vapor density problem,  
Carbon tetrachloride vapor behavior,  
  
#-----  
~Solution Control Card  
#-----  
Normal,  
Water-Oil-Air,  
1,  
0,s,100,d,10,s,10,d,1.25,8,1.e-6,  
10000,  
Variable,  
Constant,0.9e-6,m^2/s,0.9e-6,m^2/s,  
0,  
  
#-----  
~Grid Card  
#-----  
Cartesian,  
20,1,10,  
0,m,10@1,m,10@2,m,  
0,m,1,m,  
0,m,10@1,m,  
  
#-----  
~Rock/Soil Zonation Card  
#-----  
1,  
Sand,1,20,1,1,1,10,  
  
#-----  
~Mechanical Properties Card  
#-----  
Sand,2650,kg/m^3,0.4,0.4,,Millington and Quirk,  
  
#-----  
~Hydraulic Properties Card  
#-----
```

Sand,100.0,hc m/ day,,,100.0,hc m/ day,

#-----

~Saturation Function Card

#-----

72.0,dynes/cm,,,35.43,dynes/cm,  
Sand, Van Genuchten,2.5,1/m,2.0,0.10,72.0,dynes/cm,,

#-----

~Aqueous Relative Permeability Card

#-----

Sand,Mualem,,

#-----

~NAPL Relative Permeability Card

#-----

Sand,Constant,0.0,

#-----

~Gas Relative Permeability Card

#-----

Sand,Mualem,,

#-----

~Oil Properties Card

#-----

Carbontetrachloride,  
153.82,g/mol,250.,K,349.9,K,556.4,K,  
45.6,bar,275.9,cm<sup>3</sup>/mol,0.272,0.193,0.0,debyes,  
4.072e+1,2.0496e-1,-2.27e-4,8.843e-8,  
Constant,12000,Pa,  
Constant,1623,kg/m<sup>3</sup>,  
Constant,0.97e-3,Pa s,  
1.3062e8,Pa,

#-----

~Dissolved Oil Transport Card

#-----

Sand,0.2,cm,0.02,cm,linear kd,0.0,m<sup>3</sup>/kg,

#-----

~Initial Conditions Card

#-----

4,  
Aqueous Pressure,96428.24,Pa,,,,,-9793.5192,1/m,1,20,1,1,1,10,  
Gas Pressure,101319.15,Pa,,,,,-11.71,1/m,1,20,1,1,1,10,  
NAPL Pressure,-1.e9,Pa,,,,,1,20,1,1,1,10,  
NAPL Pressure,93845.17,Pa,,,,,1,1,1,1,8,8,

#-----

~Boundary Conditions Card

```
#-----  
2,  
east,hydraulic gradient,hydraulic gradient,dirichlet,  
20,20,1,1,1,10,1,  
0,d,96428.24,Pa,,,101319.15,Pa,,,1.e9,Pa,  
bottom,zero flux,zero flux,zero flux,  
1,20,1,1,1,1,1,  
0,d,101325,Pa,,,1.e9,Pa,,,1.e9,Pa,
```

```
#-----  
~Output Options Card
```

```
#-----  
6,  
1,1,8,  
1,1,5,  
5,1,1,  
6,1,8,  
6,1,5,  
20,1,1,  
1,1,day,m,6,6,6,  
3,  
aqueous saturation,,  
napl saturation,,  
oil gas concentration,g/l,  
4,  
1.0,d,  
5.0,d,  
10.0,d,  
50.0,d,  
4,  
no restart,,  
aqueous saturation,,  
napl saturation,,  
oil gas concentration,g/l,
```

## 7.4 Solutions to Selected Exercises

### Exercise 1

Henry's constant for carbon tetrachloride is given in the last entry of the Oil Properties Card ( $H = 1.3062e8$  Pa). This is the ratio of the oil vapor pressure to the mole fraction of oil in the aqueous phase. Since the vapor pressure is 12,000 Pa, the aqueous mole fraction is  $9.187e-5$ .

### Exercise 2

The density of the gas phase leads to a vertical gradient of  $-11.71$  m/Pa for the gas pressure in the soil above the water table. The lowest vertical node in the domain is 0.5 m above the water table and is therefore initialized with a pressure of  $-11.71 * 0.5 + 101325$  Pa or 101319.15 Pa.

### Exercise 3

The NAPL is forced to be residual in the NAPL Relative Permeability Card. The permeability function is specified as constant with a NAPL relative permeability of 0.0. The liquid phase NAPL will not be able to move and is in effect residual.

### Exercise 4

The plot for the case including density-driven advection is shown in Figure 7.1. The vapors are move down rapidly and are then forced to move laterally on top of the water table.

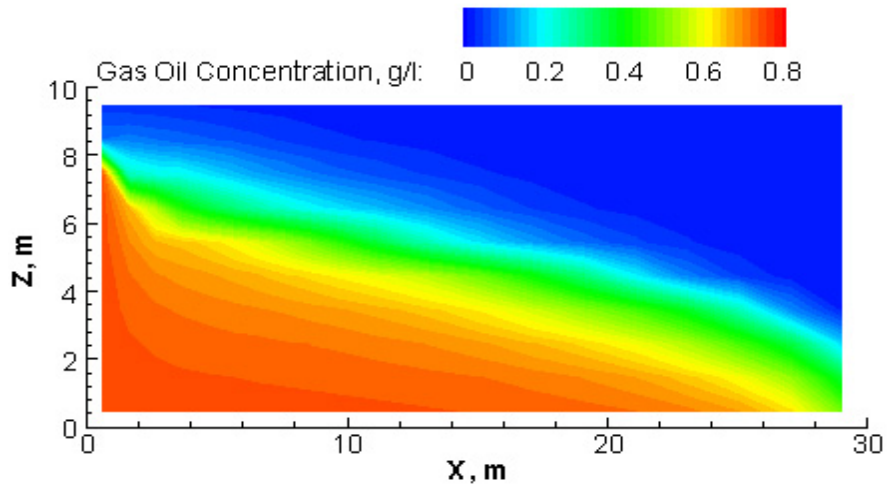


**Figure 7.1** Gas oil concentration distribution after 100 days with density-driven gaseous advection.

### Exercise 5

To remove density-driven advection, the Gas Relative Permeability Card is altered as follows:

```
#-----
~Gas Relative Permeability Card
#-----
Sand,Constant,0.0,
```

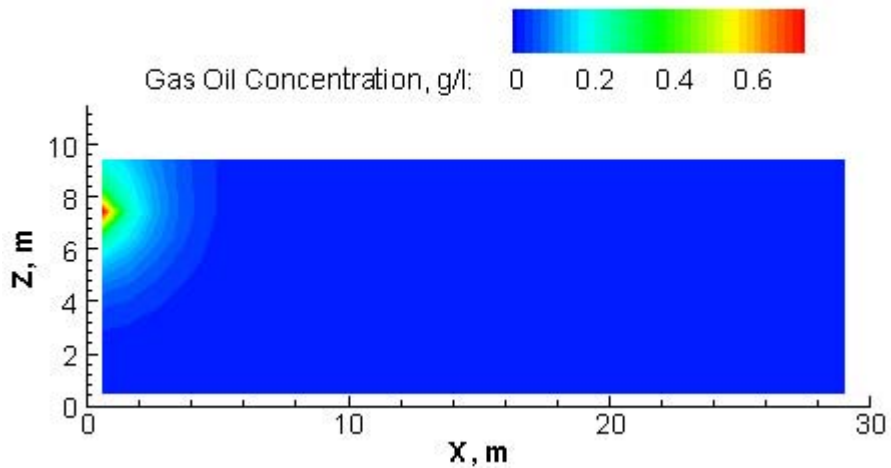


**Figure 7.2** Gas oil concentration distribution after 100 days without density-driven gaseous advection.

The resulting plot is shown in Figure 7.2. Compared to Figure 7.1, the vapor plume is less pronounced. It is obvious that ignoring density-driven advection has large effects on the simulation results.

### Exercise 6

Density-driven gaseous advection is a strong function of the permeability of the porous medium as illustrated by Figures 7.3 and 7.4. The lower the permeability, the less pronounced the density effects.

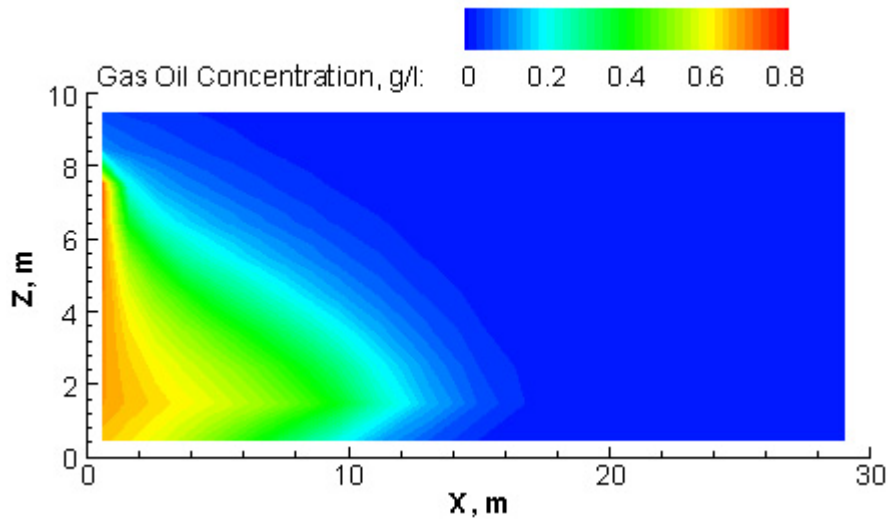


**Figure 7.3** Gas oil concentration distribution after 100 days with density driven gaseous advection. The hydraulic conductivity was reduced by a factor of 10.

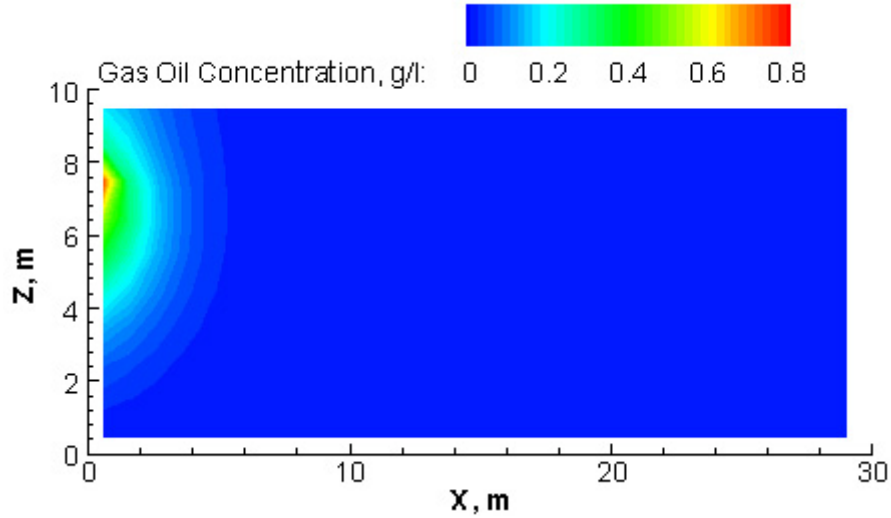


**Figure 7.4** Gas oil concentration distribution after 100 days with density driven gaseous advection. The hydraulic conductivity was reduced by a factor of 100.

### Exercise 7

A rate of 800 L/day was chosen for this exercise. The resulting plot at 6 = 100 days is shown in Figure 7.5. Compared to Figure 7.1, Figure 7.5 demonstrates that soil vapor extraction might be an effective process for this particular simulation.

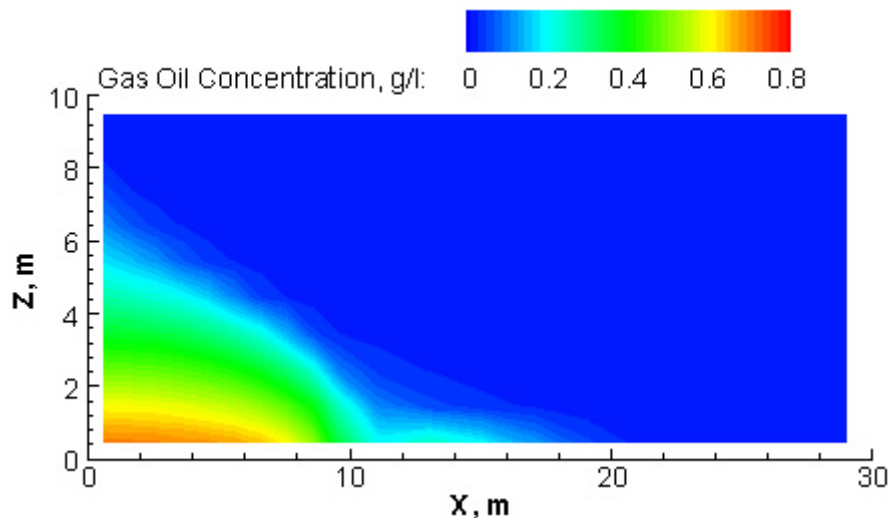


**Figure 7.5** Gas oil concentration distribution after 100 days with a 800 L/day vapor extraction system at node (10,1,1) pumping from day 25 to day 100.

## Exercise 8

Comparing Figure 7.5 and Figure 7.6 shows that the vapor extraction system is more effective closer to the source. The reduced distance to the source causes an increase in the gaseous flow rates and the original source of the contamination could be completely eliminated. The liquid NAPL evaporated into the gaseous phase more quickly because the vapor extraction system pulled the gas away quickly allowing more NAPL to evaporate.

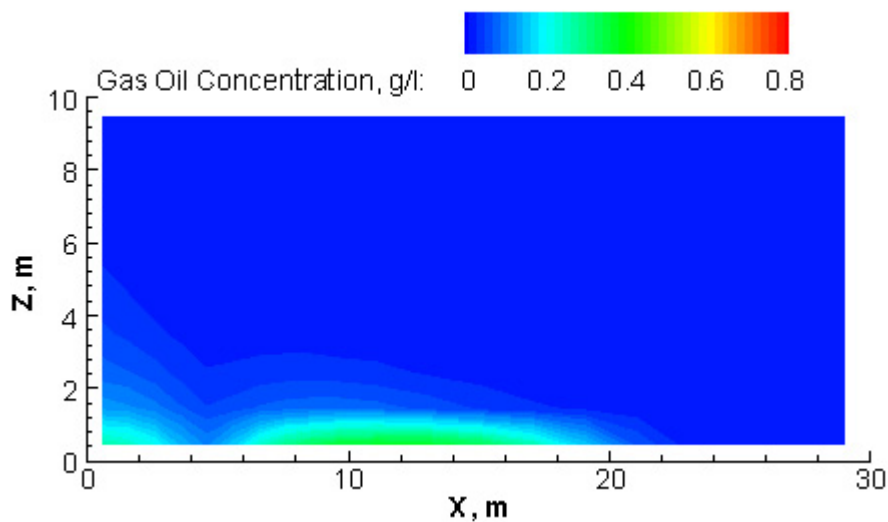


**Figure 7.6** Gas oil concentration distribution after 100 days with a 800 L/ day vapor extraction system at node (5,1,1) pumping from day 25 to day 100.

## 8. Simulation of partitioning tracer transport to detect and quantify NAPLs

**Abstract:** *In this example, the equilibrium behavior of conservative and partitioning tracers in the presence of a DNAPL is simulated. First, a 1-D experiment described by Jin et al. (1995) will be simulated with the water-oil mode. After completing the 1D simulation, the user is asked to design an input file for a 2D tracer experiment based on a conceptual model and description.*

### 8.1 Problem Description

DNAPLs occur in the subsurface at numerous contaminated sites and are usually considered to be long-term sources of groundwater contamination. The development and application of new remediation technologies require an understanding of flow and transport of DNAPLs in the subsurface. Knowledge of DNAPL distribution is important for implementation of source control strategies. Appropriate risk based decisions can not be made for a contaminated site without knowing if DNAPL is present at the site.

Current methods used for characterizing potential DNAPL sites include soil gas analysis, core sampling, cone penetrometer testing, and monitoring well sampling. These methods provide data for relatively small volumes of the subsurface and require the use of a dense sampling network and application of geostatistics to determine the overall contaminant distribution. The partitioning tracer test is an alternative, larger-scale method for locating and quantifying DNAPL saturation in the subsurface. This method involves the use of partitioning tracers, which distribute into DNAPLs, and are thus retarded and separated from non-partitioning tracers during transport.

The procedure for estimating DNAPL saturation,  $s_n$ , involves calculation of a retardation factor (R) for the partitioning tracer, which is done by a comparative moment analysis with the nonreactive tracer. The retardation factor is defined as the velocity of water (nonreactive tracer) divided by the velocity of the partitioning tracer. With knowledge of R,  $K_{ln}$  (water-DNAPL partition coefficient),  $K_d$  (sorption coefficient),  $\rho_b$  (dry soil bulk density), and  $s_l$  (aqueous saturation),  $s_n$  can be calculated from:

$$R = 1 + \frac{\rho_b}{ns_l} K_d + \frac{s_n}{1 - s_n} K_{ln} \quad 8.1$$

The terms on the right-hand side of the equation describe retention of the tracer by the aqueous, solid phase, and DNAPL phases, respectively. For a tracer with no sorption to the porous media, Eq. (2) simplifies to:

$$R = 1 + \frac{s_n}{1 - s_n} K_{ln} \quad 8.2$$

The experiment described by Jin et al. (1995; Exp. DW2) was conducted in a 30.5-cm stainless steel column with a diameter of 2.21 cm. The column was packed with Ottawa sand. The porosity of the column was 0.362 and the permeability of the sand  $15.3 \cdot 10^{-12} \text{ m}^2$ . Residual saturation of tetrachloroethylene (PCE) was established by injecting the organic liquid at a rate of 0.5 ml/min for 1.1 pore volumes in an upward direction, followed by injecting water at the same flow rate for 2.1 pore volumes in a downward direction. Using the methods of weight and volume measurements, the average residual saturation in the column was 0.202 and 0.197, respectively.

Three different tracers were used: Tritium ( $K_{ln} = 0.00$ ), isopropanol (IPA;  $K_{ln} = 0.04$ ), and 2,3 dimethyl 2-butanol (DMB;  $K_{ln} = 2.76$ ). In the experiment, 0.1 pore volumes of water containing the tracers was injected at 0.05 ml/min, followed by injection of clean water at the same rate. Inverse modeling conducted by Jin et al. (1995) yielded a porous medium dispersivity of 0.17 cm. For the molecular diffusion coefficient, a value of  $10^{-10}$  m<sup>2</sup>/s was assumed. PCE entrapment was accomplished by assuming a maximum residual saturation of 0.3 in the Saturation Function Card and a constant residual saturation of 0.2 in the Initial Conditions Card. Entrapment was only hysteretic fluid displacement process considered in the simulations. The associated input file is listed in section 8.3. The total simulation period is 2400 minutes of which the first 84.705 minutes were used to inject the tracer cocktail. The flux rate used in the Boundary Condition Cards is computed based on the diameter of column, the injected total volume and the imposed rate. The sign of the Neumann flux is negative because the fluid is injected from the top boundary in a downward direction. It is also important to note the 4 Boundary Condition times associated with the top boundary. For the bottom boundary it is assumed that the fluid outlet was kept level with the top of the column.

### *Reference*

Jin, M. M. Delshad, V. Dwarakanath, D.C. McKinney, G.A. Pope, K. Sepehrnoori, C.E. Tilburg. 1995. Partitioning tracer test for detection, estimation, and assessment of subsurface nonaqueous phase liquids. *Water Resources Research* 31: 1201-1211.

## 8.2 Exercises

1. Run the 1D problem (*input* file in section 8.3) with both standard Patankar and TVD transport. Make plots of breakthrough curves (tracer concentration vs. time) at the outlet (node 1,1,50) using the *output* file and make plots of concentration vs. elevation in the column using the various *plot* files.
2. Change the trapped DNAPL saturation from 0.2 to 0.05 and rerun the simulation (TVD transport only). Compare the breakthrough curves of tritium and DMB at the outlet.
3. Develop an input file for a 2D simulation using the 1D simulation as a basis. The experimental flow cell is 1.0 m long, 0.1 m wide, and 1.0 m high. Use the following grid card:

```
#-----  
~Grid Card  
#-----  
Cartesian,  
11,1,11,  
0,cm,10,cm,20,cm,30,cm,40,cm,47,cm,53,cm,60,cm,70,cm,80,cm,90,cm,100,cm,  
0,cm,10,cm,  
0,cm,10,cm,20,cm,30,cm,40,cm,47,cm,53,cm,60,cm,70,cm,80,cm,90,cm,100,cm,
```

Notice that this grid card allows us to specify the locations of the different sands as required below, but it also allows data to be collected at the requested locations (see Figure 8.4). The used porous media are coarse sand and fine sand. The properties of the sands are the same, except for the hydraulic conductivity. The coarse sand has a hydraulic conductivity of 100 m/day and the fine sand a hydraulic conductivity of 1 m/day. The porosity of both sands is 0.4. The fine sand is located between  $x = 0.2$  and  $0.8$  m and between  $z = 0.4$  and  $0.6$  m. The remainder of the flow cell contains the coarse sand. The aqueous relative permeability of the fine sand is assumed to be constant at 0.5. For all other

relative permeabilities, the Mualem relation can be used. Both sands have a Van Genuchten  $\alpha$  of  $2.5 \text{ 1/m}$ , a Van Genuchten  $n$  of  $2.0$ , and an irreducible water saturation of  $0.1$ . Initially, the flow cell is fully saturated and the fine sand contains a uniform trapped NAPL zone with  $15\%$  saturation. The total experimental duration is  $10$  days and water is injected for the duration with a rate of  $40 \text{ cm/day}$  at the west side. On day 2, the injected water contains two tracers with a concentration of  $1/\text{cm}^3$ . On the east side of the flow cell, a hydraulic gradient is maintained for the aqueous phase. No NAPL is allowed to move over any boundary. Three sampling locations are identified in Figure 8.1. Use partitioning coefficients similar to the values used in the 1-D problem. Make *plot* files for both tracers at several times and verify water and tracer injection through an appropriate Surface Card. Compare the breakthrough behavior of the tracers at the indicated locations. Comment on the effectiveness of the partitioning tracer test in this example.

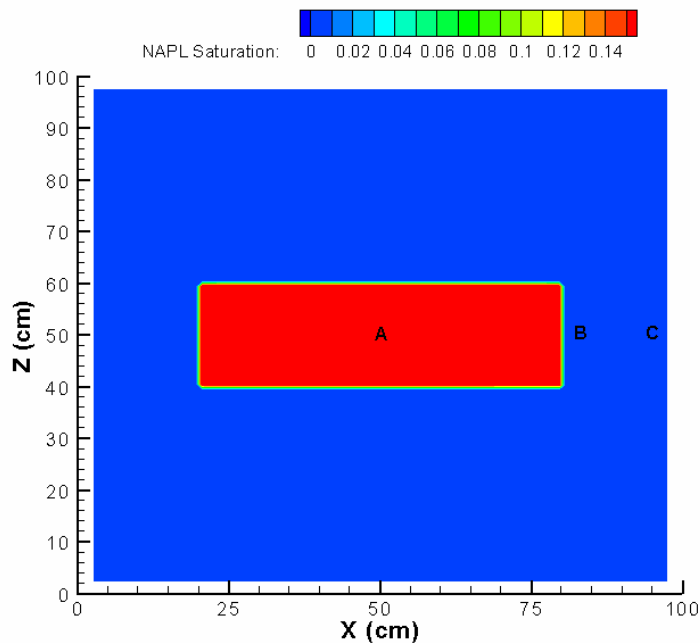


**Figure 8.1** Zone with entrapped DNAPL and sampling locations in the 2D experiment.

### 8.3 Input File

```
#-----  
~Simulation Title Card  
#-----  
1,  
STOMP Tutorial Problem 8,  
Mart Oostrom/Mark White,  
PNNL,  
June 03,  
15:00,  
4,  
Simulation of 1D partitioning tracer experiment,  
Partitioning tracer test for detection, estimation, and,  
assessment of subsurface nonaqueous phase liquids,  
Water Resources Research, Vol. 31, No. 5, Pages 1201-1211, May 1995,  
  
#-----  
~Solution Control Card  
#-----  
Normal,  
Water-Oil w/ Transport,  
1,  
0,s,2400,min,0.1,s,5,min,1.25,8,1.e-6,  
10000,  
Variable Aqueous Diffusion,  
,  
  
#-----  
~Grid Card  
#-----  
Uniform Cartesian,  
1,1,50,  
1.958562,cm,  
1.958562,cm,  
0.61,cm,  
  
#-----  
~Rock/Soil Zonation Card  
#-----  
1,  
Ottawa sand,1,1,1,1,50,  
  
#-----  
~Mechanical Properties Card  
#-----  
Ottawa sand,2650,kg/m^3,0.362,0.362,,,Millington and Quirk,  
  
#-----  
~Hydraulic Properties Card  
#-----  
Ottawa sand,,,,,1.5e-4,hc m/s,  
  
#-----  
~Saturation Function Card  
#-----  
72.0,dynes/cm,,,35.43,dynes/cm,
```

Ottawa sand,Entrapment Van Genuchten,2.7,1/m,1.23,.26,72.0,dynes/cm,,0.3,0,

#-----  
~Aqueous Relative Permeability Card  
#-----  
#Rel perm estimated from Lenhard and Parker 1987 Eq. (5)  
Ottawa sand,Constant,0.8,

#-----  
~NAPL Relative Permeability Card  
#-----  
Ottawa sand,Mualem,0.5,

#-----  
~Solute/Fluid Interactions Card  
#-----  
3,  
Tritium,1.0e-10,m^2/s,1.0e-10,m^2/s,  
Linear Isotherm,0.0,  
1.e+8,yr,  
IPA,1.0e-10,m^2/s,1.0e-10,m^2/s,  
Linear Isotherm,0.04,  
1.e+8,yr,  
DMB,1.0e-10,m^2/s,1.0e-10,m^2/s,  
Linear Isotherm,2.76,  
1.e+8,yr,  
0,

#-----  
~Dissolved Oil Transport Card  
#-----  
Ottawa sand,0.17,cm,,cm,linear kd,0.0,m^3/kg,

#-----  
~Solute/Porous Media Interactions Card  
#-----  
Ottawa sand,0.17,cm,,cm,  
tritium,Linear Isotherm,0.0,  
IPA,Linear Isotherm,0.0,  
DMB,Linear Isotherm,0.0,

#-----  
~Oil Properties Card  
#-----  
PCE,  
165.834,g/mol,251.,K,394.4,K,620.2,K,  
47.6,bar,289.6,cm^3/mol,0.2758,0.2515,0.0,debyes,  
-1.431e+1,5.506e-1,-4.513e-4,1.429e-7,  
Equation 1,-7.36067,1.82732,-3.47735,-1.00033,  
Modified Rackett,0.2758,0.2515,  
Constant,0.97e-3,Pa s,  
9.463e7,Pa,

#-----  
~Initial Conditions Card  
#-----

3,  
Aqueous Pressure,104282.15,Pa,,,,,-9793.5192,1/m,1,1,1,1,50,  
NAPL Pressure,-1.e9,Pa,,,,,1,1,1,1,50,  
Trapped NAPL Saturation,0.20,,,,,,1,1,1,1,50,

#-----  
~Boundary Conditions Card

#-----  
2,

top,neumann,zero flux,inflow aqueous,inflow aqueous,inflow aqueous,  
1,1,1,50,50,4,  
0,d,-0.013035,cm/min,0.0,-1.e9,Pa,1.0,1/cm^3,1.0,1/cm^3,1.0,1/cm^3,  
84.705,min,-0.013035,cm/min,0.0,-1.e9,Pa,1.0,1/cm^3,1.0,1/cm^3,1.0,1/cm^3,  
84.705,min,-0.013035,cm/min,0.0,-1.e9,Pa,0.0,1/cm^3,0.0,1/cm^3,0.0,1/cm^3,  
2400.,min,-0.013035,cm/min,0.0,-1.e9,Pa,0.0,1/cm^3,0.0,1/cm^3,0.0,1/cm^3,  
bottom,dirichlet,zero flux,outflow,outflow,outflow,  
1,1,1,1,1,1,  
0,d,104312.02,Pa,0.0,-1.e9,Pa,,,,,

#-----  
~Output Options Card

#-----

3,  
1,1,1,  
1,1,25,  
1,1,50,  
1,1,min,cm,6,6,6,  
6,  
napl saturation,,  
aqueous courant number,,  
z aqueous volumetric flux,cm/min,  
solute aqueous concentration,tritium,1/cm^3,  
solute aqueous concentration,IPA,1/cm^3,  
solute aqueous concentration,DMB,1/cm^3,  
4,  
84.705,min,  
6,hr,  
12,hr,  
24,hr,  
5,  
no restart,,  
napl saturation,,  
solute aqueous concentration,tritium,1/cm^3,  
solute aqueous concentration,IPA,1/cm^3,  
solute aqueous concentration,DMB,1/cm^3,

#-----  
~Surface Flux Card

#-----

5,  
solute flux,tritium,1/min,,top,1,1,1,50,50,  
solute flux,tritium,1/min,,bottom,1,1,1,1,1,1,  
solute flux,ipa,1/min,,bottom,1,1,1,1,1,1,  
solute flux,dmb,1/min,,bottom,1,1,1,1,1,1,  
aqueous volumetric flux,ml/min,ml,top,1,1,1,50,50,

## 8.4 Solutions to Selected Exercises

### Exercise 1

For the sake of graph clarity all the graphs in the simulations of the 1D problem do not include the IPA solute data. The IPA has a water-DNAPL partition coefficient that is very close to the value for the Tritium and the two solutes behave almost identically. The breakthrough behavior of the two tracers is as expected and is shown in Figures 8.2 – 8.5. The non-partitioning tritium passed through the column more quickly than the partitioning DMB. The Patankar transport scheme introduced more numerical diffusion than the TVD scheme.

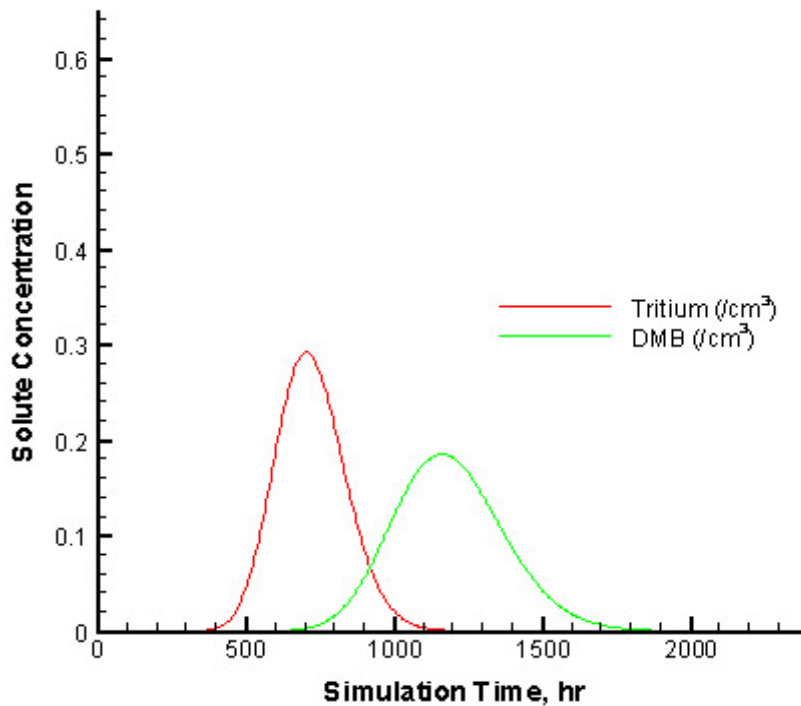


**Figure 8.2** Simulated (Patankar Transport) tritium and DMB concentrations versus time at the column outlet.

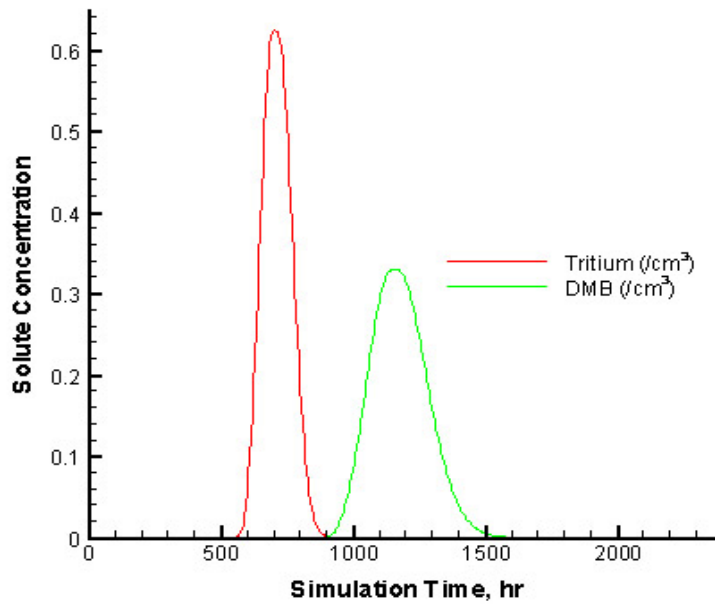
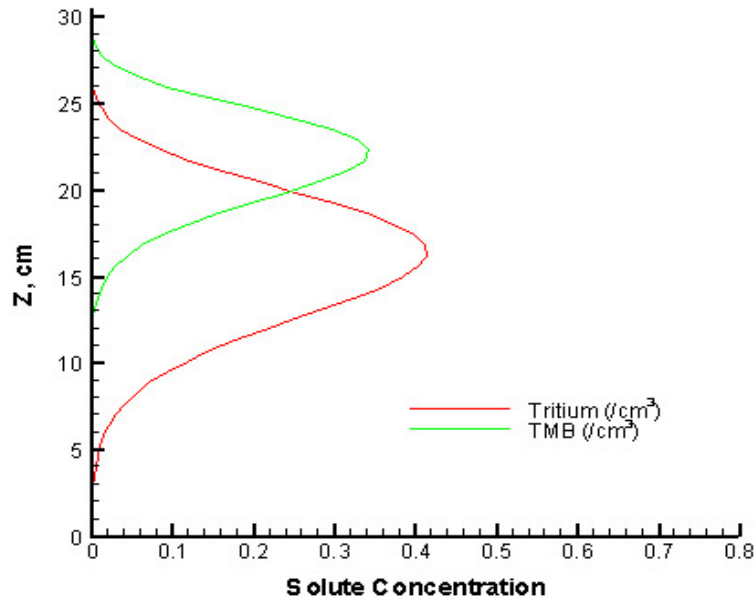


**Figure 8.3** Simulated (TVD Transport) tritium and DMB concentrations versus time at the column outlet.

Snapshots of the tracer concentrations versus column position at  $t = 6$  hours illustrate how the partition coefficient affects the spatial solute distributions (see Figures 8.4 and 8.5)



**Figures 8.4** Simulated (Patankar Transport) tritium and DMB concentrations versus column position at  $t = 6$  hours.

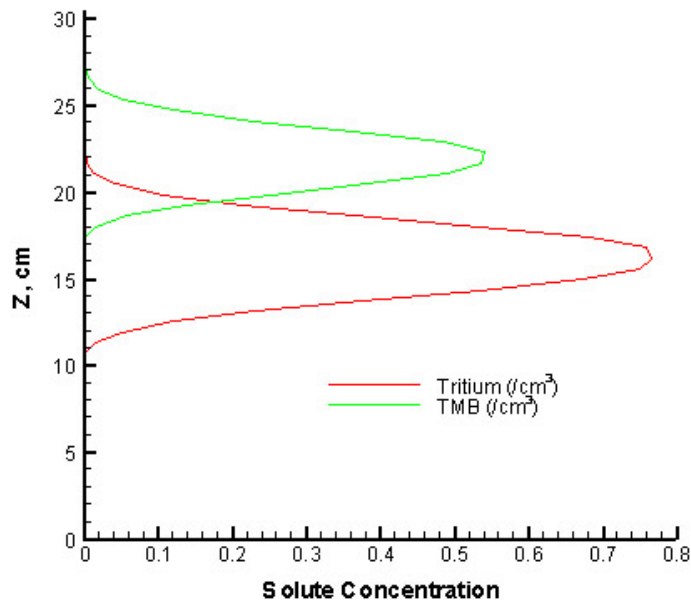


**Figure 8.5** Simulated (TVD Transport) tritium and DMB concentrations versus column position at  $t = 6$  hours.

### Exercise 2

To change the trapped DNAPL saturation from 0.2 to 0.05, just change the value on the initial conditions card. The effect is illustrated in Figure 8.6. The two solutes pass through the lowest node in the column with less of a time delay between the two indicating less initial NAPL present in the system. The breakthrough curves for the original saturation are included as dashed lines for comparison.

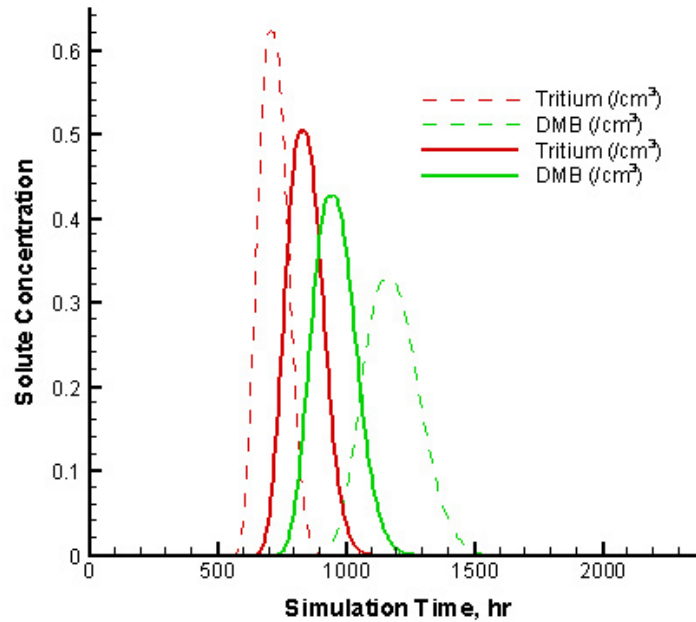


**Figure 8.6** Simulated (TVD Transport) tritium and DMB concentrations versus time at the column outlet.

**Exercise 3**

The Solution Control Card and the Boundary Conditions Card are the important cards for this exercise:

```
#-----
~Solution Control Card
#-----
Normal,
Water-Oil w/TVD Transport,
2,
0,d,2,d,.1,s,.5,d,1.24,8,1.e-6,
2,d,10,d,10,min,10,min,1.25,8,1.e-6,
10000,
Variable Aqueous Diffusion,
,

#-----
~Boundary Conditions Card
#-----
2,
west,neumann,zero flux,inflow aqueous,inflow aqueous,
1,1,1,1,1,1,6,
```

```

0,d,40,cm/d,0.0,-1.e9,Pa,0.0,1/cm^3,0.0,1/cm^3,
2,d,40,cm/d,0.0,-1.e9,Pa,0.0,1/cm^3,0.0,1/cm^3,
2,d,40,cm/d,0.0,-1.e9,Pa,1.0,1/cm^3,1.0,1/cm^3,
3,d,40,cm/d,0.0,-1.e9,Pa,1.0,1/cm^3,1.0,1/cm^3,
3,d,40,cm/d,0.0,-1.e9,Pa,0.0,1/cm^3,0.0,1/cm^3,
10,d,40,cm/d,0.0,-1.e9,Pa,0.0,1/cm^3,0.0,1/cm^3,
east,hydraulic gradient,zero flux,outflow,outflow,
11,11,1,1,1,11,1,
0,d,110628.84,Pa,0.0,-1.e9,Pa,,,,,,

```

The simulator is controlled in two execution time periods. There is no solute in the system for the first two days and the Courant and Peclet numbers are not important. In the first two days the flow is allowed to equilibrate and the trapped NAPL to re-distribute. The flow pattern is illustrated in Figure 8.7.

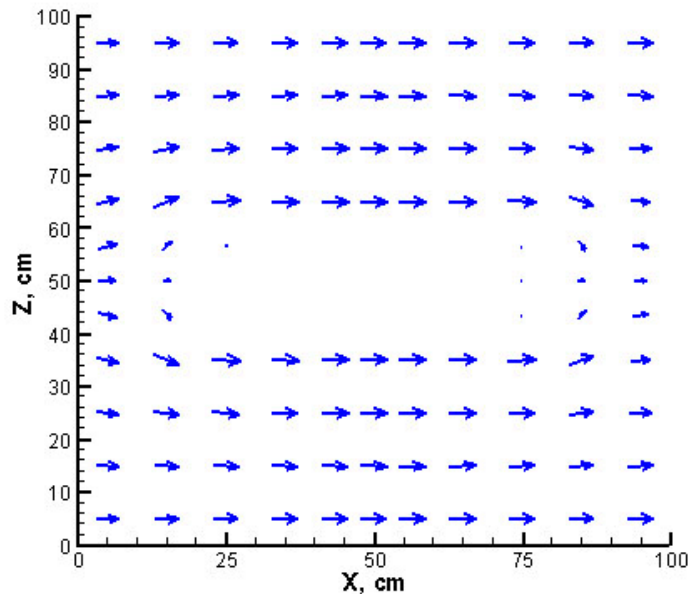


**Figure 8.7** Simulated aqueous flow field in 2D partitioning tracer transport simulation.

The flow pattern illustrates one severe limitation of the partitioning tracer method for determining the amount of NAPL in a soil system. The trapped NAPL is located in a hydraulically inaccessible region of the system and therefore the effect of the partitioning method is limited. This point is illustrated

by the solute breakthrough curves at Locations A and C in Figures 8.8 and 8.9. These curves alone would suggest that there is *not any NAPL in the system!*

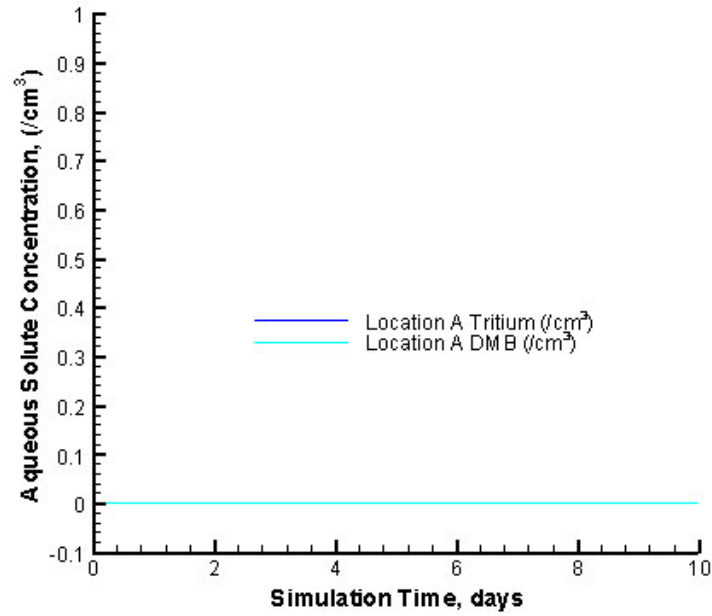


**Figure 8.8** Solute concentration as a function of time at the center of the fine sand (Location A).

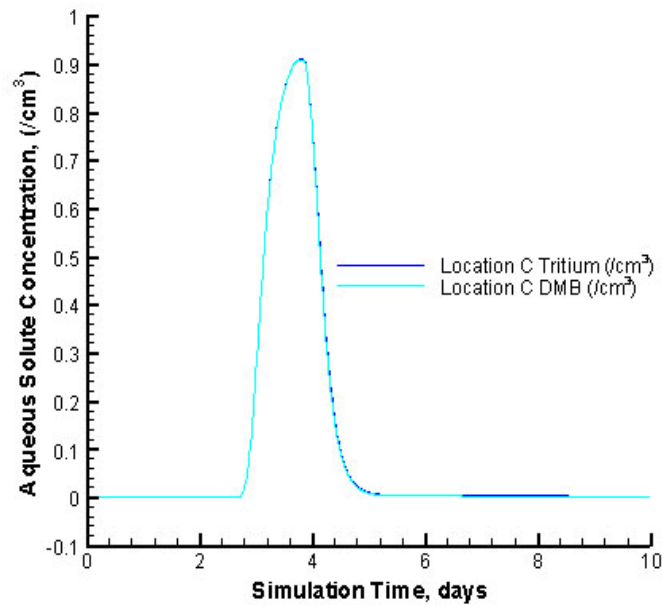


**Figure 8.9** Solute concentrations as a function of time at Location C.

There are several other important lessons to learn from this exercise. The time step used in the solution control card was not chosen at random. The courant number for TVD transport should be below 0.2. The simulator can calculate the courant number for any node at any time step. This is useful when the pore water velocities are unknown, or varying. The time step was chosen so that the courant number was below 0.2 *throughout the entire flow field*. The courant number 'distribution' is shown in Figure 8.10.

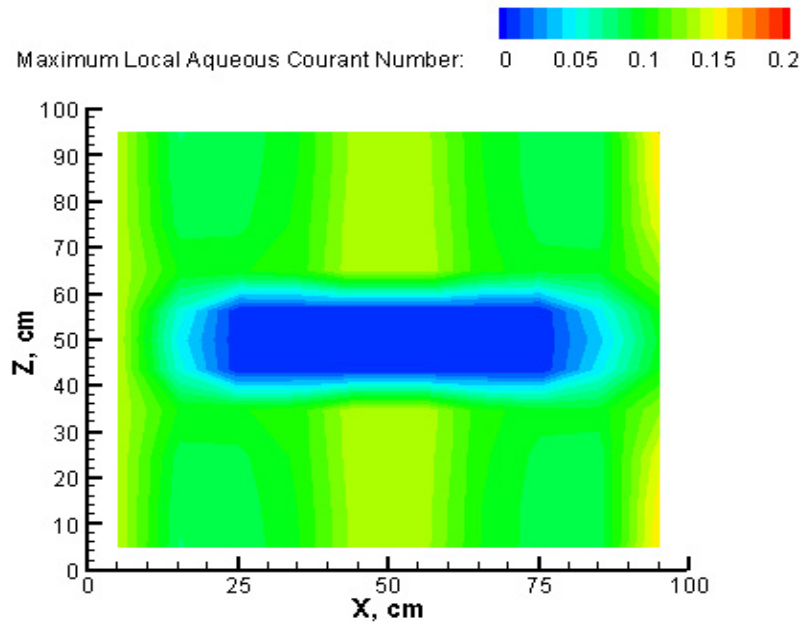


**Figure 8.10** Courant number distribution at steady-state flow in 2D solute transport simulation

The time step is forced to be 10 minutes for the 8 days of the simulation when there is solute present. If the courant number was not controlled in this manner the TVD transport method can yield bizarre results. Graphed in Figure 8.11 is the solute distribution at  $t=4$  days for time steps of 1.5 hours.

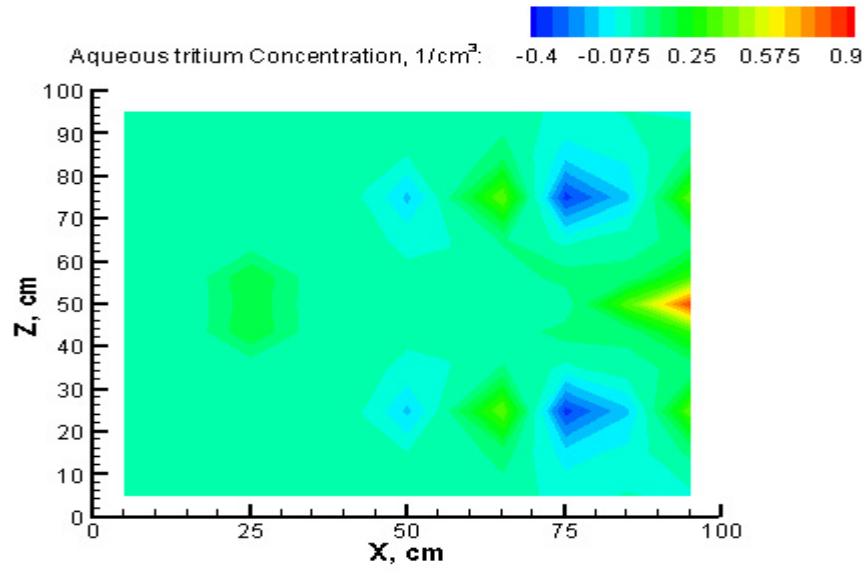


**Figure 8.11** Solute distribution without proper control of Courant Number (1.5-hour time step).

## 9. Simulation of supercritical CO<sub>2</sub> into a deep saline aquifer (CO<sub>2</sub> sequestration)

**Abstract:** *One viable scenario for geologic sequestration of anthropogenic CO<sub>2</sub> is its injection into deep saline aquifers. To evaluate the potential for a field application of this scenario, numerical simulations of the CO<sub>2</sub> injection process will be necessary. In the absence of long-term field experiments, which will be cost and time prohibitive for most applications, numerical simulation is the most comprehensive means for predicting the complex behavior of multiple fluids under complex hydrogeologic conditions and evaluating the feasibility for geologic sequestration of CO<sub>2</sub>. Numerical simulations will additionally provide critical information required to obtain regulatory permits and satisfy stakeholder concerns prior to injecting CO<sub>2</sub>, including reservoir pressure, CO<sub>2</sub> migration and dissolution behavior, and the potential for leakage to the ground surface.*

### 9.1 Problem Description

To numerically simulate CO<sub>2</sub> sequestration in deep saline aquifers, several special features are needed in the numerical model. First, the simulator must have multifluid capabilities with algorithms for handling phase transitions (i.e., phase appearances and disappearances). Depending on the system pressure and temperature, injected CO<sub>2</sub> occurs as liquid, gas, or supercritical fluid. A precondition for efficient and safe storage of CO<sub>2</sub> is that it not transition from a liquid or supercritical fluid state into a gas state, during the sequestration process. Numerical simulators for geologic sequestration of CO<sub>2</sub> should, therefore, be able to predict when such phase transitions occur. Long-term sequestration of CO<sub>2</sub> in deep saline aquifers is envisioned to occur via CO<sub>2</sub> dissolution in the brine or chemical complexation with the formation. To accurately model CO<sub>2</sub> dissolution the numerical simulator must have capabilities

for buoyancy driven flow, Rayleigh instability fingering, aqueous dissolution, molecular diffusion, hydrodynamic dispersion, and phase transitions. The *H2O-NaCl-CO2* and *H2O-NaCl-CO2-Energy* operational modes of the STOMP simulator have the capabilities described above for modeling sequestration of CO<sub>2</sub> in deep saline aquifers.

The CO<sub>2</sub> injection simulation involves a two-dimensional radial domain (36° wedge) with the injection well situated at the center of the domain. Radially, the computational domain extents from the well radius of 0.25 to 3350 ft. Vertically the computational domain ranges from 6400 to 4900 ft below ground surface. The bottom nine grid rows represent the injection formation, which is a sandstone. The overlying six grid rows constitute the immediate caprock above the injection layer. The inner-radial vertical boundary, representing the well casing is treated as a zero flux boundary and the outer-radial vertical boundary uses a unit hydraulic gradient boundary, representing hydrostatic conditions remote from the well. Upper and lower horizontal surfaces are considered zero flux boundaries. These boundary conditions allow displaced brine to only flow out the outer-radial vertical boundary. CO<sub>2</sub> injection is simulated by specifying a CO<sub>2</sub> mass injection rate for the lowest nine grid cells adjacent to the well casing, representing a screened well over the sandstone interval. An injection rate of 1 mt/yr of CO<sub>2</sub> was used, adjusted to 100 kt/yr (13727.5 lb-mole/d) for the 36° domain of the model. The simulation was executed for 20 years of injection followed by 20 years of post injection. Soil moisture retention was described using the Brooks and Corey formulation, as shown in Equation (9.1). Aqueous and gas relative permeability were described using a modified Corey function, as shown in Equation (9.2) and (9.3).

$$S_l = \left[ \frac{h_{gl}}{\psi} \right]^\lambda [1 - S_m] + S_m = \bar{S}_l [1 - S_m] + S_m \text{ for } h_{gl} > \psi \quad (9.1)$$

$$S_l = 1 = \bar{S}_l \text{ for } h_{gl} \leq \psi$$

$$k_{rl} = k_{rl}^{ref} \left[ \frac{S_l - S_{lr}}{1 - S_{lr} - S_{gr}} \right]^\beta \quad (9.2)$$

$$k_{rg} = k_{rg}^{ref} \left[ \frac{S_l - S_{lr}}{1 - S_{lr} - S_{gr}} \right]^\beta \quad (9.3)$$

The input file for this simulation, listed in section 9.3, shows how to introduce a “plug” source. The *Source Card* has one source, representing the injection of CO<sub>2</sub> mass into the column of nine nodes adjacent to the well screen. The injection period starts at time zero and continues at a constant rate of 0.352413 kg/s for each grid cell for 20 years (i.e., 7300 days). For a source with multiple time entries, the first and last time entries represents the start and stop times, respectively. By default, the simulator matches time steps with times for execution periods, sources, boundary conditions, and plot files.

Simulation results in terms of gas-saturation contours at years 10, 20, 30, and 40 are shown in Figures 9.1 through 9.4, respectively. The injected CO<sub>2</sub> forms a distinct phase, which is less dense than the ambient brine, resulting in the gross migration of CO<sub>2</sub> phase toward the caprock. There appears to be minimal to no migration of CO<sub>2</sub> phase into the caprock. During the injection and post injection periods, a large portion of the CO<sub>2</sub> mass occurs dissolved in the ambient brine. Depending on the temperature, pressure, and dissolved concentration brine with dissolved CO<sub>2</sub> can be more or less dense than the ambient brine. CO<sub>2</sub> saturated dense brine overlying ambient brine, is an

unstable situation that can lead to advective mixing of the aquifer brine, primarily via fingered flow. The computational domain was originally designed to avoid boundary condition affects on the migration behavior of the CO<sub>2</sub> phase. Clearly, from Figures 9.1 through 9.4 the outer-radial boundary is remote enough not to impact the plume formation and migration. This modeling approach, however, comes with the cost of slower execution. Ideally, the computational domain should be sized to minimize the impact on the multifluid flow processes and maximize the execution speed.

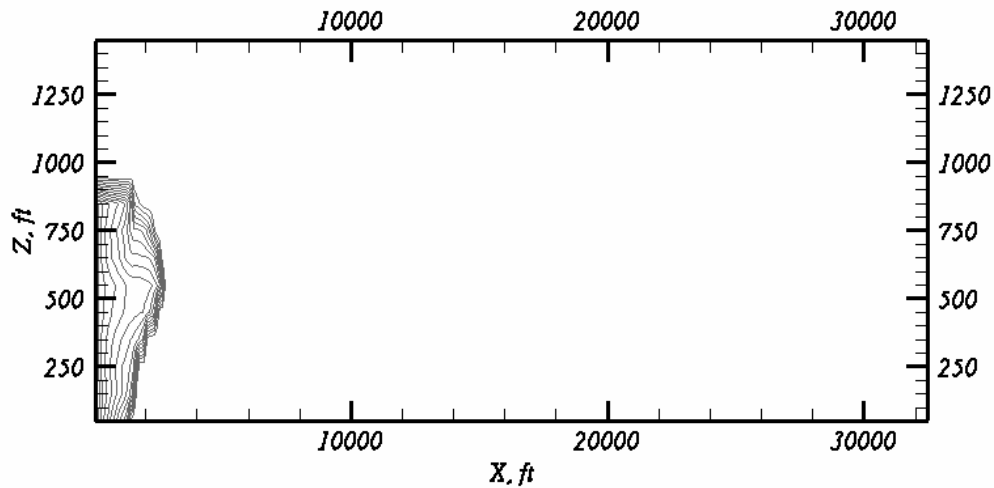


**Figure 9.1.** Gas saturation contours at 10 years

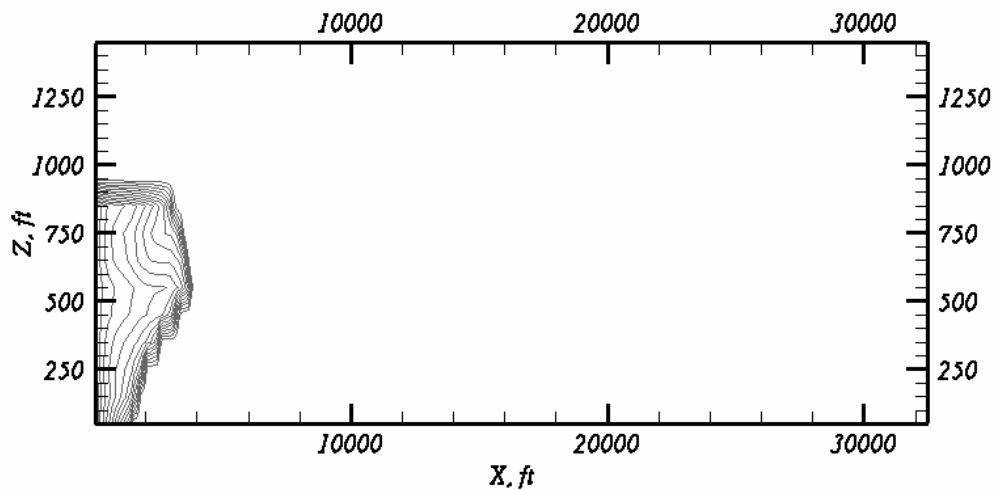


**Figure 9.2.** Gas saturation contours at 20 years

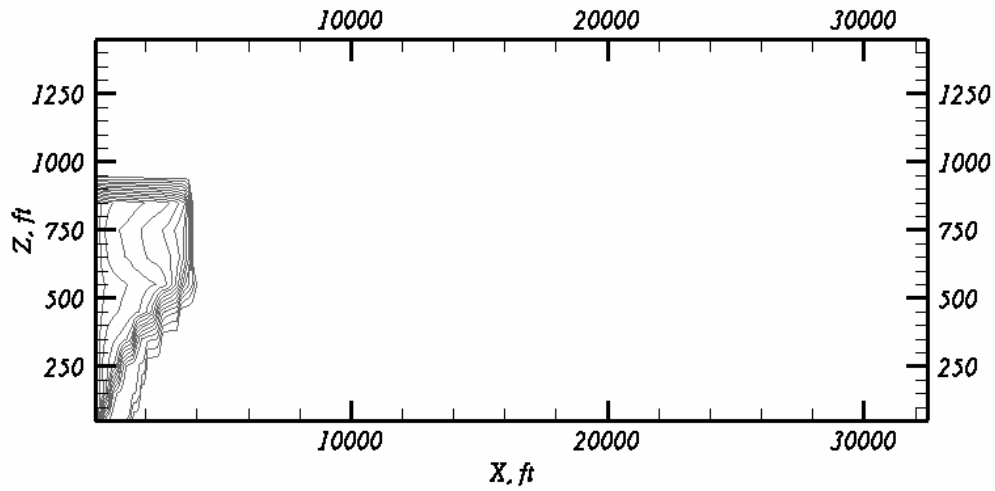


**Figure 9.3.** Gas saturation contours at 30 years

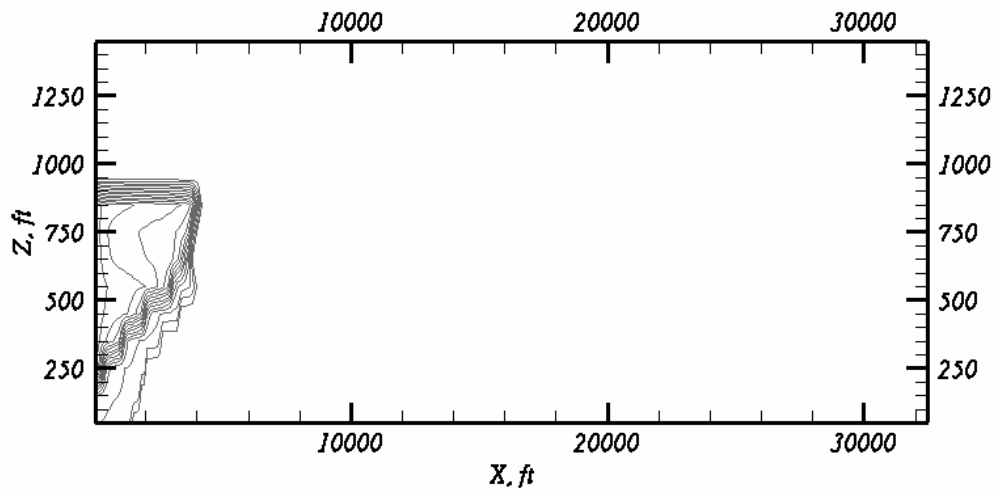


**Figure 9.4** Gas saturation contours at 40 years

## 9.2 Exercises

1. This simulation suffers from an excessive computational domain. Repeat the two-dimensional simulation using a more efficient domain that does

- not impact the multifluid flow behavior.
2. Use the plotting utility *plotTo.pl* or write a script to determine the fraction of CO<sub>2</sub> that has dissolved into the brine as a function of time.
  3. Use the plotting utility *plotTo.pl* or write a script to determine the maximum system pressure as a function of time.
  4. Design and execute a simulation to determine the solubility of CO<sub>2</sub> as a function of NaCl concentration over the range from 0 to 100% NaCl saturated solutions at 20 C and 13.8 MPa.
  5. Design and execute a simulation to determine the density of CO<sub>2</sub> saturated brine as a function of pressure from 0.1 MPa to 100 MPa, at a dissolved NaCl mass fraction of 0.178 and temperature of 20 C.

### 9.3 Input File

```

~Simulation Title Card
1,
BP_UTCOMP Comparison (Base Case),
M.D. White,
Pacific Northwest Laboratory,
30 October 2002,
04:06 PM PST,
23,
CC*****
CC BRIEF DESCRIPTION OF DATA SET: UTMCOMP ( VERSION UTMCOMP-3.5 )
CC*****
CC Radial geometry
CC Mt. Simon Sst. Run BPIN1 2D Full scale,radial model
CC (phase 1=inactivewater,phase 2 = water/oil,phase 3=co2/gas
CC LENGTH(FT):          INJECTION FLUID: CO2
CC HEIGHT(FT):          INJECTION RATE: cont. pre.
CC WIDTH(FT): variable   W/O REL. PERM:
CC POROSITY: variable    G/O REL. PERM: lindeburg
CC ABS. PERM(MD): variable 3-PHASE REL. PERM: water endpt.=1.0
CC TEMP(F): .0           WETTIBILITY:
CC PRESSURE(PSI): .    psi/ft W/O CAP. PRESSURE:
CC SOR:                  G/O CAP. PRESSURE:          *
CC SWC:                  DISPLACEMENT TYPE: HORIZONTAL
CC stop injection after 20 years run for 40 yrs,h2o k endpoint=1
CC ****NON-IDEAL MIXING, NO GRAVITY, WITH Pc, WITH X-FLOW
CC FILE NAME:

```

CC CREATED BY Neeraj Gupta  
CC MODIFIED BY Neeraj Gupta,  
CC\*\*\*\*\*

~Solution Control Card

Normal,  
H2O-NaCl-CO2,  
1,  
0,day,14600,day,1,hr,40,day,1.25,16,1.e-06,  
10000,  
#Constant Aqueous Diffusion,0.0,ft<sup>2</sup>/day,0.0,ft<sup>2</sup>/day,  
#Constant Aqueous Diffusion,4.0e-3,ft<sup>2</sup>/day,4.0e-3,ft<sup>2</sup>/day,  
Variable Aqueous Diffusion,  
Variable Gas Diffusion,  
0,

~Grid Card

Cylindrical,  
70,1,15,  
0.25,ft,100,ft,29@100,ft,5@150,ft,5@200,ft,5@300,ft,  
5@450,ft,5@700,ft,5@1000,ft,7@1500,ft,3@2000,ft,  
0.0,deg,36.0,deg,  
0.0,ft,15@100.0,ft,

~Rock/Soil Zonation Card

6,  
Eau Claire Carbonate,1,70,1,1,14,15,  
Eau Claire Shale,1,70,1,1,11,13,  
Lower Eau Claire,1,70,1,1,10,10,  
Upper Mt. Simon,1,70,1,1,7,9,  
Middle Mt. Simon,1,70,1,1,4,6,  
Lower Mt. Simon,1,70,1,1,1,3,

~Mechanical Properties Card

EauClaireCarbonate,2650,kg/m<sup>3</sup>,0.032,0.032,Compressibility,0.032e5,1/psi,14.7,psi,constant,1.0,  
1.0,  
Eau Claire Shale,2650,kg/m<sup>3</sup>,0.028,0.028,Compressibility,0.028e-5,1/psi,14.7,psi,constant,1.0,1.0,  
LowerEauClaire,2650,kg/m<sup>3</sup>,0.064,0.064,Compressibility,0.064e-5,1/psi,14.7,psi,constant,1.0,1.0,  
UpperMt.Simon,2650,kg/m<sup>3</sup>,0.065,0.065,Compressibility,0.065e-5,1/psi,14.7,psi,constant,1.0,1.0,  
MiddleMt.Simon,2650,kg/m<sup>3</sup>,0.093,0.093,Compressibility,0.093e5,1/psi,14.7,psi,constant,1.0,1.0,  
LowerMt.Simon,2650,kg/m<sup>3</sup>,0.044,0.044,Compressibility,0.044e-5,1/psi,14.7,psi,constant,1.0,1.0,

~Hydraulic Properties Card

Eau Claire Carbonate,3.e-7,Darcy,,,3.e-7,Darcy,  
Eau Claire Shale,7.e-9,Darcy,,,7.e-9,Darcy,  
Lower Eau Claire,3.e-6,Darcy,,,3.e-6,Darcy,  
Upper Mt. Simon,3.8e-3,Darcy,,,3.8e-3,Darcy,  
Middle Mt. Simon,2.1e-2,Darcy,,,2.1e-2,Darcy,  
Lower Mt. Simon,7.1e-3,Darcy,,,7.1e-3,Darcy,

~Saturation Function Card

Eau Claire Carbonate,Brooks and Corey,1.404e-2,m,0.5,0.2,

Eau Claire Shale, Brooks and Corey, 2.239e-2, m, 0.5, 0.2,  
Lower Eau Claire, Brooks and Corey, 3.14e-2, m, 0.5, 0.2,  
Upper Mt. Simon, Brooks and Corey, 1.109e-2, m, 0.5, 0.2,  
Middle Mt. Simon, Brooks and Corey, 2.179e-2, m, 0.5, 0.2,  
Lower Mt. Simon, Brooks and Corey, 1.842e-2, m, 0.5, 0.2,

~Aqueous Relative Permeability Card

Eau Claire Carbonate, Free Corey, 1.0, 3.25, 0.2, 0.1,  
Eau Claire Shale, Free Corey, 1.0, 3.25, 0.2, 0.1,  
Lower Eau Claire, Free Corey, 1.0, 3.25, 0.2, 0.1,  
Upper Mt. Simon, Free Corey, 1.0, 3.25, 0.2, 0.1,  
Middle Mt. Simon, Free Corey, 1.0, 3.25, 0.2, 0.1,  
Lower Mt. Simon, Free Corey, 1.0, 3.25, 0.2, 0.1,

~Gas Relative Permeability Card

Eau Claire Carbonate, Free Corey, 0.9, 2.9, 0.2, 0.1,  
Eau Claire Shale, Free Corey, 0.9, 2.9, 0.2, 0.1,  
Lower Eau Claire, Free Corey, 0.9, 2.9, 0.2, 0.1,  
Upper Mt. Simon, Free Corey, 0.9, 2.9, 0.2, 0.1,  
Middle Mt. Simon, Free Corey, 0.9, 2.9, 0.2, 0.1,  
Lower Mt. Simon, Free Corey, 0.9, 2.9, 0.2, 0.1,

~Salt Transport Card

Eau Claire Carbonate, 20.0, ft, 5.0, ft,  
Eau Claire Shale, 20.0, ft, 5.0, ft,  
Lower Eau Claire, 20.0, ft, 5.0, ft,  
Upper Mt. Simon, 20.0, ft, 5.0, ft,  
Middle Mt. Simon, 20.0, ft, 5.0, ft,  
Lower Mt. Simon, 20.0, ft, 5.0, ft,

~Initial Conditions Card

Gas Pressure, Aqueous Pressure,  
4,  
Gas Pressure, 2857, Psi, -0.45, 1/ft, 1, 70, 1, 1, 1, 15,  
Aqueous Pressure, 2857, Psi, -0.45, 1/ft, 1, 70, 1, 1, 1, 15,  
Temperature, 50.0, C, 1, 70, 1, 1, 1, 15,  
Salt Mass Fraction, 0.178, 1, 70, 1, 1, 1, 15,

~Source Card

1,  
Gas Mass Rate, Water-Vapor Mass Fraction, 1, 1, 1, 1, 9, 2,  
0, day, 0.352413, kg/s, 0.0,  
7300, day, 0.352413, kg/s, 0.0,

~Boundary Conditions Card

1,  
East, Aqu. Initial Conditions, Gas Initial Conditions, Aqu. Mass Frac.,  
70, 70, 1, 1, 1, 15, 1,  
0, s, 0.0, 1.0, 0.178,,

~Output Options Card

4,

1,1,1,  
10,1,1,  
20,1,1,  
30,1,1,  
1,1,day,ft,deg,6,6,6,  
6,  
Gas Saturation,,  
Integrated CO2 Mass,kg,  
Salt Aqueous Mass Fraction,,  
CO2 Aqueous Mass Fraction,,  
Gas Pressure,psi,  
Diffusive Porosity,,  
19,  
1,day,  
10,day,  
30,day,  
182,day,  
365,day,  
730,day,  
1095,day,  
1460,day,  
1825,day,  
3650,day,  
5475,day,  
7300,day,  
7301,day,  
7330,day,  
7665,day,  
8030,day,  
8395,day,  
10950,day,  
12775,day,  
6,  
Gas Saturation,,  
CO2 Aqueous Mole Fraction,,  
Salt Aqueous Mass Fraction,,  
CO2 Aqueous Mass Fraction,,  
Gas Pressure,psi,  
Diffusive Porosity,,

## 9.4 Solutions to Selected Exercises

### Exercise 1

The gas saturation contours at 40 years (Fig. 9.4) indicate that the radial extent of the computational domain is excessive. The computation domain and execution time can be reduced by decreasing the number of nodes (from 72 to 50) in the radial direction, bringing the overall radial distance down from 30,000 to 10,000 ft. The following *Grid Card* shows this change:

```
~Grid Card
Cylindrical,
52,1,15,
0.25,ft,100,ft,29@100,ft,5@150,ft,5@200,ft,5@300,ft,
5@450,ft,2@700,ft,
0.0,deg,36.0,deg,
0.0,ft,15@100.0,ft,
```

When the simulation is executed using the smaller computational domain gas saturation results are unaltered.

### Exercise 2

The STOMP H<sub>2</sub>O-CO<sub>2</sub>-NaCl operational mode has two reference-node variables that make this exercise straightforward. Include “Integrated CO<sub>2</sub> Mass” and “Integrated Aqueous CO<sub>2</sub> Mass” on the *Output Control Card* as reference-node variables. The reference node itself is arbitrary, as the variables record the spatially integrated amounts of the respective masses for the entire domain. Then, simply divide the CO<sub>2</sub> in the aqueous phase (i.e., integrated aqueous CO<sub>2</sub> mass) by the total CO<sub>2</sub> (i.e., integrated CO<sub>2</sub> mass) in the system to obtain the fraction of CO<sub>2</sub> that has dissolved. The fraction of injected CO<sub>2</sub> that is dissolved versus simulation time is shown in Figure 9.5. This plot illustrates that

20 years after the 20-year injection period, the fraction of injected CO<sub>2</sub> that has been sequestered as dissolved CO<sub>2</sub> is less than 10%.

### Exercise 3

CO<sub>2</sub> sequestration increases the pressure in the confined saline aquifer. The cap rock above an aquifer must be able to withstand this additional pressure without allowing the CO<sub>2</sub> to escape into the layers above. The gas pressure is a plot file variable and a reference node variable. The maximum gas pressure can be determined, at a point in time, by extracting the gas pressure field variable from a *plot.x* file and searching for the maximum value. The maximum gas pressure at a point in space can be determined by extracting the gas pressure field variable from the output file and searching for the maximum value.

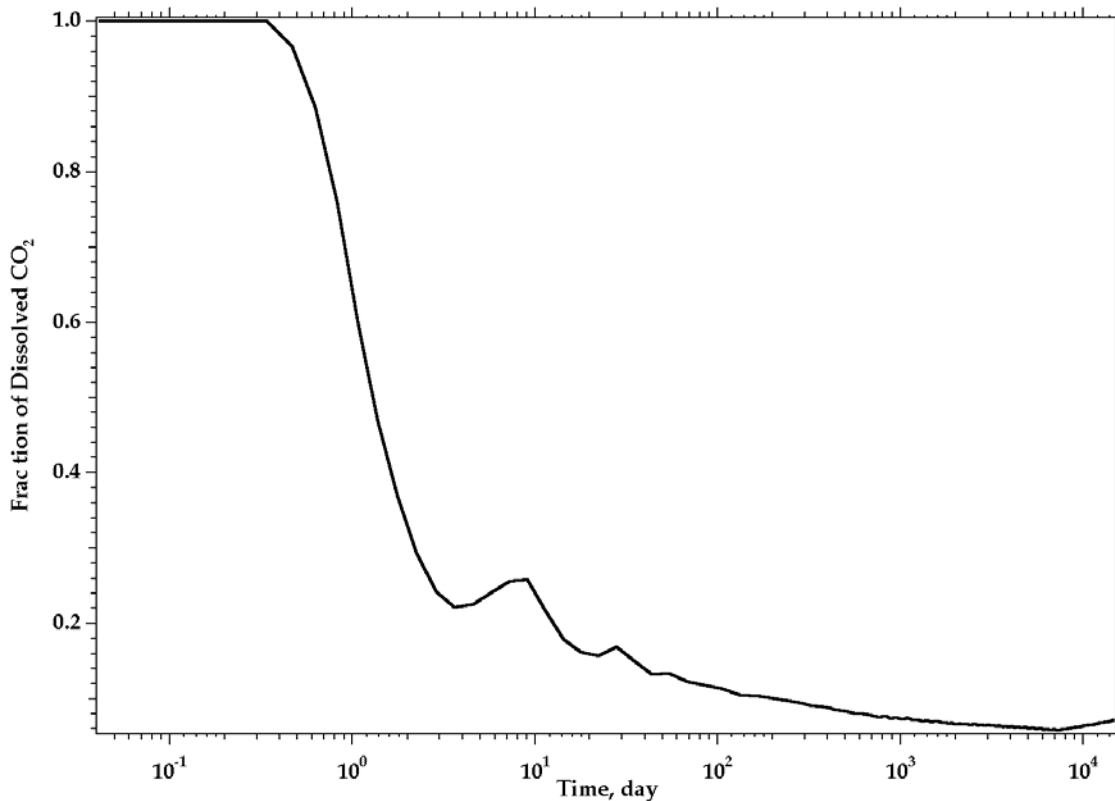


**Figure 9.5.** Fraction of aqueous dissolved CO<sub>2</sub>.

#### **Exercise 4**

An efficient way to use the STOMP simulator for solving this problem is to use a one-dimensional array of grid cells, with each node having unique initial NaCl saturation (0 to 100%) and then execute an equilibrium simulation. The *Initial Conditions* execution mode computes equilibrium conditions, using the equation-of-state module and then stops. For this simulation, it is important to set the initial aqueous saturation to values less than 1.0, to create two-phase conditions (CO<sub>2</sub>-aqueous).

#### **Exercise 5**

The approach to solving this problem is essentially the same as in Exercise 4. The *Initial Conditions* execution mode is ideal for this type of problem. As mentioned in the problem statement, depending on the temperature, pressure, and dissolved concentration, brine with dissolved CO<sub>2</sub> can be denser than the ambient brine. This can lead to advective mixing and increase the rate at which CO<sub>2</sub> enters the aqueous phase. Try and simulate these conditions with the physical system detailed in this problem.

## 10. Simulation of countercurrent flow and heat transport with local evaporation and condensation (natural heat pipe)

**Abstract:** *This heat pipe problem demonstrates the simulator's ability to model countercurrent aqueous and gas flow in variably saturated geologic media, including saturations below residual saturation. As posed, the problem involves one-dimensional horizontal flow and heat transport, but this classic multifluid subsurface flow and transport problem involves complex flow behavior, which is subtle to changes in soil properties. The user will first explore the affects of changes in soil thermal conductivity, specific heat, and enhanced vapor transport on the formation and temperature distribution for a horizontal one-dimensional heat pipe. After completing these investigations the user is asked to design an input file for a two-dimensional problem involving dynamic heat pipe flow.*

### 1.1 Problem Description

Because of their ability to transport large quantities of heat over small temperature differences and surface areas, engineered heat pipes are commonly used in thermal engineering applications. Natural heat pipes can occur in partially saturated soils, subjected to thermal gradients. The typical scenario for a natural heat pipe occurs when a heated engineered surface is in contact with the subsurface (e.g., nuclear waste repository containers, nuclear waste storage tanks, or in-situ soil heating). The general requirements for creating countercurrent hydrothermal (i.e., heat pipe) flow in geologic media are a heat source and heat sink separated by partially saturated porous media. The heat source causes pore water to evaporate, creating a locally elevated gas pressure and water vapor concentration. Evaporation of the pore water reduces the

saturation near the heat source, which in turn elevates the local capillary pressure. The heat sink causes water vapor to condense, creating a locally reduced gas pressure and water vapor concentration. The condensing water vapor also increases the local saturation. The pressure and water vapor gradients in the gas phase produce a flow of water vapor and associated heat from the heat source to the heat sink. Conversely, the capillary draw created by the elevated capillary pressures near the heat sink produces flow of liquid water towards the heat source. This countercurrent flow of water vapor in the gas phase and liquid water in the aqueous phase yields a net flow of heat from the heat source to the heat sink. Because of the importance of heat pipe flow to the overall heat transfer of engineered geologic systems, the ability of the numerical simulator to accurately and efficiently predict these complex and multiple-phase flow structures is imperative. The heat pipe problem chosen for solution is a modified version of the problem posed and solved by Udell and Fitch (1985).

The heat pipe problem solved by Udell and Fitch involved a one-dimensional horizontal cylinder (2.25-m in length) of porous media, which was assumed perfectly insulated on the sides, subjected to a constant heat flux (100-W/m<sup>2</sup>) on one end, and maintained at a constant temperature (70°C) on the other end. The heat flux end of the cylinder was sealed and the constant temperature end was maintained under total-liquid saturation conditions. Initial conditions for the porous media were a total-liquid saturation of 0.7, a temperature of 70°C, and an absolute gas pressure of 101,330 Pa. Initial conditions and boundary conditions are listed for reference in Table 10-1.

The constitutive functions used in this problem differ slightly from those used by Udell and Fitch. Soil-moisture retention was described using the van Genuchten formulation (van Genuchten 1980) with a modification to the residual saturation that allows aqueous saturation to fall below the residual saturation, as

shown in Equations (10.1) and (10.2). The aqueous and gas relative permeabilities were described by the Fatt and Klikoff formulations, as shown in Equations (10.3) and (10.4), respectively. The effective thermal conductivity of the partially saturated porous media was described by the formulation of Sommertson (1974), according to Equation (10.5). Parameter values are shown in Table 10-1.

$$S_l = \left[ 1 + (\alpha h_{gl})^n \right]^{-m} \left[ 1 - \bar{S}_m \right] + \bar{S}_m = \bar{S}_l \left[ 1 - \bar{S}_m \right] + \bar{S}_m \quad (10.1)$$

$$\bar{S}_m = \left[ 1 - \frac{\ln(h_{gl})}{\ln(h_{od})} \right] S_m \quad (10.2)$$

$$k_{rl} = \bar{S}_l^3 \quad (10.3)$$

$$k_{rg} = (1 - \bar{S}_l)^3 \quad (10.4)$$

$$k_e = k_{unsat} + \sqrt{\bar{S}_l} (k_{sat} - k_{unsat}) \quad (10.5)$$

**Table 10-1.** Simulation Parameter Values

Parameter Description	Parameter Value
Unsaturated Thermal Conductivity	0.582 W/m K
Saturated Thermal Conductivity	1.13 W/m K
Intrinsic Permeability	$10^{-12} \text{ m}^2$
Porosity	0.4
Grain Density	2650. kg/m <sup>3</sup>
Grain Specific Heat	700. J/kg K
Tortuosity	0.5
van Genuchten $\alpha$	1.5631 m <sup>-1</sup>
van Genuchten $n$	5.4

Residual Saturation	0.15
---------------------	------

The relative high van Genuchten  $n$  parameter is representative of well-drained soils and is numerically difficult to resolve, as it yields a strongly nonlinear function between capillary head and saturation. To reduce convergence problems with this simulation, the time stepping was controlled using three execution periods over the 10,000-day span of the simulation. During the first 10-day period the maximum time step was limited to 0.1 day. During the second execution period from day 10 to day 100 the maximum time step was increased to 1 day, and during the final period from day 100 to day 10,000, the maximum time step was increased to 1000 day. The simulation will execute without this manual time-stepping control, but the simulation suffers from numerous convergence errors and primary variable exceptions. Both of these errors are trapped by STOMP and result in a reduction in the current time step.

Simulation results, in terms of profiles of temperature, aqueous saturation, and water vapor mass fraction at days 2, 5, 10, 50, and 10,000 are shown in Figures 10.1 through 10.5, respectively. In these plots the aqueous saturated boundary at 70 C is on the left side and the heated, flow-impermeable boundary is on the right. After 2 days, Figure 10.1, the temperature on the heated boundary has risen from 70 C to 96.7 C and water has started to imbibe from the saturated boundary. The water-vapor mass fraction in the gas phase is primarily a function of vapor pressure, which is a function of temperature. The water-vapor mass fraction profile, therefore, tracks the temperature profile. After 5 days, Figure 10.2, the heated boundary temperature exceeds 100 C and the soil moisture begins to evaporate. After 10 days, Figure 10.3, the 100-C temperature point has nearly reached the mid-point of the column and water is now being forced out the saturated boundary. At this point in time, the zone of

countercurrent flow, (i.e., gas evaporating and moving toward the left and water being drawn back toward the right via capillary pressure) is still expanding. After 10,000 days, Figure 10.4, the simulation has reached steady-flow conditions and the column is exhibiting three heat transport regimes. In the left portion of the domain, heat transfer is via conduction, advection, and mass diffusion, as shown by the non-linear temperature profile; in the middle portion heat transfer is primarily via countercurrent advection and mass diffusion, as shown by the flat temperature profile; and in the right portion heat transfer is primarily by conduction as shown by the linear temperature profile. Under steady-flow conditions the right side of the column has aqueous saturations below the residual saturation and the gas phase comprises primarily water-vapor.

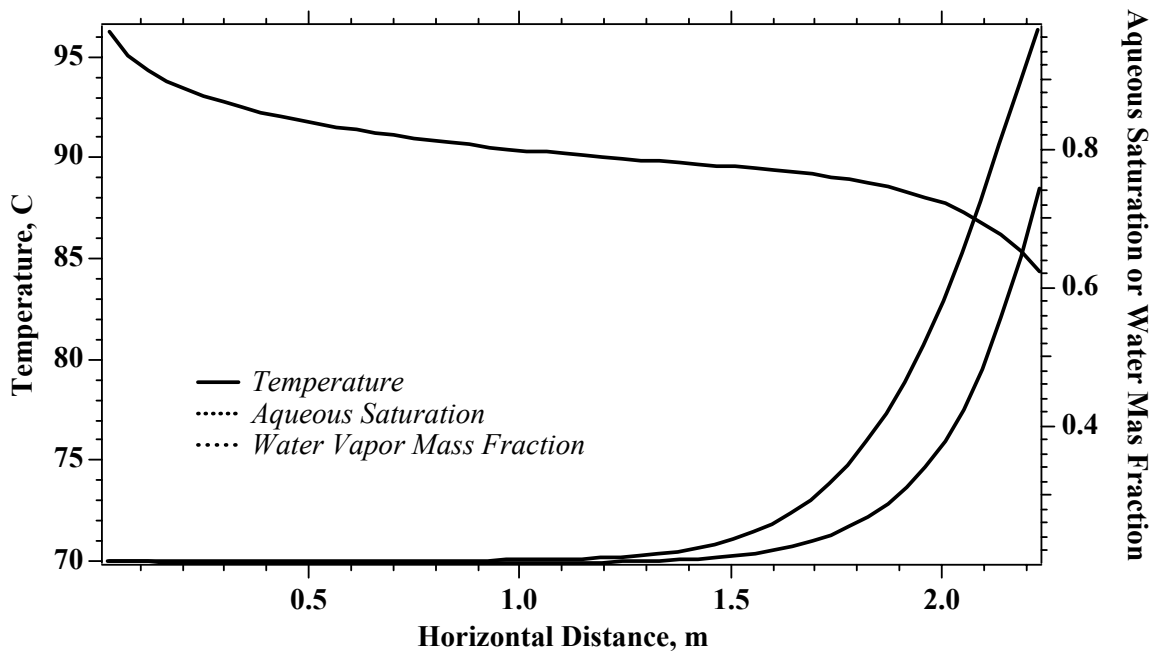


**Figure 10.1.** Temperature, aqueous saturation, and water vapor mass fraction profiles at 2 days

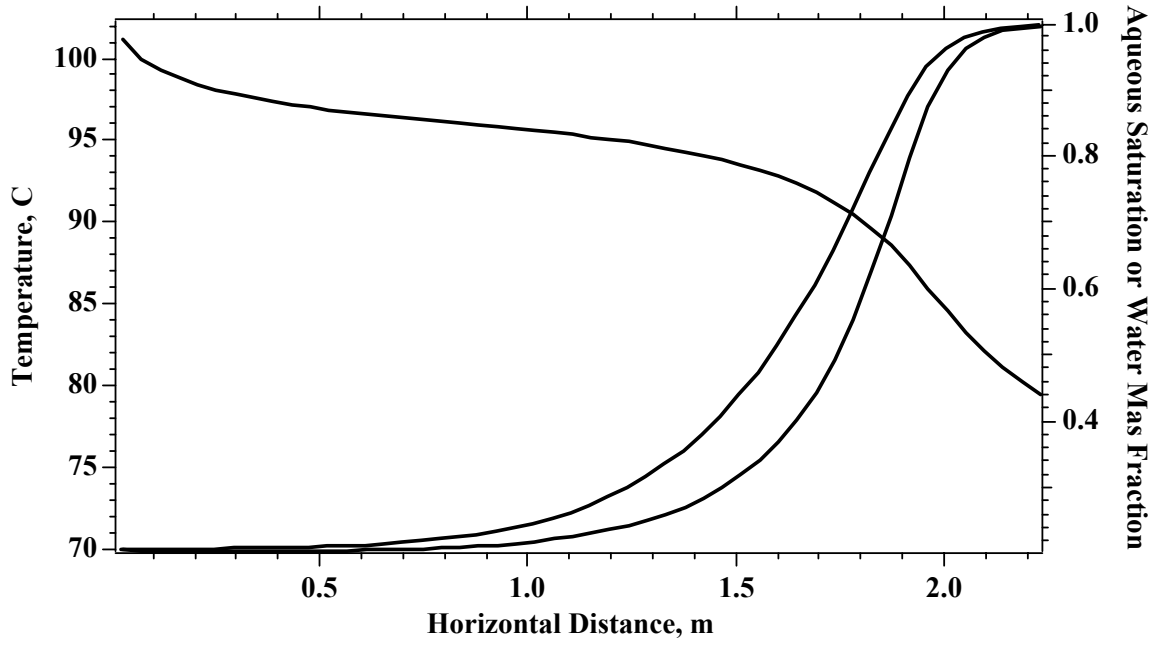


**Figure 10.2.** Temperature, aqueous saturation, and water vapor mass fraction profiles at 5 days

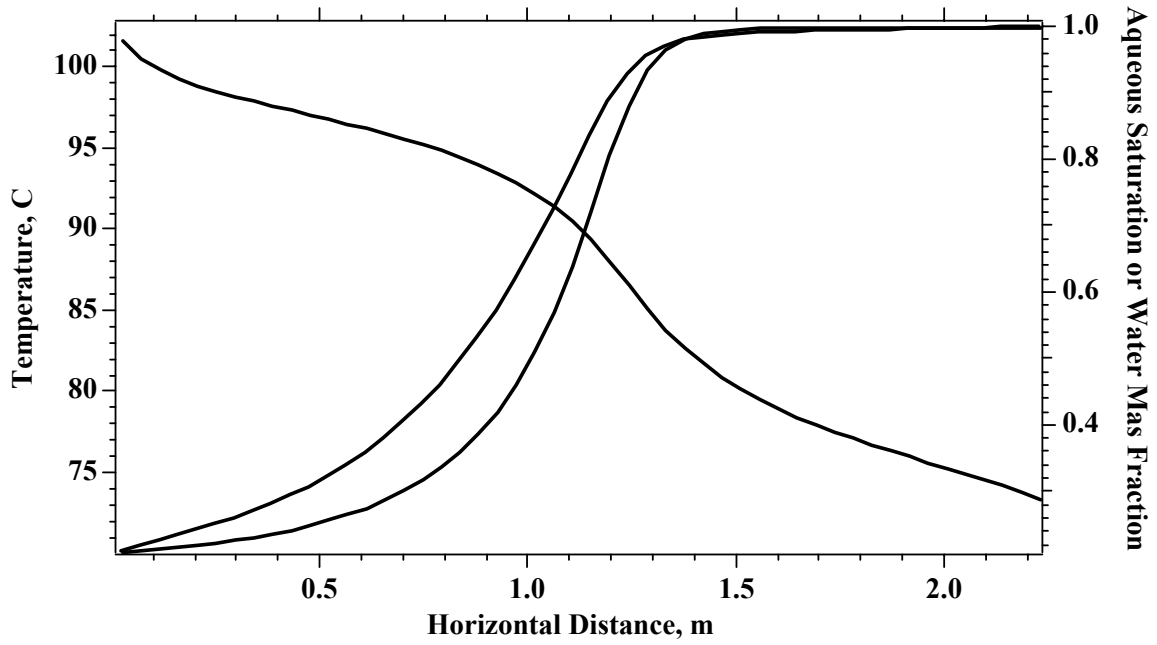


**Figure 10.3.** Temperature, aqueous saturation, and water vapor mass fraction profiles at 10 days

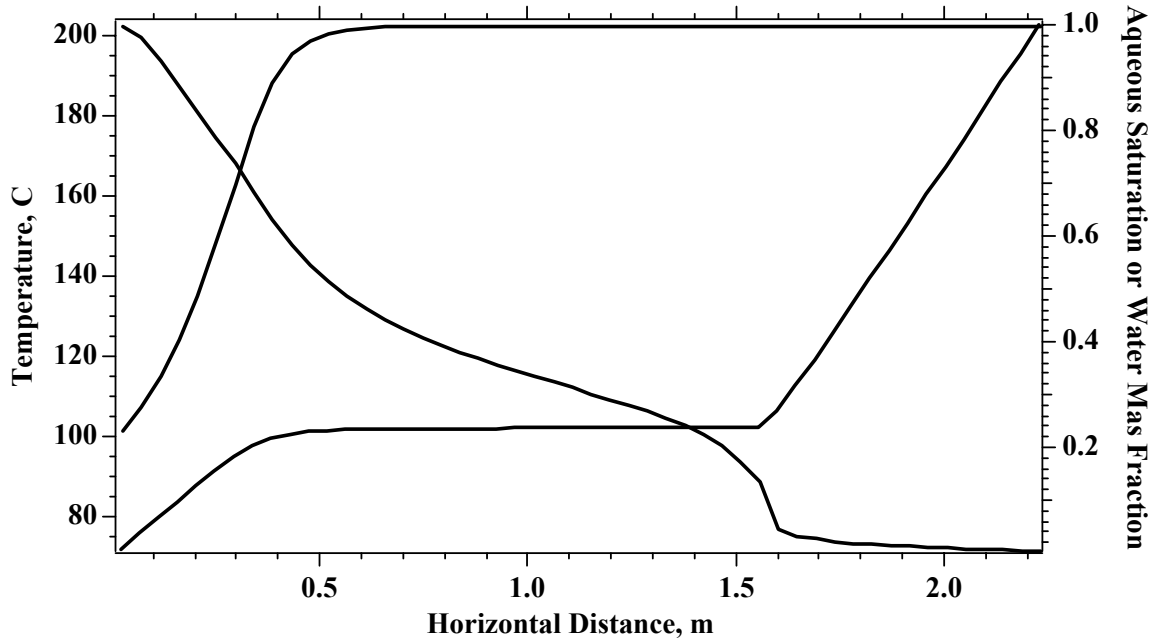


**Figure 10.4.** Temperature, aqueous saturation, and water vapor mass fraction profiles at 10,000 days

The heat-pipe problem, which was solved using an semi-analytical approach by Udell and Fitch (1985), differs from the current problem in several aspects. First, the Udell and Fitch problem used constant physical properties, whereas the STOMP simulation included temperature and pressure dependent physical properties for the gas and aqueous phases. Second, nitrogen gas, instead of air, was used as the noncondensable in the Udell and Fitch problem. Third, the saturation-capillary function in the Udell and Fitch formulation used the Leverett function (Leverett 1941) without extensions below the residual saturation, whereas the STOMP simulation used a van Genuchten function which closely matched the Leverett function. In spite of these differences the results show good agreement between the solution of Udell and Fitch and the STOMP simulation for the steady-state conditions; the Udell and Fitch solution is valid only for the steady-state solution. Both results show temperature profiles with mixed conduction and advection/diffusion heat transport near the saturated boundary and nearly pure countercurrent gas and aqueous flow heat

transport in the center portion of the heat pipe. The Udell and Fitch solution stops short of the dry-out region with the minimum saturation being the residual saturation level. The STOMP solution allows a region near the heated boundary to dry out, thus creating elevated temperatures, in comparison to the Udell and Fitch results.

### *References*

Fayer, M.J., and C.S. Simmons. 1995. Modified soil water retention function for all matric suctions. *Water Resources Research*, 31(5), 1233-1238.

Leverett, M.C. 1941. Capillary behavior in porous solids. *AIME Transactions*, 142-152.

Somerton, W.H., A.H. El-shaarani, and S.M. Mobarak. 1974. High temperature behavior of rocks associated with geothermal type reservoirs. Paper SPE-4897, presented at the 44<sup>th</sup> Annual California Regional Meeting of the Society of Petroleum Engineers, San Francisco, California.

Udell, K.S., and J.S. Fitch. 1985. Heat and mass transfer in capillary porous media considering evaporation, condensation, and non-condensable gas effects, In *Proceedings of 23<sup>rd</sup> ASME/AIChE National Heat Transfer Conference*, Denver, Colorado.

van Genuchten, M. Th. 1980. A closed-form equation for predicting the hydraulic conductivity of unsaturated soils. *Soil Sci. Soc. Am. J.*, 44:892-898.

White, M.D., and M. Oostrom. 2000. *STOMP Subsurface Transport Over Multiple Phases, Version 2.0, Theory Guide*, PNNL-12030, UC-2010, Pacific Northwest National Laboratory, Richland, Washington.

## **10.2 Exercises**

6. (Basic) Repeat the one-dimensional horizontal column simulation changing the unsaturated and saturated thermal conductivities (*Thermal Properties Card*), grain density (*Mechanical Properties Card*) and grain

- specific heat (*Thermal Properties Card*). Compare the steady-flow temperature, aqueous saturation, and water-vapor mass fraction profiles against those reported herein.
7. (Intermediate) Repeat the one-dimensional horizontal column simulation using various time stepping controls (*Execution Time Periods, Solution Control Card*). Check for differences in the simulation results at 2, 5, 10, 50, and 10,000 days.
  8. (Intermediate) Repeat the one-dimensional horizontal column simulation using the *Enhanced Gas Diffusion Option*, changing the clay mass fraction (*Solution Control Card*). Compare the steady-flow temperature, aqueous saturation, and water-vapor mass fraction profiles against those reported herein.
  9. (Advanced) Design and execute a two-dimensional heat pipe simulation with heat emanating from an impermeable subsurface structure (e.g., pipe, nuclear waste canister, nuclear waste repository, heating element). Simulate the system with time varying heat source to form a dynamic heat pipe. Create a time sequence of temperature and aqueous saturation contours to visualize the dynamic heat pipe.

### 10.3 Input File

```
#-----
~Simulation Title Card
#-----
1,
STOMP Tutorial Problem 10,
Mart Oostrom/Mark White,
PNNL,
June 2003 20,
15:15,
4,
This application problem follows the heat-pipe problem solved
semi-analytically by Udell and Fitch. The soil moisture retention
function has been changed to a modified van Genuchten function to
allow saturations for all matric suctions.
```

```

#-----
~Solution Control Card
#-----
Normal,
Water-Air-Energy,
3,
0,day,10,day,1,s,0.1,day,1.25,16,1.e-06,
10,day,100,day,0.1,day,1,day,1.25,16,1.e-06,
100,day,10000,day,1,day,1000,day,1.25,16,1.e-06,
1000,
Variable Aqueous Diffusion,
Variable Gas Diffusion,
0,

#-----
~Grid Card
#-----
Uniform Cartesian,
50,1,1,
4.5,cm,
10.0,cm,
10.0,cm,
#-----
~Rock/Soil Zonation Card
#-----
1,
Sand,1,50,1,1,1,1,

#-----
~Mechanical Properties Card
#-----
Sand,2650,kg/m^3,0.4,0.4,,,Constant,0.5,0.5,

#-----
~Hydraulic Properties Card
#-----
Sand,1.e-12,m^2,,,,,

#-----
~Thermal Properties Card
#-----
Sand,Somerton,0.582,W/m K,,,,,1.13,W/m K,,,,,700,J/kg K,

#-----
~Saturation Function Card
#-----
Sand,van Genuchten,1.563,1/m,5.4,0.15,,

#-----
~Aqueous Relative Permeability Card
#-----
Sand,Fatt and Klikoff,

```

#-----  
~Gas Relative Permeability Card

#-----  
Sand,Fatt and Klikoff,

#-----  
~Initial Conditions Card

#-----  
Aqueous Saturation,Gas Pressure,  
3,  
Aqueous Saturation,0.7,,,,,,1,50,1,1,1,1,  
Gas Pressure,101330,Pa,,,,,,1,50,1,1,1,1,  
Temperature,70.0,C,,,,,,1,50,1,1,1,1,

#-----  
~Boundary Conditions Card

#-----  
2,  
West,Dirichlet Energy,Dirichlet Aqueous,Dirichlet Gas,  
1,1,1,1,1,1,  
0,day,70,C,101330,Pa,1.0,101330,Pa,1.0,  
East,Neumann Energy,Zero Flux Aqueous,Zero Flux Gas,  
50,50,1,1,1,1,1,  
0,day,-100,W/m^2,,,,,,

#-----  
~Output Options Card

#-----  
2,  
1,1,1,  
50,1,1,  
1,1,day,m,5,5,5,  
6,  
Temperature,,  
Aqueous saturation,,  
Phase condition,,  
Water gas mass frac.,,  
Aqueous pressure,,  
Gas pressure,,  
4,  
2,day,  
5,day,  
10,day,  
50,day,  
6,  
Temperature,,  
Aqueous saturation,,  
Phase condition,,  
Water gas mass frac.,,  
Aqueous pressure,,  
Gas pressure,,

## 10.4 Solution to Selected Exercises

### Exercise 1

As thermal conductivity is a coefficient for heat transfer, we expect changes in thermal conductivity to change the transient and steady-flow profiles. Strong coupling between the thermal and hydrologic system, typical of heat-pipe flows, additionally makes us expect changes in both the temperature and saturation profiles with changes in the thermal conductivity. The Somerton model for calculating the effective thermal conductivity of partially saturated soils is dependent on the aqueous saturation and the saturated and unsaturated thermal conductivity of the soil. We, therefore, expect changes in the transient and steady-flow profiles with changes in both the unsaturated and saturated thermal conductivities. The affect of increasing the saturated thermal conductivity and decreasing the unsaturated thermal conductivity are shown in Figures 10.5 and 10.6, respectively. Increasing the saturated thermal conductivity (Figure 10.5) lessens the slope in the temperature profile in the regions of higher saturation (i.e., left-hand side). Consequentially, this shifts the region of countercurrent flow toward the heated side (i.e., right-hand side), eliminating the region of saturation values below residual. Decreasing the unsaturated thermal conductivity (Figure 10.6) has little effect on the steady-flow profiles in the regions of higher saturations (i.e., right-hand side). The slope of the temperature profile in the unsaturated region is steeper, resulting in higher peak temperatures and slight increases in soil drying in the unsaturated region (i.e., left-hand side). The grain density and grain specific heat are variables which only appear in the thermal storage term of the energy conservation equation. Under steady-flow conditions the thermal storage term is zero; therefore, changing the grain density and specific heat has no affect on the steady-flow profiles.

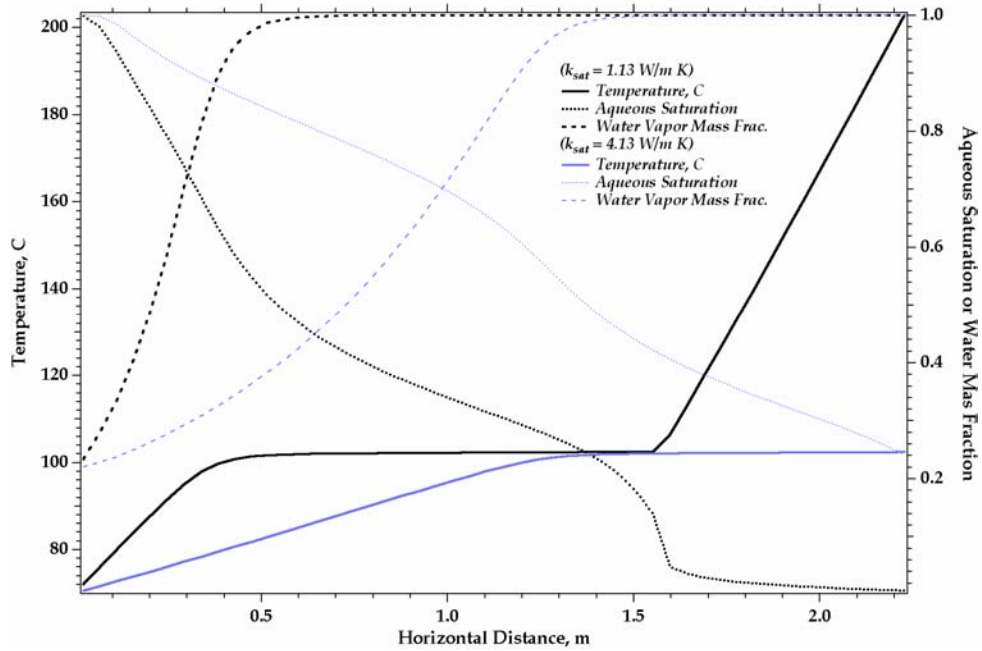


**Figure 10.5.** Temperature, aqueous saturation, and water vapor mass fraction profiles under steady-flow conditions for different unsaturated thermal conductivities.

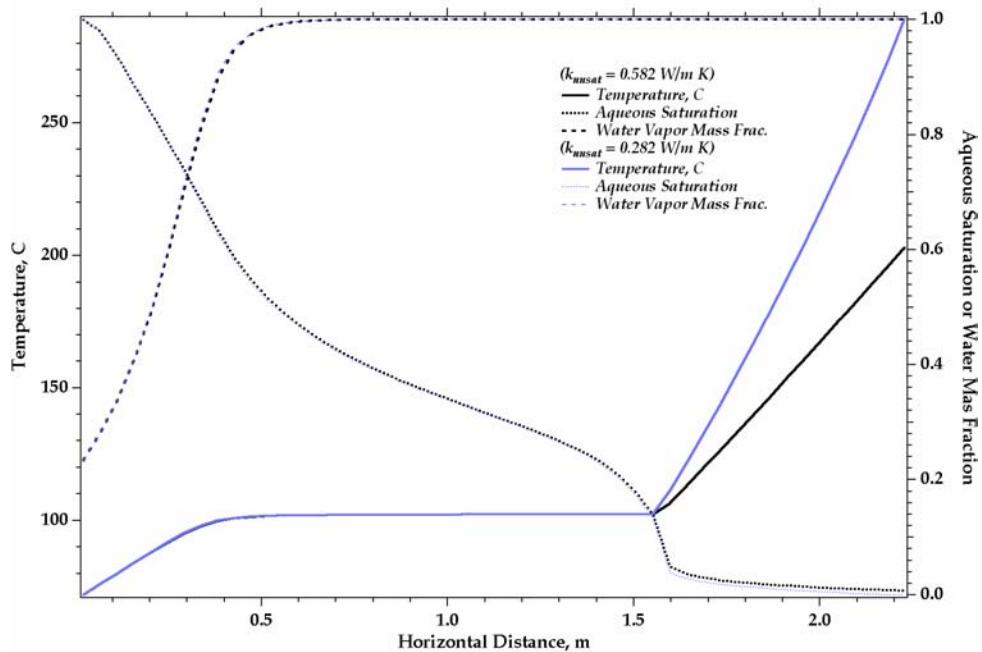


**Figure 10.6.** Temperature, aqueous saturation, and water vapor mass fraction profiles under steady-flow conditions for different unsaturated thermal conductivities.

## Exercise 2

The original Solution Control Card, used three execution periods that controlled the maximum time step (i.e., 0.1 day for the first 10 days, 1 day from 10 to 100 days, and 1000 days from 100 to 10,000 days). The time-step controlled simulation required 271 time steps to reach steady-flow conditions at 10,000 days. The affect of no time step control can be seen by executing the simulation with the following simpler Solution Control Card, shown below.

```
#-----  
~Solution Control Card  
#-----  
Normal,  
Water-Air-Energy,  
1,  
0,day,10000,day,100,s,5000,day,1.25,16,1.e-06,  
1000,  
Variable Aqueous Diffusion,  
Variable Gas Diffusion,  
0,
```

Whereas, the simulation reached steady-flow conditions at 10,000 days after 93 time steps, the transient portion of the simulation required forced time-step reductions because of convergence failures. Although no differences in results are apparent in the profiles of temperature, aqueous saturation and water-vapor mass fraction at steady-flow conditions, there are differences in these profiles at 10 days, as illustrated in Figure 10.8. Theoretically, the simulator will produce more accurate solutions, to a point, using smaller time steps. There is, however, dimensioning return on increased accuracy with smaller and smaller time steps. It is the onus of the user to select time stepping schemes that achieve the desired accuracy at minimal computational effort. An effective approach for achieving the appropriate time stepping scheme is to systematically reduce the time steps until no further change in the results are noticed.

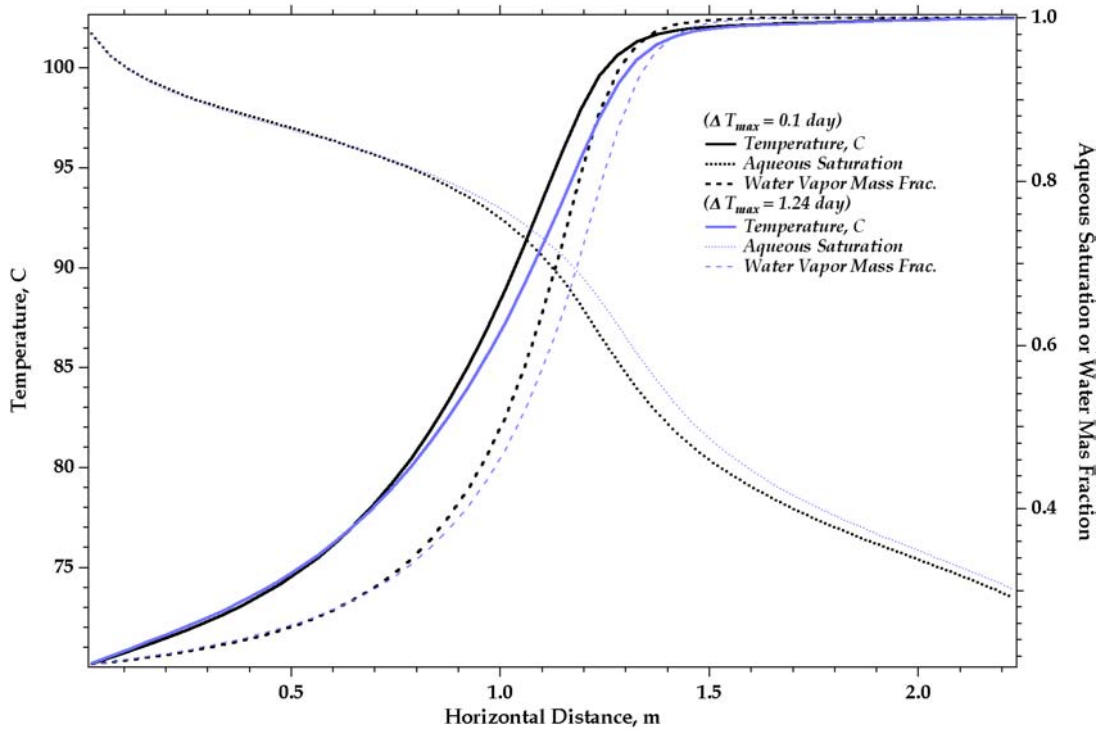


**Figure 10.8.** Temperature, aqueous saturation and water-vapor mass fraction profiles at 10 days, with different time-step control.

### Exercise 3

Water-vapor diffusion in the gas phase in porous media occurs at rates greater than those in free gas. This affect is often referred to as enhanced vapor diffusion. Enhanced vapor diffusion can be simulated in the STOMP simulator through the *Enhanced Gas Diffusion Option* and specifying a clay mass fraction for the soil. The affect of using a clay mass fraction of 0.1 to enhance the water-vapor mass diffusion is apparent in the steady-flow profiles of temperature, aqueous saturation and water-vapor mass fraction, shown in Figure 10.9. The enhanced water-vapor diffusion has a significant impact on all profiles at steady-flow conditions. The flat temperature profile in the countercurrent flow region is replaced with a sloped temperature profile caused by the gradient in water-vapor mass fraction in this region. The aqueous saturation profile is shifted toward the left, yielding an increased region below residual saturation and the

enhanced water-vapor diffusion allows air to exist in the drier regions (i.e., right-hand side).

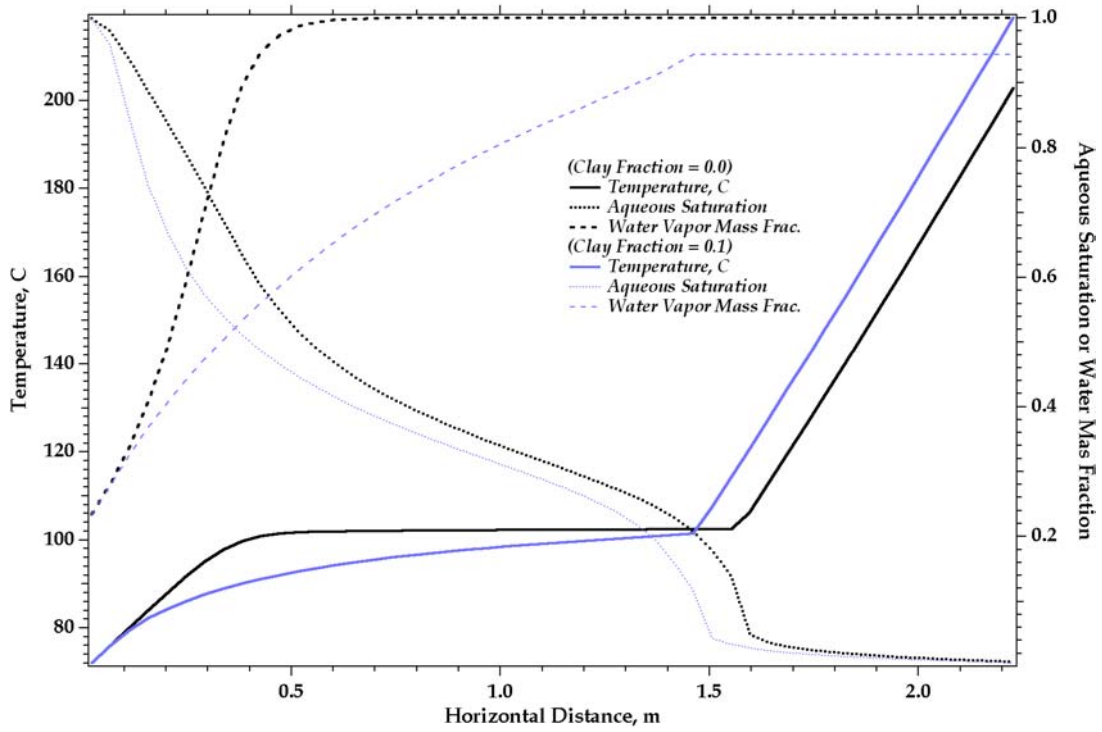


**Figure 10.9.** Temperature, aqueous saturation, water-vapor mass fraction profiles at steady-flow conditions with different clay mass fractions